

UNIVERSIDADE DE BRASÍLIA  
FACULDADE DE CIÊNCIAS DA SAÚDE

GLEICE ROCHA FERREIRA BORGES

ATIVIDADE DE DERIVADOS DE DIINDOLILMETANO E DE URACIL EM  
RECEPTORES DE ÁCIDOS GRAXOS 1 E 4 (FFAR1 E FFAR4)

BRASÍLIA

2018

Gleice Rocha Ferreira Borges

ATIVIDADE DE DERIVADOS DE DIINDOLILMETANO E DE URACIL EM  
RECEPTORES DE ÁCIDOS GRAXOS 1 E 4 (FFAR1 E FFAR4)

Dissertação apresentada ao Programa de Pós-Graduação em Ciências Farmacêuticas da Faculdade de Ciências da Saúde, Universidade de Brasília, como requisito parcial à obtenção do título de Mestre em Ciências Farmacêuticas.

Orientador: Prof. Dr. Luiz Alberto Simeoni

Coorientador: Dr. Dominik Thimm

Brasília

2018

Autorizo a reprodução parcial ou total deste trabalho, por qualquer meio convencional ou eletrônico, para fins de ensino, estudo ou pesquisa, desde que citada a fonte.

### Catálogo da publicação

Ficha catalográfica elaborada automaticamente,  
com os dados fornecidos pelo(a) autor(a)

RB732a Rocha Ferreira Borges , Gleice  
Atividade de derivados de diindolilmetano e de uracil em  
receptores de ácidos graxos 1 e 4 (FFAR1 e FFAR4). /  
Gleice Rocha Ferreira Borges ; orientador Luiz Alberto  
Simeoni; co-orientador Dominik Thimm. -- Brasília, 2018.  
141 p.

Dissertação (Mestrado - Mestrado em Ciências  
Farmacêuticas) -- Universidade de Brasília, 2018.

1. GPCR. 2. receptores de ácidos graxos. 3.  
diindolilmetano. 4. uracil. 5. adipogênese. I. Simeoni,  
Luiz Alberto, orient. II. Thimm, Dominik, co-orient. III.  
Título.

Gleice Rocha Ferreira Borges

ATIVIDADE DE DERIVADOS DE DIINDOLILMETANO E DE URACIL EM RECEPTORES DE ÁCIDOS GRAXOS 1 E 4 (FFAR1 E FFAR4)

Dissertação apresentada ao Programa de Pós-Graduação em Ciências Farmacêuticas, Faculdade de Ciências da Saúde, Universidade de Brasília, como requisito parcial à obtenção do título de Mestre em Ciências Farmacêuticas.

Aprovada em 09 de março de 2018.

**Banca Examinadora**

---

Prof. Dr. Luiz Alberto Simeoni - Universidade de Brasília (Presidente)

---

Profa. Dra. Angélica Amorim Amato - Universidade de Brasília

---

Prof. Dr. Carlos Frederico de Souza Castro - Instituto Federal Goiano

---

Dra. Mariella Guimarães Lacerda - Universidade de Brasília (Suplente)

*À minha mãe Amparo;  
porque antes mesmo que eu acreditasse, você acreditou em mim.*

## ACKNOWLEDGMENTS

Primeiramente eu gostaria de agradecer à CAPES pelo fornecimento das bolsas de intercâmbio acadêmico do Ciências sem Fronteiras e de mestrado, as quais permitiram que este trabalho fosse realizado.

Ao meu orientador Prof. Simeoni. Muito obrigada por ter me dado a oportunidade de fazer pesquisa e ser orientada por você desde o PIBIC! Obrigada por ter aceitado esse projeto, por todas as discussões que tivemos, pelo seu carinho e por sua eterna paciência comigo.

Dominik, thank you so much for accepting me under your supervision. Thanks for your huge patience at teaching me while I was at AK Müller. I will not forget all the nice and funny moments we had together in the lab.

Prof. Christa Müller, many thanks for giving me the opportunity to work in a high-level research group as yours. The experience I had while working in your group was extremely important for my personal and professional development.

Obrigada Prof. Francisco por ter aceitado esse projeto e por todas as considerações e discussões sobre o meu trabalho!

A todos os professores do Farmol: Angélica, Adriana, Carine, Djane, Enrique, Fátima, Guilherme, Marie, Marília, Michella. Obrigada por fazerem parte da minha formação e pelas ricas discussões que tivemos no Farmol.

Carol Lourenço, obrigada por existir! Você é um dos meus maiores exemplos de excelência, tanto no nível pessoal quanto no profissional. Eu te admiro muito! Obrigada por compartilhar um pouco da sua experiência em RT-qPCR comigo!

Cíntia, obrigada por ter me ajudado com todos os reagentes e materiais que eu precisei durante o mestrado. Obrigada pela sua companhia no laboratório, por todas

às idas ao RU e ao Mendes e por todos os bons (e maus) momentos que passamos juntas. Pode não parecer, mas eu gosto muito de você!

Henrique, esse mestrado não seria o mesmo sem você. Você me ensinou muito sobre pesquisa e sobre como ser uma boa pesquisadora! Obrigada por me ajudar desde o planejamento até a análise dos experimentos. Obrigada por me fazer rir, por me escutar, por tudo que compartilhamos, e pela sua preciosa amizade!

Mariella, muito obrigada por você ser exatamente como é! Eu admiro muito o seu amor pela pesquisa, o seu conhecimento e sua didática ao ensinar os outros! Obrigada por eu ter sido muitas vezes uma dessas pessoas.

A todas as Angelicats, especialmente à Bruna, Carol e Fefê que me ajudaram tanto com as minhas infindáveis dúvidas sobre adipogênese. Obrigada pelas conversas, risadas, paciência e pelo carinho de vocês!

Luizetes Anyk, Isadora, Simone, Yuri, obrigada fazerem nosso grupo de pesquisa o mais lindo e especial!

Ao grupo Cromatina. Bel, Camyla, Kaian, obrigada pelos risos de nervoso e pelos de felicidade também. Kaian, muito obrigada por me ajudar com a parte molecular da coisa.

À todo o grupo da Prof. Fátima, mas, especialmente à Laíza por ter gentilmente me ajudado com o ensaio de gene repórter.

Rilva, muito obrigada por ter tirado tempo pra me ensinar e me ajudar com todas as minhas dúvidas desde que entrei no Farmol. Eu aprendi muito com você e agradeço pelo seu trabalho no laboratório!

Ao trabalho do Luciano e de todos os estagiários do Farmol. Vocês são muito importantes para o andamento do laboratório!

Yessica, Sazan, Muhammad, Isaac thank you for the happy moments in the lab! Thank you for helping me with all my doubts about assays and techniques while I was in Bonn. Moreover, thank you for always motivating me!

Pietro, muito obrigada por me dar todo o carinho e suporte que eu precisei durante esse período e por me motivar a ser melhor todos os dias. Eu sou muito agradecida pela sua ajuda nas análises dos meus resultados e por sempre ter paciência comigo. Obrigada por fazer parte do meu mundo!

Aos meus amigos (e vocês sabem quem são), eu amo vocês! Obrigada por sempre torcerem por mim!

À minha família. Sem vocês eu não chegaria aqui. Obrigada por sempre me ajudarem a progredir nos estudos e a me tornar quem eu sou. Eu espero poder orgulhar vocês! Eu amo muito vocês!!!

À Deus toda honra e glória, pelos séculos dos séculos. Amém.



## RESUMO EXTENDIDO

O diabetes *mellitus* tipo 2 (DM2) é um dos maiores problemas de saúde em todo o mundo e a sua prevalência tem crescido notavelmente (DAVIS et al., 2012). Essa doença, crônica e progressiva, caracteriza-se por hiperglicemia causada por produção insuficiente de insulina pelo pâncreas e por resistência à ação da insulina nos tecidos (FENG et al., 2012). O tratamento da DM2 tem como base melhorar o controle glicêmico e alguns medicamentos estão disponíveis atualmente porém, muitas vezes, associados com diversos efeitos adversos como ganho ponderal e hipoglicemia (sulfonilureias), desconforto gástrico (biguanidas) e aumento do risco de fraturas ósseas (tiazolidinadionas) (AHRÉN, 2009). Novos fármacos como os similares ao peptídeo análogo do glucagon 1 (GLP-1) e os inibidores da enzima dipeptidil peptidase 4 (DPPIV) têm se mostrado superiores visto que não causam hipoglicemia e tornam as células  $\beta$ -pancreáticas defeituosas mais sensíveis à glicose (DEFOSSA; WAGNER, 2014; FORTI, 2006).

O sucesso do GLP-1 é argumento para a busca de novos alvos de forma a melhorar a terapêutica (DEFOSSA; WAGNER, 2014). Neste contexto, os receptores de ácidos graxos têm emergido como alvos promissores uma vez que pesquisas recentes têm indicado o envolvimento destes receptores com a secreção de insulina apenas em presença de glicose, de maneira similar à ação do GLP-1, abolindo assim o risco de hipoglicemia iatrogênica (MANCINI; POITOUT, 2013). A ativação dos receptores também está ligada à diminuição da resistência à ação da insulina bem como a outros efeitos benéficos como diminuição da inflamação (LIN et al., 2011; OH; WALENTA, 2014). Sendo assim, os receptores de ácidos graxos 1 e 4 (FFAR1 e FFAR4) têm sido investigados como potenciais alvos farmacêuticos para o tratamento da doença. Alguns ligantes para estes receptores já foram descritos, mas até o momento nenhum obteve sucesso em todas as fases clínicas. Desta forma, faz-se necessário a busca por novos ligantes, norteados o desenvolvimento de novos fármacos (FENG et al., 2012).

Com objetivo de encontrar novos ligantes para os receptores em questão, primeiramente os genes FFAR1 e a isoforma curta do FFAR4 foram amplificados por meio de reação em cadeia da polimerase (PCR) e em seguida, purificados.

Utilizando enzimas de restrição e técnicas de DNA recombinante, o cDNA amplificado de cada receptor e de vetores apropriados foram clivados por enzimas de restrição e ligados por meio da enzima T4 ligase. Os plasmídeos formados foram amplificados por meio de transformação bacteriana e extraídos e purificados por reação do tipo Miniprep. A confirmação da correta clonagem deu-se por meio de sequenciamento pelo método Sanger. Para criar linhagens celulares que expressassem os receptores de forma estável, células de ovário de hamster chinês (CHO) e células de astrocitoma humano 1321N1 foram transfectadas com os plasmídeos pelo sistema Lipofectamine<sup>®</sup> 2000 (Invitrogen). Em seguida, as bibliotecas de derivados de diindolilmetano, uracil, alguns compostos de produtos naturais e comerciais foram testados para avaliação da atividade por meio do ensaio de recrutamento de  $\beta$ -arrestina (FFAR4) e por meio do ensaio de mobilização de cálcio (FFAR1). Para moléculas encontradas como ligantes dos receptores foram feitas curvas concentração-efeito e as potências foram calculadas em valor de EC<sub>50</sub> e IC<sub>50</sub>.

Desta forma, no total seis ligantes com atividade moderada foram encontrados. Para o receptor FFAR1, quatro derivados (Yazh 3, Yazh 4, Yazh 16, Yazh 357) puderam antagonizar o receptor, enquanto que o produto natural stemphol foi capaz de ativá-lo. Apenas a digitonina foi encontrada como um agonista do FFAR4. Por meio da avaliação da estrutura versus atividade dos compostos, foi visto que substitutos longos não foram bem tolerados na ponte de metileno. Igualmente apenas átomos altamente eletronegativos de flúor na posição 4 geraram atividade da molécula.

Com objetivo de avaliar o potencial adipogênico dos ligantes, células 3T3-L1 foram induzidas a diferenciarem-se com coquetel de indução (IBMX, insulina e dexametasona), e foram tratadas com veículo ou ligantes por 3 ou 10 dias. Em seguida, o RNA total foi coletado, extraído e purificado, e a expressão gênica foi avaliada pelo sistema Power SYBR<sup>®</sup> Green RNA-to-CT 1-Step (Applied Biosystems). Dos ligantes avaliados, Yazh 357 foi capaz de promover a diferenciação de preadipócitos. Células expostas a este ligante apresentaram uma alta na expressão do marcador adipocitário FABP4, do fator de transcrição PPAR- $\gamma$  e do receptor FFAR4 quando comparadas com o veículo DMSO. Além disto, esse

composto pode ser um agonista parcial de PPAR- $\gamma$ .

Entretanto, estudos complementares são necessários para confirmar o potencial adipogênico desse composto, além da investigação sobre o possível agonismo parcial em PPAR- $\gamma$ , buscando seu correto alvo celular durante o processo de diferenciação.

## RESUMO

BORGES, Gleice Rocha Ferreira. **Atividade de derivados de diindolilmetano e de uracil em receptores de ácidos graxos 1 e 4 (FFAR1 e FFAR4)**. Brasília, 2018. Dissertação (Mestrado em Ciências Farmacêuticas) - Faculdade de Ciências da Saúde, Universidade de Brasília, Brasília, 2018.

Doenças metabólicas como o diabetes tipo 2 têm crescido em prevalência em todo o mundo. Diversas alternativas farmacológicas têm sido usadas, porém com importantes efeitos adversos, como exemplo, a hipoglicemia. Os receptores de ácidos graxos 1 e 4 (FFAR1 e FFAR4) têm sido investigados como possíveis alvos para o tratamento de diabéticos, porém, até o momento, nenhum fármaco com alvo nestes receptores atingiu sucesso em todas as fases clínicas. Com objetivo de encontrar novos ligantes, diversos compostos foram testados para atividade agonista e antagonista nos receptores FFAR1 e FFAR4 em ensaios de recrutamento de  $\beta$ -arrestina e de mobilização de cálcio. Foram encontrados quatro antagonistas e um agonista com atividade moderada para o receptor FFAR1, e um agonista moderado para FFAR4. A análise de estrutura-atividade (SAR) dos derivados de diindolilmetano mostrou que substitutos longos não foram bem tolerados na ponte de metileno e apenas substitutos altamente eletronegativos de flúor foram tolerados na posição 4 de cada indol da molécula. Os ligantes foram também testados para a atividade adipogênica *in vitro*. Desses, apenas Yazh 357 mostrou um potencial adipogênico com aumento da expressão gênica de *Fabp4*, *Pparg* e *Ffar4* durante o processo de diferenciação. Estudos adicionais são necessários para esclarecer o possível alvo desse ligante no processo de maturação do adipócito.

Palavras-chave: diabetes, GPCR, receptores de ácidos graxos, diindolilmetano, uracil, SAR, adipogênese

## ABSTRACT

BORGES, Gleice Rocha Ferreira. **Activity of diindolylmethane and uracil derivatives at the free fatty acid receptors 1 and 4 (FFAR1 and FFAR4)**. Brasília, 2018. Dissertação (Mestrado em Ciências Farmacêuticas) - Faculdade de Ciências da Saúde, Universidade de Brasília, Brasília, 2018.

Metabolic diseases, like type 2 diabetes, are increasing in prevalence worldwide. Several pharmacologic alternatives have been used, however with side effects such as the hypoglycemia. The free fatty acids receptor 1 and 4 (FFAR1 and FFAR4) have been investigated as possible alternatives for the treatment of these patients, but so far none medicine targeting these receptors could reach success in all the clinical trials. Aiming to find new ligands, many compounds were tested for agonist and antagonist activity at FFAR1 and FFAR4 using  $\beta$ -arrestin recruitment and calcium mobilization assays. Four antagonists and one agonist were found with moderate activity at FFAR1, while for FFAR4 one moderate agonist was found. The structure activity relationship (SAR) of diindolylmethane derivatives showed that long substitutes were not well tolerated in the methylene bridge, and only the highly electronegative substitute fluorine was tolerated at position 4 of each distal aromatic system of the molecule. The ligands were also tested for their adipogenic activity *in vitro*. Only Yazh 357 showed an adipogenic potential, increasing the gene expression of *Fabp4*, *Pparg* e *Ffar4* during the differentiation process. Additional studies are necessary to clarify the possible target of this ligand in the process of adipocyte maturation.

Keywords: diabetes, GPCR, free fatty acid receptors, diindolylmethane, uracil, SAR, adipogenesis

## LIST OF FIGURES

- Figure 1. Basic structure of a GPCR
- Figure 2. The role of FFAR1 in insulin release
- Figure 3. The physiological role of FFAR4 in adipocyte and macrophage.
- Figure 4. Agarose gel electrophoresis after amplification of human FFAR1.
- Figure 5. Agarose gel electrophoresis after Nested PCR of human FFAR1.
- Figure 6. Agarose gel electrophoresis after amplification of human FFAR4short.
- Figure 7.  $\beta$ -arrestin recruitment assays at human FFAR1, performed with commercially and an adapted detection reagent.
- Figure 8.  $\beta$ -arrestin recruitment assays at human FFAR4s, performed with commercially and an adapted detection reagent.
- Figure 9.  $\beta$ -arrestin recruitment assays at human FFAR1 using monoclonal cell lines.
- Figure 10.  $\beta$ -arrestin recruitment assays at human FFAR4s using monoclonal cell lines.
- Figure 11.  $\beta$ -arrestin recruitment assays using monoclonal cell lines expressing human FFAR4s tagged with ProLink2-ARMS2.
- Figure 12.  $\beta$ -arrestin recruitment assay at human FFAR1, performed under different conditions
- Figure 13.  $\beta$ -arrestin recruitment assay at human FFAR4s, performed under different conditions
- Figure 14.  $\beta$ -arrestin recruitment assays at ProLink2-ARMS2-tagged human FFAR4s under standard and condition II.
- Figure 15.  $\beta$ -arrestin recruitment assays at human FFAR1 and FFAR4 using polyclonal CHO cell line.
- Figure 16.  $\beta$ -arrestin recruitment assays at ProLink2-ARMS1-tagged human FFAR4s performing under three different conditions.
- Figure 17. Dose-response curve of TUG-891 in  $\beta$ -arrestin recruitment assay performed with CHO cells expressing the human FFA4short receptor.
- Figure 18. Dose-response curves of TUG-424 in calcium mobilization assays performed with 1321N1 astrocytoma cells expressing the human FFA1

receptor.

- Figure 19. Dose-response curves of diindolylmethane derivatives (Yazh library) with antagonist activity at human FFAR1
- Figure 20. Structure-activity relationship of diindolylmethane derivatives for antagonist activity at human FFAR1
- Figure 21. Dose-response curve of stemphol at human FFAR1.
- Figure 22. Dose-response curve and structure of digitonin at human FFAR4s.
- Figure 23. Relative cell viability using MTT in 3T3-L1 cells.
- Figure 24. Relative cell viability using MTT in C3H/10T1/2 cells.
- Figure 25. Differentiation assay to adipocytes using Oil Red O staining.
- Figure 26. Relative mRNA expression of genes involved in adipogenesis on the third day of differentiation.
- Figure 27. Relative mRNA expression of genes involved in adipogenesis on the tenth day of differentiation.
- Figure 28. Activity of Yazh 357 at human PPAR- $\gamma$ .

## LIST OF TABLES

- Table 1. Main agonists of human FFAR1.
- Table 2. Antagonists of human FFAR1.
- Table 3. Principal agonists of human FFAR4.
- Table 4. Antagonist of human FFAR4.
- Table 5. Potency of diindolylmethane derivatives (Yazh library) at the human FFAR1 and FFAR4.
- Table 6. Potency of uracil derivatives (Yazh library) at the human FFAR1 and FFAR4.
- Table 7. Potency of AK König and AK Piel library compounds at the human FFAR1 and FFAR4s.



## LIST OF ABBREVIATIONS

[Ca <sup>2+</sup> ]	calcium concentration
7-TM	7-transmembrane
ALA	$\alpha$ -linolenic acid
ATP	adenosine triphosphate
C/EBP	CCAAT-enhancer-binding protein
cAMP	cyclic adenosine monophosphate
CB <sub>1</sub>	cannabinoid type 1 receptor
CCK	cholecystokinin
cDNA	complementary DNA
CHO	chinese hamster ovarian cells
COX-2	prostaglandin-endoperoxide synthase 2
cPLA2	cytosolic phospholipase A
DAG	diacylglycerol
DHA	docosahexaenoic acid
DM2, T2DM	type 2 diabetes <i>mellitus</i>
DPPIV	dipeptidyl peptidase IV
EP4	prostaglandin E receptor 4
EPA	eicosapentaenoic acid
ERK	extracellular signal - related
FABP4, Fabp4	fatty acid binding protein 4
FAs	fatty acids
FFAR1	free fatty acids receptor 1
FFAR4	free fatty acids receptor 4
FFAR4s / FFAR4short	free fatty acids receptor 4 short isoform
FFAs	free fatty acids
gDNA	genomic DNA
GDP	guanosine diphosphate
GEF	guanine nucleotide exchange factor
GIP	glucose-dependent insulintropic polypeptide
GIRK	G protein-coupled inwardly-rectifying potassium
GLP-1	glucagon-like peptide-1
GLUT4	glucose transporter 4
GPCR	G protein-coupled receptor
GRK	G protein-coupled receptor kinase
GTP	guanosine triphosphate
HFD	high-fat diet
icv	intracerebroventricular injection
IP <sub>3</sub>	inositol-1,4,5-trisphosphate
IP <sub>3</sub> R	inositol-1,4,5-trisphosphate receptor
JNK	c - Jun N - terminal kinases
KO	knockout
LA	linoleic acid
LPC	lysophosphatidylcholine
MAPKs	mitogen - activated protein kinases
MDI	induction media

MTT	3-(4,5-dimethylthiazol-2-yl)-2,5-diphenyltetrazolium bromide
NFκB	factor nuclear kappa B
ORF	open reading frames
ORO	Oil Red O staining
PC	pooled cells
PCR	polymerase chain reaction
PDK1	protein-dependent kinase 1
PGE2	prostaglandin E2
PI3K	phosphatidylinositol-4,5-bisphosphate 3-kinase
PIP2	phosphatidylinositol-4,5-bisphosphate
PKA	protein kinase A
PLC	phospholipase C
PPAR-γ, Pparg	peroxisome proliferator- activated receptor-γ
PPRE	peroxisome proliferator-activated receptor response element
RLU	relative luminescence unit
RT-qPCR	reverse-transcription quantitative polymerase chain reaction
SAR	structure-activity relationship
TAB1	TAK1-binding protein 1
TAK1	TGF-β-activated kinase 1
TGI	gastrointestinal tract
TM	transmembrane α-helices
TNF-α	tumor necrosis factor-α
VDCCs	voltage-dependent calcium channel
VLP	virus-like particle
WAT	white adipose tissue

## CONTENTS

1. INTRODUCTION.....	21
1.1 G protein-coupled receptors (GPCRs).....	21
1.1.1 Structure.....	21
1.1.2 Classification.....	22
1.1.3 Signalling.....	23
1.2. Free fatty acid receptors (FFARs).....	25
1.2.1 GPR40/ FFAR1.....	25
1.2.1.1 Expression/Tissue distribution.....	26
1.2.1.2 Pharmacology.....	27
1.2.1.3 Ligands.....	28
1.2.1.4 Mutagenesis studies.....	35
1.2.1.5 (Patho) physiology.....	37
1.2.2. GPR120/FFAR4.....	400
1.2.2.1 Expression/Tissue distribution.....	40
1.2.2.2 Pharmacology.....	42
1.2.2.3 Ligands.....	43
1.2.2.4 Mutagenesis studies.....	47
1.2.2.5 (Patho) physiology.....	48
AIM OF THE WORK.....	500
2. MATERIALS AND METHODS.....	511
3. RESULTS AND DISCUSSION.....	800
Part 1. Screening of compound libraries at human FFAR1 and FFAR4 and SAR of ligands.....	800
3.1. Cloning of the human FFAR1 and FFAR4short receptors.....	800
3.2. Biological assays.....	833
3.3 Compound screening.....	97
Part 2. Adipogenic activity of ligands.....	118
3.4. Cell viability assay.....	118

3.5. Differentiation assay into adipocytes.....	1211
3.5.1 Oil Red O staining to validate the protocol for adipogenesis .....	1211
3.5.2 Gene expression during adipogenesis .....	1222
Perspectives.....	127
4. CONCLUSION .....	129
5. REFERENCES.....	130

## 1. INTRODUCTION

### 1.1 G protein-coupled receptors (GPCRs)

A particular molecule can produce physiological responses e.g. by binding and activating a receptor. This concept derives from the research of Paul Ehrlich and John Newport Langley from the beginning of the 20th century (MAEHLE, 2009). Up to now, identified receptors have been divided into four main classes: ion-channels, G protein-coupled receptors, tyrosin kinases and nuclear receptors (IUPHAR/BPS).

G protein-coupled receptors (GPCRs) are plasma membrane-localized glycoproteins that couple to heterotrimeric guanine nucleotide binding proteins (G proteins) (INSEL et al., 2012). Due to their conserved seven transmembrane helical domains, GPCRs are also known as 7-transmembrane (7-TM) receptors. They represent one of the largest gene families with approximately 800 G protein-coupled receptors genes in humans (BJARNADÓTTIR et al., 2006). With a wide variety of ligands and involved in diverse body functions, they are targets of about 30 % of the current drugs (INSEL et al., 2012; VASSILATIS et al., 2003; HOPKINS; GROOM, 2002). Therefore GPCRs are hot targets to investigate biological processes and diseases, leading to drug discovery (FILMORE, 2004).

#### 1.1.1 Structure

The characteristic structures of GPCRs are an extracellular N-terminus, followed by seven transmembrane  $\alpha$ -helices (TM1 - TM7) which are connected by three intracellular (C1 - C3) and three extracellular loops (E1 - E3), and an intracellular C-terminus (Figure 1). The  $\alpha$ -helices are composed of about 25 – 35 mostly hydrophobic amino acid residues that span the plasma membrane (SCHIÖTH; FREDRIKSSON, 2005).

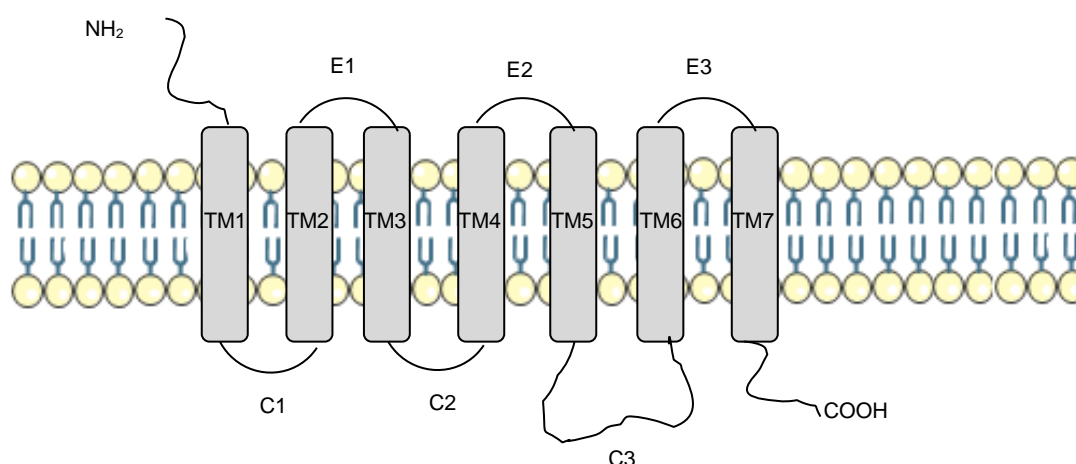


Figure 1. Basic structure of a GPCR.

### 1.1.2 Classification

There are several classification systems to sort this superfamily of receptors, either by how their ligand bind, or by their physiological and structural features. One of the most frequently used systems divides the receptors in classes A to F, and it is designed to cover all GPCRs in eukaryotes (ATTWOOD; FINDLAY, 1994). However, this classification was replaced by another recent classification system called GRAFS, which was designed after a phylogenetic analysis of GPCRs in humans (SCHIÖTH; FREDRIKSSON, 2005). In this system, GPCRs are divided based on sequence homology and functional similarity in five main families, i.e., glutamate (G), rhodopsin (R), adhesion (A), frizzled/taste2 (F), and secretin (S) (SCHIÖTH; FREDRIKSSON, 2005).

#### 1.1.2.1 Rhodopsin-like receptors (or class A)

Class A GPCRs is by far the group with most members, including the receptors for light (rhodopsin), purinergic, adrenergic and olfactory receptors (PIERCE; PREMONT; LEFKOWITZ, 2002). Therefore rhodopsin-like receptors have been implicated in a wide array of biological processes. Based on the GRAFS system this family can be subdivided into four groups  $\alpha$ ,  $\beta$ ,  $\gamma$  and  $\delta$  (SCHIÖTH; FREDRIKSSON, 2005) although other researchers suggest other ways of classification (PELÉ et al., 2011; JOOST; METHNER, 2002).

The rhodopsin-like characterization is based mainly on 25 conserved residues in TM regions (TRZASKOWSKI et al., 2012). A cysteine residue in N-terminus, the

DRY (ASP-ARG-TYR) motif in TM3, the TM6 CWxP (CYS-TRP-x-PRO) motif and the NPxxY (ASN-PRO-x-x-TYR) motif within TM7 have been found to be important conserved residues and motifs (TRZASKOWSKI et al., 2012; SCHIÖTH; FREDRIKSSON, 2005). Diverse types of ligands, such as photons, small molecules, and peptides, bind to the rhodopsin-like receptors despite the similarity and the phylogenetic relationship of this family (SCHIÖTH; FREDRIKSSON, 2005). The orthosteric binding site was found to be constituted by TM regions, extracellular loops and, less frequently, the N-terminal region (TRZASKOWSKI et al., 2012), while effectors can interact with the intracellular loops and the C-terminus domain (TUTEJA, 2009).

### 1.1.3 Signalling

Regarding signalling, a substance can be named according to the response produced at a receptor. The concept of agonist refers to the ligand which binds to a receptor, resulting in a biological response similar to the endogenous ligand. A full agonist reaches the maximum receptor signal (i.e., highest efficacy) while a partial agonist does not cause a comparably high effect under same conditions (KATZUNG, 2014). On the other hand, inverse agonists produce opposite effect of an agonist (GOODMAN; GILMAN, 2005). Alternatively, an antagonist binds to the receptor however without producing any effect itself and therefore no efficacy conditions (KATZUNG, 2014). It can also prevent or reduce the effect of agonists by blocking their binding to the receptor (KATZUNG, 2014). Antagonists can be divided into surmountable (competitive) and insurmountable (non-competitive). Competitive antagonists share the orthosteric site with an agonist, but increasing the concentration of the latter in the assay system can reverse the antagonism (KATZUNG, 2014). Partial agonists can also act as competitive antagonists in the presence of a full agonist, reducing the potency of the latter (KATZUNG, 2014). In contrast, an insurmountable antagonist binds strongly (covalently or allosterically) to the receptor, and even in the presence of an agonist, the inhibitory effect cannot be overcome (ATAK; LAVREYSEN, 2010).

When an agonist binds to the GPCR, a structural rearrangement in the TM helices orientation occurs (PIERCE; PREMONT; LEFKOWITZ, 2002). Due to this

rearrangement, the receptor acts as a guanine nucleotide exchange factor (GEF), mediated by amino acids residues of C2 and C3 along with adjacent residues of the associated TM helices (PIERCE; PREMONT; LEFKOWITZ, 2002). The exchange of guanosine diphosphate (GDP) for guanosine triphosphate (GTP) results in the activation of G proteins. The G protein's  $\alpha$  subunit, with the bound GTP, can then dissociate from the  $\beta\gamma$  subunits to activate target functional proteins (WETTSCHURECK; OFFERMANN, 2005).

#### 1.1.3.1 $G\alpha_s$ signalling

In this pathway, the dissociated  $G\alpha_s$  subunit binds to and activates adenylate cyclase, which catalyzes the conversion of adenosine triphosphate (ATP) into cyclic adenosine monophosphate (cAMP), thus increasing cAMP levels. The cAMP can activate the protein kinase A (PKA), which has two regulatory and two catalytic subunits. To activate PKA, two cAMP molecules bind to each of the two regulatory subunits, detaching them, and thus exposing the two activated catalytic subunits. The activated PKA can then activate further effectors by phosphorylation (PIERCE; PREMONT; LEFKOWITZ, 2002).

#### 1.1.3.2 $G\alpha_i$ signalling

Unlike  $G\alpha_s$ ,  $G\alpha_i$  protein inhibit the activity of adenylate cyclase, which decreases the production of cAMP from ATP. The result is a reduction of cAMP-dependent signalling.  $G\alpha_i$  signalling is also related to activation of G protein-coupled inwardly-rectifying potassium (GIRK) channels, which are involved in cell hyperpolarization (PIERCE; PREMONT; LEFKOWITZ, 2002).

#### 1.1.3.3 $G\alpha_{q/11}$ signalling

In the signalling involving the G proteins  $G\alpha_{q/11}$ , the  $\alpha$  subunit activates phospholipase C (PLC), which cleaves phosphatidylinositol-4,5-bisphosphate (PIP<sub>2</sub>) to produce inositol-1,4,5-trisphosphate (IP<sub>3</sub>) and diacylglycerol (DAG). DAG promotes the phosphorylation of protein-dependent kinase 1 (PDK1) leading to its activation. PDK1 then can phosphorylate and activate effector proteins, producing a physiological response (MANCINI; POITOUT, 2013). Another pathway is mediated by



IP<sub>3</sub>, which binds to its receptor (IP<sub>3</sub>R) on the endoplasmic reticulum, leading to an intracellular calcium release (SMRCKA et al., 1991).

#### 1.1.3.4 $\beta$ -arrestin signalling

To suppress the receptor activity, GPCRs can be phosphorylated by G protein-coupled receptor kinases (GRK) and thus proteins called arrestins can be recruited (SCHIÖTH; FREDRIKSSON, 2005). Arrestins are ubiquitously present in animal cells, and so far four subtypes have been discovered (1 to 4) (GUREVICH; GUREVICH, 2006).  $\beta$ -arrestins bind to the cytoplasm phosphorylated sites of GPCRs, blocking further interaction with G proteins and allowing the endocytose of the receptor. GPCRs can then either be degraded within the endosome or be recycled, returning to the cell membrane (PIERCE; PREMONT; LEFKOWITZ, 2002).

However, recent studies demonstrated that these proteins could also help transduce signals.  $\beta$ -arrestins have been investigated as a scaffold molecules for effector proteins in the mitogen-activated protein kinases (MAPKs) signalling, such as for extracellular signal-related (ERK) and c - Jun N - terminal kinases (JNK) (DEWIRE et al., 2007; MCDONALD et al., 2000). Upon the activation of a receptor,  $\beta$ -arrestins can form complexes with the stimulated receptor and kinases, generating the signal transduction (LEFKOWITZ; RAJAGOPAL; WHALEN, 2006).

## 1.2. Free fatty acid receptors (FFARs)

### 1.2.1 GPR40/ FFAR1

Free fatty acid receptor 1, previously known as G protein-coupled receptor 40 (GPR40), is a rhodopsin-like receptor (JOOST; METHNER, 2002). It was first described in 1997 by the analysis of open reading frames (ORF) in the 19q13.1 chromosome (SAWZDARGO et al., 1997). Six years later, the receptor was deorphanized and characterized and it was discovered to be activated by endogenous medium- and long-chain fatty acids (FAs), such as eicosapentaenoic acid (EPA), docosahexaenoic acid (DHA), and linoleic acid (LA) (BRISCOE et al., 2003; ITOH et al., 2003). Since then FFAR1 has been associated with the glucose-dependent insulin secretion and has been studied as a potential target for the treatment of type 2 diabetes *mellitus* (T2DM).

### 1.2.1.1 Expression/Tissue distribution

#### 1.2.1.1.1 Rat (*Rattus norvegicus*)

Performing reverse-transcription quantitative polymerase chain reaction (RT-qPCR) it has been found that *Ffar1* mRNA is almost exclusively expressed in the pancreas, but also low expressed in the gastrointestinal tract (TGI) (ITOH et al., 2003). In rat pancreatic islets, *Ffar1* mRNA levels were found to be approximately 17-fold higher than the levels in the pancreas as a whole, suggesting selective expression in pancreatic islets (ITOH et al., 2003). The expression of this receptor in pancreatic  $\beta$ -cells has also been confirmed by *in situ* hybridization (BRISCOE et al., 2003; ITOH et al., 2003).

#### 1.2.1.1.2 Mouse (*Mus musculus*)

*Ffar1* has been found highly expressed in mice pancreatic islets when performing *in situ* hybridization (STENEBERG et al., 2005; EDFALK; STENEBERG; EDLUND, 2008). The receptor was also found expressed in pancreatic islet  $\alpha$ -cells by immunohistochemistry and RT-qPCR, and it could be involved in glucagon synthesis and secretion (FENG et al., 2006; FLODGREN et al., 2007). Applying X-gal staining and *in situ* hybridization, EDFALK; STENEBERG; EDLUND (2008) showed the expression also in enteroendocrine cells, implying that the activation of the receptor could lead to secretion of incretin hormones. Additionally, *Ffar1* expression was shown in the spleen, bone marrow, testis and lung (REGARD; SATO; COUGHLIN, 2008).

#### 1.2.1.1.3 Human (*Homo sapiens*)

In comparison to rat and mouse, *FFAR1* has been found to be expressed in more tissues in human until now. Like in rodents, *FFAR1* was found to be particularly expressed in pancreatic islets when performing RT-qPCR (BRISCOE et al., 2003). The receptor was also notably expressed in the brain (especially in the medulla oblongata and substantia nigra) (BRISCOE et al., 2003). Additionally, low expression was found in monocytes and TGI.

## 1.2.1.2 Pharmacology

### 1.2.1.2.1 Signalling pathway of FFAR1

FFAR1 is mainly coupled to  $G\alpha_{q/11}$ , but it has  $G\alpha_s$  as secondary transduction mechanism (FENG et al., 2006; HARDY et al., 2005; ITOH et al., 2003). Increases in cytoplasmic  $[Ca^{2+}]$  by activation of the receptor promote insulin release, which further leads to lowering of blood glucose levels (Figure 2). Also, PLC activation leads to cytoplasmic increase of DAG, which can further cause remodeling of actin filaments. This remodeling in pancreatic  $\beta$ -cells moreover stimulates insulin secretion. Interestingly, the FFAR1 insulinotropic effects occur in a glucose-dependent manner, reducing the risk of hypoglycemia (DEFOSSA; WAGNER, 2014).

As secondary transduction mechanism, FENG et al. (2006) demonstrated the involvement of cAMP in insulin release by reduction of the voltage-gated  $K^+$  current induced by the FFAR1 agonist linoleic acid. The activated PKA may phosphorylate the  $\alpha_{11.2}$ -subunit of voltage-dependent calcium channel (VDCCs) enhancing  $[Ca^{2+}]$  influx and boosting insulin granule exocytosis (AMMÄLÄ; ASHCROFT; RORSMAN, 1993; FLOCK et al., 2015; LEISER; FLEISCHER, 1996).

Connected to the activation of the FFAR1 in enteroendocrine cells, several studies focused on what may contribute to secrete the incretin hormones glucagon-like peptide 1 (GLP-1) and glucose-dependent insulinotropic polypeptide (GIP) (Figure 2) (EDFALK; STENEBERG; EDLUND, 2008; LUO et al., 2012). These hormones can increase the cAMP concentration within the pancreatic  $\beta$ -cells, allowing the insulin release and further reduction of plasma glucose (LUO et al., 2012).

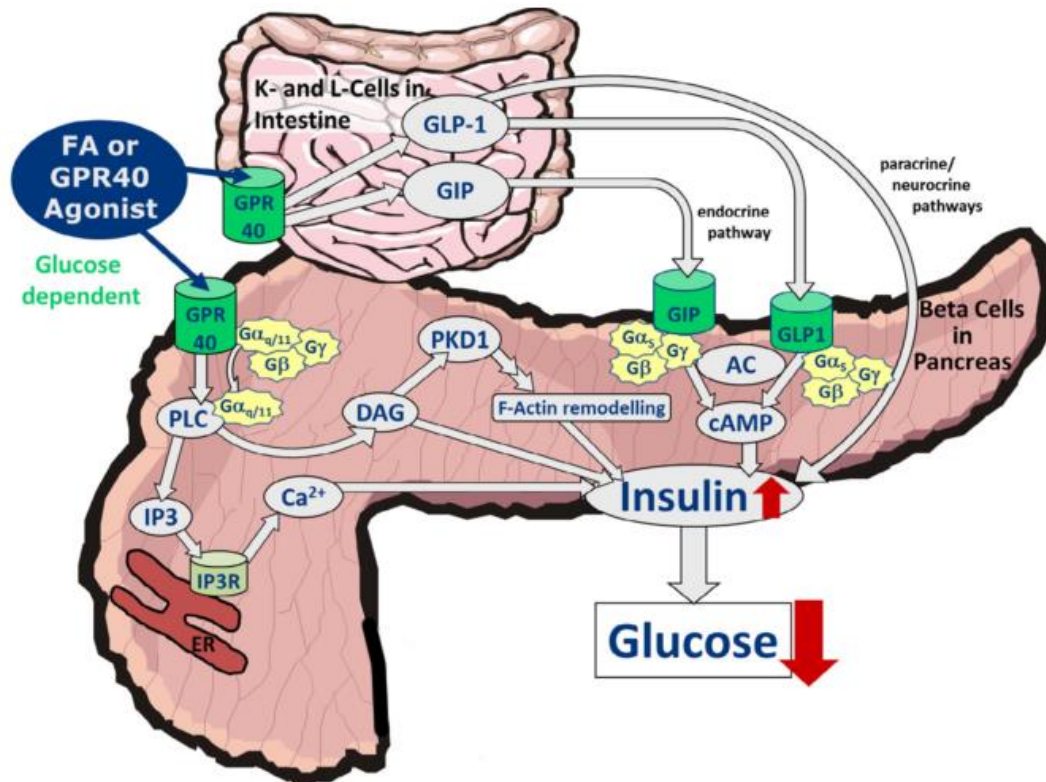


Figure 2. The role of FFAR1 in insulin release. The figure is taken and adapted from DEFOSSA; WAGNER (2014).

To date, the information about  $G\alpha_s$  and  $\beta$ -arrestin recruitment signalling through FFAR1 is still scarce (MANCINI; POITOUT, 2013). For some compounds as TAK-875 a biased agonism could be observed for FFAR1; in which its signalling occurs preferably through  $G\alpha_{q/11}$  rather than through  $\beta$ -arrestin recruitment (MANCINI et al., 2015).

Signalling through mitogen-activated protein kinase (MAPK) and activation of ERK1/2 induced by long-chain FFAs was shown to occur (ITOH et al., 2003; QIAN et al., 2017). Considering that MAPK activation plays a role in cellular proliferation and differentiation, the mechanism through which FFAR1 may be related not only to insulin secretion but to other cellular processes (ITOH et al., 2003).

### 1.2.1.3 Ligands

Nowadays, several ligands for FFAR1 were found. BRISCOE et al. (2003) identified for the first time that this receptor could be endogenously activated by

medium- to long-chain fatty acids, which was confirmed by further works (KOTARSKY et al., 2003a; ITOH et al., 2003). Besides, the FFAR1 dual mechanisms of blood glucose lowering with reduced risk of hypoglycemia have encouraged the search for new medicines for type 2 diabetes. Therefore a crescent number of compounds have been discovered and synthesized, and the so far discovered agonists at FFAR1 are shown in Table 1. Among them, the synthetic CNX-011-67 is the agonist with the highest potency, while for FFAs DHA was shown to be the most potent at FFAR1. Interestingly, Faslifam (TAK-875) was found to be an effective drug against type 2 diabetes. The drug, developed by Takeda Ltd, reached the phase III clinical trials but its development was interrupted due to hepatotoxicity by inhibition of hepatobiliary transporters (Li X, et al. 2015). Together with other structures, analogs of TAK-875 have been tested, and several of them are active in pre- and clinical trials (LI et al., 2016a).

**Table1. Main agonists of human FFAR1**

(Table to be continued)

Ligand	Structure	Potency EC <sub>50</sub> ( $\mu$ M)	Type	Reference
CNX-011-67		0.00024 <sup>a</sup>	Agonist	(GOWDA et al., 2013)
Compound 5		0.0012 <sup>a</sup>	Agonist	(AGARWAL et al., 2016)
Compound 28a		0.0013 <sup>a</sup>	Full agonist	(LU et al., 2013)
DS-1558		0.004 <sup>a</sup>	Agonist	(TAKANO et al., 2015)
TUG-770		0.006 <sup>a</sup>	Full agonist	(CHRISTIAN SEN et al., 2013)
LY2922470		0.007 <sup>b</sup>	Full agonist	(HAMDOUCH I et al., 2016)
AMG-837		0.013 <sup>a</sup>	Partial agonist	(LIN et al., 2011)

(Table continued)

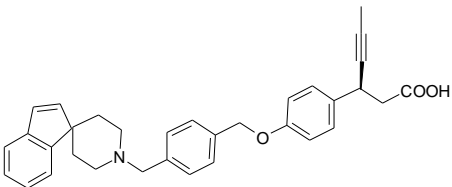
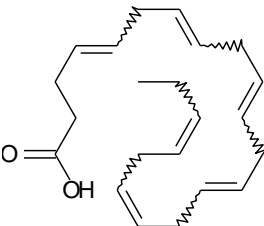
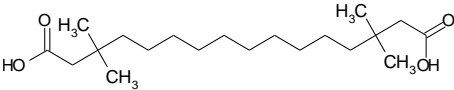
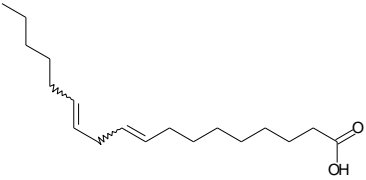
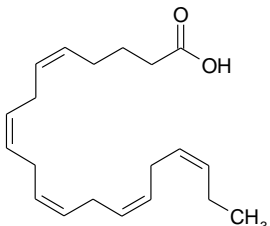
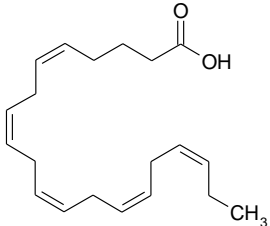
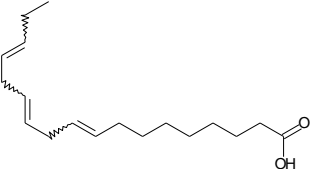
Ligand	Structure	Potency EC <sub>50</sub> ( $\mu$ M)	Type	Reference
Fasiglifam (TAK-875)		0.014 <sup>a</sup>	Partial agonist	(NEGORO et al., 2010)
11k		0.016 <sup>a</sup>	Full agonist	(YANG et al., 2016)
TUG-469		0.019 <sup>a</sup>	Full agonist	(Christiansen, E. et al. 2010)
TUG-424		0.032 <sup>a</sup>	Full agonist	(CHRISTIAN SEN et al., 2008)
Compound 11		0.035 <sup>a</sup>	Agonist	(LI et al., 2016b)
MR1704		0.035 <sup>a</sup>	Partial agonist	(TSUDA et al., 2017)
GW9508		0.047 <sup>a</sup>	Partial agonist	(BRISCOE et al., 2006)
Yhhu4488		0.05 <sup>a</sup>	Full agonist	(GUO et al., 2015)

(Table continued)

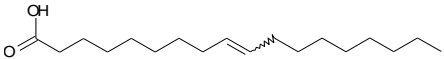
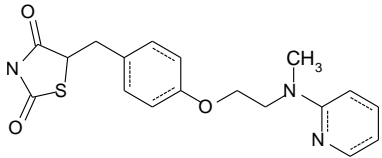
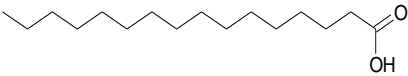
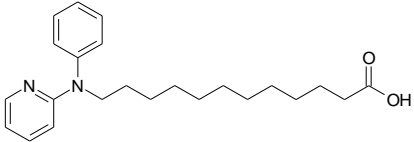
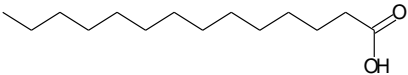
Ligand	Structure	Potency EC <sub>50</sub> ( $\mu$ M)	Type	Reference
Compound 18b		0.062 <sup>a</sup>	Agonist	(WANG et al., 2015)
Compound 7		0.071 <sup>a</sup>	Agonist	(WALSH et al., 2011)
AM-5262		0.081 <sup>c</sup>	Full agonist	(WANG et al., 2013)
(R)-7k		0.081 <sup>a</sup>	Full agonist	(LI et al., 2017)
Compound B		0.088 <sup>a</sup>	Full agonist	(TAN et al., 2008)
AM-6226		0.13 <sup>c</sup>	Full agonist	(LUO et al., 2012)
AMG-1638		0.16 <sup>c</sup>	Full agonist	(LUO et al., 2012)



(Table continued)

Ligand	Structure	Potency EC <sub>50</sub> ( $\mu$ M)	Type	Reference
LY2881835		0.23 <sup>a</sup>	Full agonist	(HAMDOUCH I et al., 2016; HAMDOUCH; LINESWALA; MAITI, 2011)
Docosahexanoic acid (DHA)		1.1 - 4.3 <sup>a</sup>	Full agonist	(BRISCOE et al., 2003)
Medica 16		1.22 <sup>d</sup>	Full agonist	(KOTARSKY et al., 2003)
Linoleic acid (LA)		1.8 - 39.8 <sup>a,d</sup>	Full agonist	(BRISCOE et al., 2003; ITOH et al., 2003; KOTARSKY et al., 2003)
cis-5,8,11,14,17-eicosapentaenoic acid		1.86 <sup>a</sup>	Full agonist	(BRISCOE et al., 2006)
cis-5,8,11,14,17-eicosapentaenoic acid		1.86 <sup>a</sup>	Full agonist	(BRISCOE et al., 2006)
$\alpha$ -linolenic acid		2.0 - 25.1 <sup>a,d</sup>	Full agonist	(ITOH et al., 2003; KOTARSKY et al., 2003)

(Table concluded)

Ligand	Structure	Potency EC <sub>50</sub> ( $\mu$ M)	Type	Reference
Oleic acid		2.0 - 126.0 a,d	Full agonist	(BRISCOE et al., 2003; ITOH et al., 2003; KOTARSKY et al., 2003)
Rosiglitazone		2.8 <sup>d</sup>	Full agonist	(KOTARSKY et al., 2003)
Palmitic acid		5.01 - 158.0 <sup>a</sup>	Full agonist	(BRISCOE et al., 2003; ITOH et al., 2003; KOTARSKY et al., 2003)
NCG75		5.11 <sup>a</sup>	Full agonist	(TAKEUCHI et al., 2013)
Myristic acid		7.7 - 31.6 a,d	Full agonist	(BRISCOE et al., 2003; ITOH et al., 2003; KOTARSKY et al., 2003)

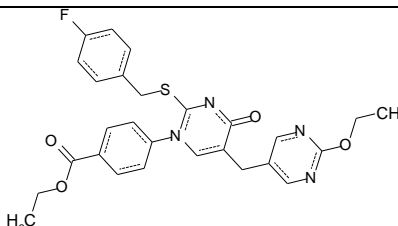
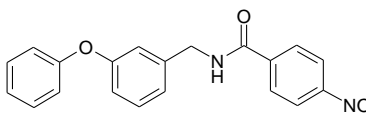
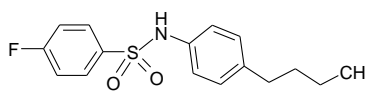
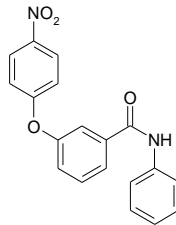
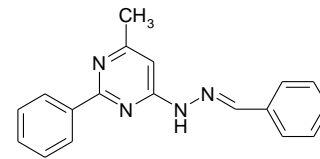
<sup>a</sup> Determined in calcium mobilization assay; <sup>b</sup>  $\beta$ -arrestin recruitment assay; <sup>c</sup> aequorin calcium assay;

<sup>d</sup> HFF11 reporter assay.

Up to date, only a few molecules were found to antagonize the FFA1 receptor. GW1100, discovered by Briscoe et al. (2003), is the most potent antagonist of FFAR1. Although lowering insulin secretion, these molecules could be useful to investigate the function of the receptor and to lead the development of new drugs.

Additionally, SUN et al. (2013) showed that FFAR1 antagonist DC26126 could protect pancreatic  $\beta$ -cells of obese *db/db* mice from dysfunction and improve insulin sensitivity, suggesting a possible positive effect on FFAR1 inhibition. Antagonists are shown in Table 2.

**Table 2. Antagonists of FFAR1.**

Ligand	Structure	Inhibition IC <sub>50</sub> ( $\mu$ M)	Type	Reference
GW1100		0.977 <sup>a, 1</sup>	Non-competitive antagonist <sup>a</sup>	(BRISCOE et al., 2006)
Compound 8		2.8 <sup>c, 1</sup>	Pure antagonist <sup>c</sup>	(TIKHONOV A et al., 2008)
DC260126		4.6 – 7.0 <sup>b, 1</sup>	Competitive antagonist <sup>b</sup>	(HU et al., 2009)
Compound 20		5.3 <sup>c, 1</sup>	Pure antagonist <sup>c</sup>	(TIKHONOV A et al., 2008)
ANT203		Data not available <sup>1</sup>	Competitive antagonist <sup>d</sup>	(KRISTINSS ON et al., 2013)

<sup>1</sup> Determined in calcium mobilization assay. <sup>a</sup> When tested against 10  $\mu$ M of agonist LA and 1  $\mu$ M of agonist GW9508. <sup>b</sup> Tested against 5  $\mu$ M of agonist LA, 5  $\mu$ M of oleic acid, 3  $\mu$ M of palmitoleic acid and 4  $\mu$ M of lauric acid. <sup>c</sup> Tested against 10  $\mu$ M of LA and 0.1  $\mu$ M of GW9508. <sup>d</sup> Tested against elaidic acid.

#### 1.2.1.4 Mutagenesis studies

An interesting approach of the mutagenesis is to investigate the role of a specific amino acid of a receptor sequence and its involvement in the receptor ligand

binding. In this way, it is possible to study the structure-activity relationship of ligands in a particular receptor.

TIKHONOVA et al. (2007) demonstrated for the first time the amino acid residues directly associated with the binding of FFAR1 receptor and ligands. Using computational binding predictions followed by mutagenesis studies the group showed that H137, R183, N244, and R258 are important residues for the interaction with the synthetic agonist GW9508. Likewise, mutations at R183 and R258 impair the activation of the receptor when tested with synthetic agonists such as AM837 (LIN et al., 2012). Mutations at H137 to alanine or phenylalanine decreases the potency of this ligand, as well as the alterations R183A, R258A, and N244A. Interestingly the mutant R258L could restore the potency partially, indicating the presence of hydrogen bonds or electrostatic interactions in the binding mechanism. Also, the examination of the conserved residue histidine at position 137 demonstrated that changes in this position resulted in potency decreasing of GW9508, but not of linoleic acid (SUM et al., 2007; TIKHONOVA et al., 2007). Additionally, the interaction between H137 and GW9508 seems to be a NH- $\pi$  interaction, which plays a role in the stability of the molecule in the binding pocket and allows the contact with other relevant residues such as Y91 (LU et al., 2011).

Subsequent mutagenesis studies based on amino acids located in the binding pocket suggested that Y12, Y91, and L186 are essential residues for receptor activation since mutations on them headed to loss of function of the receptor and alterations in the ligand binding (SUM et al., 2007). Although the agonists GW9508 and linoleic acid share similar amino acids when binding to FFAR1, GW9508 seems to have stronger interactions, which could explain the higher potency of this ligand.

Considering this knowledge and using virtual screening, some new ligands for the receptor were discovered (TIKHONOVA et al., 2008), both agonists and antagonists. Interestingly, some ligands were also shown to interact with other residues in the binding pocket such as H86, and even slight changes on them could alter pharmacological parameters as efficacy and potency of the test compounds.

Futhermore, HIROZANE et al. (2014) analysed a four-point FFAR1 mutant (L42A/F88A/G103A/Y202F) and the binding of the FFAR1 agonist fasiglifam, by combining a size-exclusion chromatography/liquid chromatography mass

spectroscopy (SEC/LC-MS)-based binding assay with transient overexpression in mammalian virus-like particles (VLP). The combination could ensure the thermostability of the receptor and with no requirement of a radiolabeled ligand. The mutant had lower signalling after activation by fasiglifam, but alterations in the binding affinity were not observed, establishing this protocol suitable to identify thermostabilized mutant GPCRs optimized for particular ligands.

Recently, a *Ffar1*<sup>R258W/R258W</sup> mouse model was engineered after the analysis of missense mutations in the extracellular protein domain (SABRAUTZKI et al., 2017). In contrast to the wild type, the primary culture of mutant islets showed an impairment in insulin secretion in the presence of palmitate (50  $\mu$ M) and TUG-469 (3  $\mu$ M). Also, no significant differences were seen for insulin content and gene expression of *Ffar1*, *Glp1r*, *Ins2*, and *Ppard* between the groups. Interestingly, a high-fat diet (HFD) could induce glucose intolerance in wild-type but not in the mutant mice. Therefore, this point mutation could abolish insulin secretion without causing glucose intolerance in mice.

#### 1.2.1.5 (Patho) physiology

##### 1.2.1.5.1 Rodents

Since its discovery, FFAR1 has been mainly associated with the glucose metabolism when activated by free fatty acids endogenously. According to STENEBERG et al. (2005), the overexpression of FFAR1 in mouse pancreatic  $\beta$ -cells was associated with impaired  $\beta$ -cell function and hypoinsulinemia. In contrast, the FFAR1 knockout  $\beta$ -cells showed a decrease in insulin secretion; and animals lacking the receptor were less susceptible to obesity-induced hyperinsulinemia, hyperglycemia, glucose intolerance, lipids disorder and hepatic steatosis, even in high FFAs feeding (STENEBERG et al., 2005). LATOUR et al. (2007) confirmed that islets from FFAR1-KO animals exhibited impairment in insulin secretion after FFAs chronic exposure. However, the exact FFAR1 physiology remains controversial. In contradiction to prior findings, LATOUR et al. (2007) showed that a FFAR1 knockout leads to significant glucose intolerance in animals on a normal chow diet. Also, LAN et al. (2008) demonstrated that both wild-type and FFAR1<sup>-/-</sup> mice had the same weight, bad lipid profile, and hyperinsulinemia when submitted to HFD.

Differential expression of the protein in pancreatic  $\alpha$ -cells was also investigated. Overexpression of FFAR1 in glucagon-secreting cell line could promote the FFA-induced glucagon production (FLODGREN et al., 2007). FFAR1-null mice secrete less glucagon than the wild type in response to raised levels of circulating FAs (LAN et al., 2008). The incretin response was also found to be reduced in knockout animals (EDFALK; STENEBERG; EDLUND, 2008).

In accordance with its expression in brain, FFAR1 may be involved in pain modulation in mice. A FFAR1-deficient mouse model exhibited exacerbated incision-induced mechanical allodynia in comparison to a wild-type mouse. Accordingly, chronic treatment with GW1100 could increase allodynia and reduce the pain threshold in mice; and high levels of long-chain FFAs were detected two days after the injury in the hypothalamus, a known nociceptive modulator (NAKAMOTO et al., 2012, 2017). The FFAR1 knockout has also been found to cause abnormal behavior in mice. FFAR1<sup>-/-</sup> female mice showed higher offspring negligence and infanticide when compared to wild-type female mice. Those animals exhibited anxiety- and depression-related behavior, which could be explained by a misbalance in noradrenaline in the brain (AIZAWA et al., 2016; NAKAMOTO et al., 2017).

#### 1.2.1.5.2 Human

Increasing evidence reveals that FFAR1 is involved in cancer cell genesis, progression, and migration. In pancreatic cancer cells, the expression of *FFAR1* could reduce cell migration and its knock-down increased the cell tumorigenicity (FUKUSHIMA et al., 2015). Accordingly, *FFAR1* expression and activation were related to a reduction in HT1080 fibrosarcoma and osteosarcoma motile and invasive activities (ISHII et al., 2016; TAKAHASHI et al., 2017). However, in melanoma cells, the activation of the receptor could promote the cell motility when they were treated with 12-O-tetradecanoylphorbol-13-acetate (TPA), a known carcinogen (FUKUSHIMA et al., 2016). Treatment with TPA enhanced the expression of FFAR1 in melanoma cells, likewise the treatment of liver epithelial cells with the tumor-promoting agent ethionine (ISHII et al., 2015a). Nevertheless, the inhibition of the receptor with GW1100 increased the motility of these cells, while in lung cancer cell lines the reduced FFAR1 expression or inhibition decreased the cell tumorigenicity (KITA et al.,

2016). HOPKINS et al. (2016) showed that FFAR1 regulates negatively the proliferation of breast cancer lines MCF-7 and MDA-MB-231. However, a previous study shows that FFAR1 overexpression and activation by oleate amplified the proliferation of MCF-7, MDA-MB-231, and T47D, while FFAR1 knock-down decreased it (HARDY et al., 2005). The receptor was also found highly expressed in serous ovarian carcinomas, and its inhibition could reduce cell energy metabolism, therefore reducing the viability of cancer cells (MUNKARAH et al., 2016). These findings suggest that FFAR1 has differential roles in cancer cells, being pro- or anti-tumorigenic depending on tumor type.

### 1.2.2. GPR120/FFAR4

Free fatty acids receptor 4 (FFAR4) is a G protein-coupled receptor, previously known as GPR120. It was first named by FREDRIKSSON et al. (2003) while performing large-scale GPCRs screening of the human genome. Besides, orthologues in several species were described in this study. Soon after, the receptor was orphanized, and its physiological role was suggested by HIRASAWA et al. (2005). Performing a large-scale screening, FFAR4 was found to be particularly activated by C<sub>14</sub> to C<sub>18</sub> saturated and C<sub>16</sub> to C<sub>22</sub> unsaturated FFAs, i.e., long chain free fatty acids. Its signalling through FFAs was able to increase GLP-1 release in mouse enteroendocrine cell line STC-1 and *in vivo* using C57BL/6 mice. Recently, the receptor was also connected to an anti-inflammatory function by inhibition of cytokine production in macrophages (LIU et al., 2014). Therefore this receptor has been investigated for its potential role in the treatment of diabetes and insulin resistance. Two isoforms (a long NM\_181745 and a shorter BC101175 variant) have been found for the human FFAR4, while only the shorter sequence has been reported for mice and rodents (MOORE et al., 2009).

#### 1.2.2.1 Expression/Tissue distribution

##### 1.2.2.1.1 Rat (*Rattus norvegicus*)

By performing RT-qPCR and Western blot, MATSUMURA et al. (2007) made a comparison between FFAR1 and FFAR4 expression in rodents. In contrast to FFAR1, *Ffar4* mRNA was detected in the lingual epithelium containing taste buds. The same research group demonstrated the expression of *Ffar4* in enteroendocrine cells of the colon via immunohistochemistry. Besides, the presence of *Ffar4* in the rat intestinal tract, especially in the colon was confirmed when applying RT-qPCR (TANAKA et al., 2008). This receptor was also found in rat spleen, lung, muscle, thalamus, and thymus (TANAKA et al., 2008).

##### 1.2.2.1.2 Mouse (*Mus musculus*)

The FFA4 receptor was demonstrated to be widely expressed among mice tissues. Real-time PCR showed high expression of *Ffar4* mRNA in lungs and TGI,



including rectum, colon, and cecum (HIRASAWA et al., 2005). The study also revealed medium expression in adrenal gland and low expression in thymus, ileum, and spleen. Using the same technique, another study showed the expression of the receptor in the TGI mucosa, with the highest expression in the colon (ITO et al., 2009). RT-qPCR has been performed in several studies confirming the receptor expression in MIN6 cells, isolated islets and glucose-dependent insulinotropic polypeptide - secreting K cells, which can be mainly found in the duodenum and proximal jejunum (CALANNA et al., 2013; KEBEDE et al., 2009; PARKER et al., 2009). As in rats, mouse *Ffar4* is distributed in taste cells, especially in type II taste cells. This expression profile has been identified via immunohistochemistry and double immunostaining. (CARTONI et al., 2010; MATSUMURA et al., 2009). GOTOH et al. (2007) reported high expression in mature adipocytes and medium expression in stromal vascular cells when performing semi-quantitative RT-PCR. The receptor was also found expressed in pituitary and kidney, as well in pro-inflammatory macrophages (D. OH et al., 2011; GOTOH et al., 2007). The distribution in adipose tissue as well as in large intestine and lung was also shown by immunohistochemistry (MIYAUCHI et al., 2009).

#### 1.2.2.1.3 Human (*Homo sapiens*)

HIRASAWA et al. (2005) investigated the expression of *FFAR4* using RT-qPCR and identified a high level of mRNA in the lung, mean expression in the intestinal tract, while in brain, thymus and adrenal gland a low expression of the protein was found. In the same study, *FFAR4* was detected in colonic intraepithelial neuroendocrine cells and GLP-1 positive cells via *in situ* hybridization. In the same manner, as in mice, the receptor mRNA could be detected in adipose tissue and gustatory epithelia (GALINDO et al., 2012; GOTOH et al., 2007). It has also been shown to be expressed in the stomach when performing expressed sequence tag (EST). (FREDRIKSSON et al., 2003). Expression in several human cell lines (breast cancer cell MDA-MB-231, breast adenocarcinoma MCF-7; osteoclast-like RAW264.7) was confirmed as well (CORNISH et al., 2008; NAVARRO-TITO; ROBLEDO; SALAZAR, 2008; SOTO-GUZMAN et al., 2008).

## 1.2.2.2 Pharmacology

### 1.2.2.2.1 Signalling of FFAR4

The main FFAR4 signalling pathway in adipocytes, gastrointestinal and taste bud cells is mediated by  $G\alpha_{q/11}$  proteins (ZHANG; LEUNG, 2014). The PLC activation in enteroendocrine cells causes an increase in intracellular  $[Ca^{2+}]$ , promoting the release of incretins (the insulinotropic GLP-1 and cholecystokinin, CCK), further lowering blood glucose levels (ZHANG; LEUNG, 2014). FFAR4 activation is also known to promote the translocation of glucose transporter 4 (GLUT4) by phosphatidylinositol-4,5-bisphosphate 3-kinase (PI3K) in adipocytes. GLUT4 is responsible for cellular glucose uptake, which in turn reduces the blood glucose (D. OH et al., 2011; LIU et al., 2012; ZHANG; LEUNG, 2014). Besides, PI3K and ERK1/2 phosphorylation resulted from  $G\alpha_{q/11}$  signalling leads to inhibition of apoptosis in mice intestinal STC-1 cells and prevent ghrelin secretion, possibly enhancing insulin secretion (GONG et al., 2014; KATSUMA et al., 2005; LU et al., 2012).

Furthermore, the receptor can also transduce a signal through recruitment of  $\beta$ -arrestin. In this case,  $\beta$ -arrestin2 signalling promotes the internalization of the FFAR4/ $\beta$ -arrestin2 complex (OH; WALENTA, 2014). Moreover, it binds to TAK1-binding protein 1 (TAB1); and this association blocks the binding of TAB1 to TGF- $\beta$ -activated kinase 1 (TAK1), resulting in inhibition of TAK1 phosphorylation and activation. The inactivation of TAK1 interrupts the inflammation in adipose tissue macrophages generated by cytokines and receptors that promote cytokine releases, such as tumor necrosis factor- $\alpha$  (TNF- $\alpha$ ) and toll-like receptor (OH; OLEFSKY, 2012; TAKAESU et al., 2003). The FFAR4/ $\beta$ -arrestin2 complex binds as well to the nucleotide-binding oligomerization leucine-rich repeat and pyrin domain-containing protein (NLRP)3/1b and inhibits the formation of interleukins 18 and 1 $\beta$  by caspase-1 (YAN et al., 2013). Furthermore FFAR4 can increase the concentration of prostaglandin E2 (PGE2) via stimulation of cytosolic phospholipase A (cPLA2) and prostaglandin-endoperoxide synthase 2 (COX-2). Therefore PGE2 blocks nuclear kappa B (NF $\kappa$ B) signalling by activating prostaglandin E receptor 4 (EP4), reducing inflammation (GAO et al., 2015; LIU et al., 2014; OH; WALENTA, 2014).

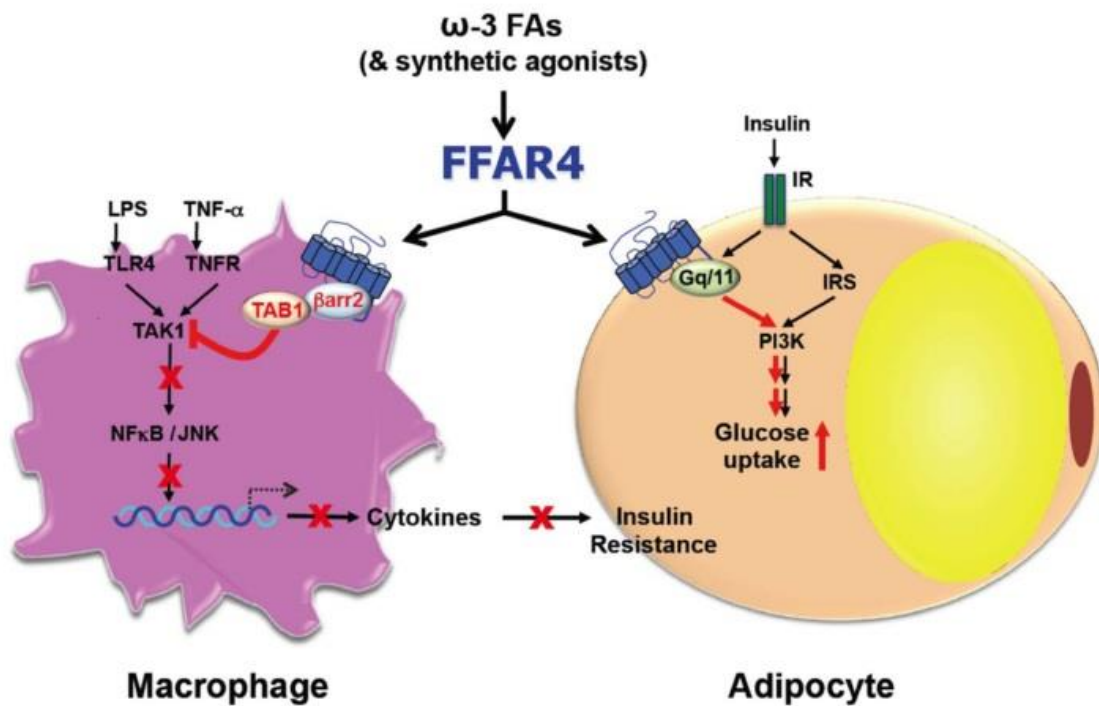


Figure 3. The physiological role of FFAR4 in adipocyte and macrophage. Adapted from OH; WALENTA (2014).

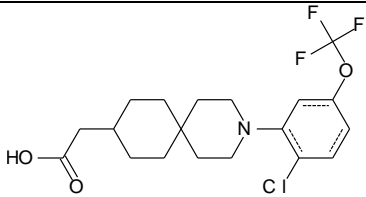
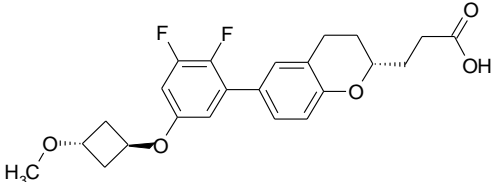
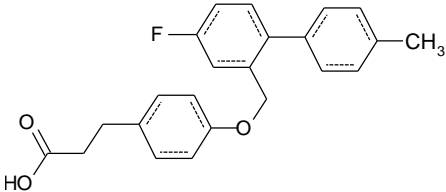
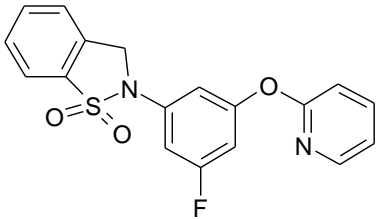
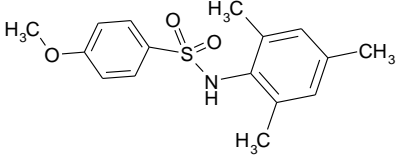
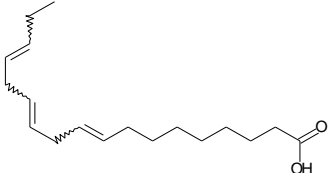
### 1.2.2.3 Ligands

GPR120 was deorphanized by HIRASAWA et al. (2005) when long chain saturated, and unsaturated fatty acids were found to bind and activate the receptor endogenously. Among them, the  $\omega$ -3 unsaturated FFAs are the ones with the highest potency. Palmitoleic acid, DHA and  $\alpha$ -linolenic acid (ALA) are shown to be the most potent and common endogenous ligands of FFAR4 (Table 3) (HIRASAWA et al., 2005). The first synthetic ligand found was GW9508, however with poor selectivity since it can also activate FFAR1 (BRISCOE et al., 2006). Considering that both receptors share several ligands, the major challenge in the development of new agonist is finding molecules with high selectivity towards FFAR4 only. Subsequently, NCG21 and TUG-891 were developed as potent and selective agonists (SUZUKI et al., 2008; HUDSON et al., 2013). Bearing in mind the druggable potential of FFAR4 for the treatment of T2DM, several other structures have been proposed as possible ligands for the receptor (see Table 3). Noticeably, all the natural and most of the

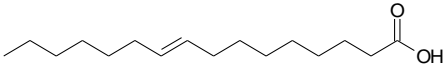
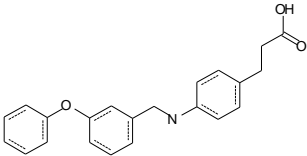
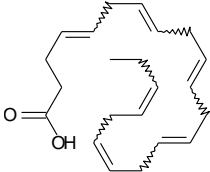
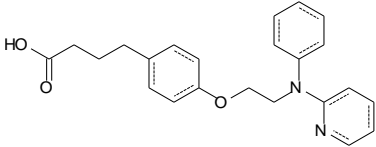
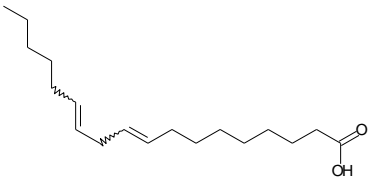
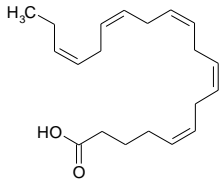
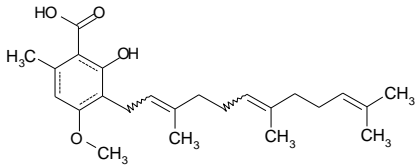
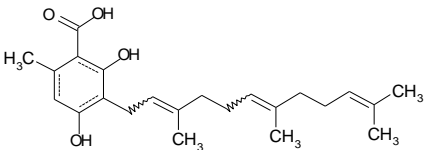
synthetic agonists contain a carboxyl group, which is required for their activity at the receptor (HIRASAWA et al., 2005).

**Table 3. Principal agonists at human FFAR4.**

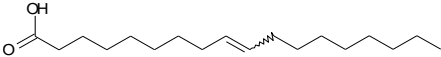
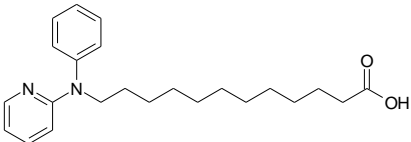
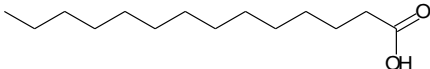
(Table to be continued)

Ligand	Structure	Potency EC <sub>50</sub> ( $\mu$ M)	Type	Reference
Cpd A		0.024 <sup>a</sup>	Full agonist	(OH et al., 2014)
Compound 18		0.024 - 0.035 <sup>b, c</sup>	Full agonist	(ADAMS et al., 2017)
TUG-891		0.044 - 1.48 <sup>d, a</sup>	Full agonist	(HUDSON et al., 2013)
Compound 34		0.12 - 0.23 <sup>a, b</sup>	Full agonist	(AZEVEDO et al., 2016)
GSK137647		0.5 <sup>a</sup>	Full agonist	(SPARKS et al., 2014)
$\alpha$ -linolenic acid		0.55 <sup>a</sup>	Full agonist	(BRISCOE et al., 2006)

(Table continued)

Ligand	Structure	Potency EC <sub>50</sub> ( $\mu$ M)	Type	Reference
Palmitoleic acid		0.76 <sup>a</sup>	Full agonist	(BRISCOE et al., 2006)
GW9508		0.85 - 3.16 <sup>a</sup>	Full agonist	(BRISCOE et al., 2006; GARRIDO et al., 2006)
DHA		1 - 10 <sup>e</sup>	Full agonist	(D. OH et al., 2011)
NCG21		1.2 <sup>a</sup>	Full agonist	(SUZUKI et al., 2008)
Linoleic acid (LA)		1.28 <sup>a</sup>	Full agonist	(BRISCOE et al., 2006)
Eicosapentaenoic acid (EPA)		10 <sup>e</sup>	Partial agonist	(D. OH et al., 2011)
Grifolic acid methyl ether		Data not shown <sup>a</sup>	Partial agonist	(HARA et al., 2009)
Grifolic acid		Data not shown <sup>a</sup>	Partial agonist	(HARA et al., 2009)

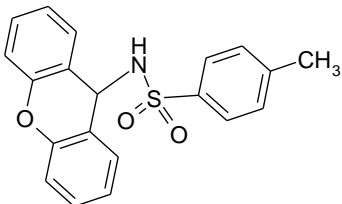
(Table concluded)

Ligand	Structure	Potency EC <sub>50</sub> ( $\mu$ M)	Type	Reference
Oleic acid		20 <sup>a</sup>	Full agonist	(WATSON; BROWN; HOLLIDAY, 2012)
NCG75		46.2 <sup>a</sup>	Partial agonist	(TAKEUCHI et al., 2013)
Myristic acid		63.1 <sup>a</sup>	Full agonist	(WATSON; BROWN; HOLLIDAY, 2012)

<sup>a</sup> Determined in calcium mobilization assay; <sup>b</sup>  $\beta$ -arrestin recruitment assay; <sup>c</sup> D-myo-inositol-1-phosphate assay; <sup>d</sup> BRET  $\beta$ -arrestin interaction; <sup>e</sup> SRE-driven reporter system.

Thus far only one antagonist was identified for FFAR4 while screening a series of diarylsulfonamide derivatives at the receptor (Table 4). Compound 39 could block the [Ca<sup>2+</sup>] release induced by LA and GSK137647 in competition assays. The compound was shown as a selective, non-competitive antagonist with comparable effects at rat and mouse FFAR4 (SPARKS et al., 2014).

**Table 4. Antagonist at human FFAR4**

Ligand	Structure	Inhibition IC <sub>50</sub> ( $\mu$ M)	Type	Reference
AH 7614 (Compound 39, NSC 3117)		0.08 <sup>1</sup>	Non-competitive antagonist <sup>a</sup>	(SPARKS et al., 2014)

<sup>1</sup> Determined in calcium mobilization assay. <sup>a</sup> When tested against linoleic acid and GSK137647.

#### 1.2.2.4. Mutagenesis data

Mutagenesis studies by HUDSON et al.(2014) indicate that the FFAR4 ligands share the same binding pocket. Among many mutations made, for the W104A, F115A, F211A, W277A, W207A, F303H, and F304A mutants the response to all tested agonists was abolished (ALA, TUG-891, GW9508, TUG-670). Also, for the mutants T119A, N215A, I280A, I126A, and V212A a significant decrease in potency of TUG-891 was observed, while N215 and T119 were described as essential residues for GW9508 potency. The F88A mutant could reduce the potency of ALA, TUG-891, and TUG-670 with no significant change for the effect of GW9508. For the F311A mutant only the potency of GW9508 was affected, suggesting that the compound may bind differently to the receptor. Interestingly, the I281V mutant increased the potency of all four tested ligands at FFAR4.

Another study showed that the receptor phosphorylation occurs specifically at the Thr<sup>347</sup>, Thr<sup>349</sup>, Ser<sup>350</sup>, Ser<sup>357</sup> and Ser<sup>361</sup> residues in the C-terminus (PRIHANDOKO et al., 2016). Moreover, FFAR4 activation was shown to be regulated by the pattern of phosphorylation. Exchange for alanine resulted in complete abolishment of phosphorylation for mouse FFAR4. Interestingly, they demonstrated that signalling through ERK1/2 is phosphorylation independent, depending however on G $\alpha_{q/11}$  coupling. Also,  $\beta$ -arrestin recruitment and internalization depend particularly on the phosphorylation of the Ser<sup>357</sup> and Ser<sup>361</sup> residues (PRIHANDOKO et al., 2016).

#### 1.2.2.4.2. Naturally occurring variants and polymorphisms

Two FFAR4 splice variants have been found in the human transcriptome. The longer variant (GPR120-L, NM\_181745) has 16 additional amino acids starting at position 231 in intracellular loop 3; and only the shorter form (GPR120-S, NM\_001195755 or BC101175) has been found in rodents (WATSON; BROWN; HOLLIDAY, 2012). In rhodopsin-like GPCRs, the C3 plays a role in the G protein recognition (ROSENBAUM; RASMUSSEN; KOBILKA, 2009). Furthermore, WATSON; BROWN; HOLLIDAY (2012) confirmed an impairment of the long isoform to couple to G $\alpha_{q/11}$  and further calcium release but with no effect on  $\beta$ -arrestin recruitment and signalling. The fact characterizes the long isoform FFAR4 as a native

$\beta$ -arrestin-biased receptor.

#### 1.2.2.5 (Patho) physiology

Since its deorphanization, the free fatty acid receptor 4 has been connected to the (patho)physiology of insulin resistance and obesity. As FFAR4 KO mice exhibited an insulin-resistant condition on a regular chow diet (D. OH et al., 2011). In vivo studies showed that  $\omega$ -3 FAs supplementation reduced the insulin resistance caused by a HFD in wild-type but not in FFAR4 KO mice. Using a diet-induced obesity model, the administration of FAs could reduce hypothalamus inflammation and the weight of animals (CINTRA et al., 2012). Additionally, intracerebroventricular injection (icv) of FAs in obese mice decreased food intake and body mass gain upon FFAR4 activation (CINTRA et al., 2012). In accordance, AUGUSTE et al. (2016) showed that icv injections of FFAR4 agonist could reduce food intake and high-fat/-sugar food reward, as well as anxiety-like behavior in mice. Therefore, FFAR4 seems to be responsible for the appetite reduction promoted by  $\omega$ -3 polyunsaturated fatty acids, and it may be a target for the development of anxiolytics.

Several single nucleotide polymorphisms were found for the human FFAR4, which result in the amino acid exchanges Q257R, R254H, R67C, and R270H. The latter polymorphism (dbSNP rs116454156) has a minor allele frequency of about 1 - 3 % in the studied European population, composed of about 30,000 subjects from different nationalities (French, Italian, Finish, Danish, Belgian, Swiss and Greek) (ICHIMURA et al., 2012; LAMRI et al., 2016; VESTMAR et al., 2016). Allele frequency data from other populations are scarce. Alterations in the FFAR4 gene, located in the chromosomal region 10q23.33, may be related to the susceptibility to obesity since alterations in the locus 10q have been linked to the disease (DONG et al., 2003; ICHIMURA et al., 2012). However, this link is still controversial. ICHIMURA et al. (2012) suggested that p.R270H causes impaired  $G_{\alpha q/11}$  coupled signalling and increases the risk of obesity. However recent studies showed that no significant relation was seen between this polymorphism and obesity (LAMRI et al., 2016; VESTMAR et al., 2016). Nevertheless, a significant connection between p.R270H individuals and risk of type 2 diabetes was suggested (LAMRI et al., 2016).

In consideration of the high expression in human and mouse adipose tissues,



there is evidence that FFAR4 is involved in adipogenesis. GOTOH et al. (2007) found that the FFAR4 mRNA increases over the course of differentiation in 3T3-L1 cells and it is not detected in preadipocytes. Similar results were seen with the major transcription factor of adipogenesis, the peroxisome proliferator-activated receptor- $\gamma$ 2 (PPAR- $\gamma$ 2). Accordingly, the receptor knock-down prevented the adipogenesis, and dramatically reduced adipogenic genes, such as *Pparg* and the fatty acid binding protein 4, *Fabp4* (also called adipocyte Protein 2, aP2). Later on, the molecular mechanism of the adipogenic differentiation through FFAR4 was elucidated by SONG et al. (2016). By applying the FFAR4 agonists TUG-891 and ALA, an increase in intracellular  $[Ca^{2+}]$  and ERK1/2 phosphorylation was seen in the adipogenesis using 3T3-L1. Likewise, ERK1/2 and intracellular  $[Ca^{2+}]$  inhibitors diminished the differentiation of the cells, confirming that FFAR4 is involved in the process by upregulating PPAR $\gamma$  via  $[Ca^{2+}]$  and ERK1/2 signalling. Moreover, a high expression of the receptor in humans has been observed in obese in comparison to slim subjects (ICHIMURA et al., 2012). Interestingly, a recent study shows that the receptor activation can promote the browning of mice white adipose tissue (WAT) by the release of fibroblast growth factor-21 (FGF21) (QUESADA-LÓPEZ et al., 2016). Therefore FFAR4 seems to be involved in the metabolism of adipose tissues.

FFAR4 appears to contradict the effects of FFAR1 in cancer. FFAR4 was found to reduce the tumorigenicity in melanoma, lung, breast, prostatic and ovarian cancer cells, while for fibrosarcoma, liver epithelial cells, pancreatic and colon cancer cells the receptor has been associated with an increase in migration and metastasis (FUKUSHIMA et al., 2015, 2016; HOPKINS et al., 2016; ISHII et al., 2015b; LIU et al., 2015; WU et al., 2013). Besides, activation of FFAR4 by platinum-induced fatty acid (hexadeca-4,7,10,13-tetraenoic acid, 16:4(n-3)) could reduce the chemotherapeutic activity of cisplatin *in vivo* (HOUTHUIJZEN et al., 2017). The chemoresistance was related to the release of an isoform of lysophosphatidylcholine (LPC) in splenic macrophages.

In brief, FFAR4 functions have been gradually explored, and the precise consequences of the patho- and physiological FFAR4 signalling need to be studied further.

## **AIM OF THE WORK**

The general aim of this work is to test the activity of diindolylmethane and uracil derivatives at the free fatty acid receptors 1 and 4.

Therefore, some specific objectives are:

1. Cloning of the receptors and generating human FFAR1 and FFAR4 transfected cell lines;
2. Screening of compounds *in vitro* and determination of the potency of ligands at both receptors, as well as the structure-activity relationships (SAR);
3. Evaluation of the adipogenic activity of the ligands.

## 2. MATERIALS AND METHODS

### 2.1 Cells

CHO-K1-cells (Ovary cells, <i>Cricetulus griseus</i> )	ATCC®, CCL-61™
C3H/10T1/2 cells (Embryo fibroblast, <i>Mus musculus</i> )	ATCC®, CCL-226™
GP <sup>+env</sup> AM-12 (Fibroblast, <i>Mus musculus</i> )	ATCC®, CRL-9641™
PathHunter® CHO-K1 β-Arrestin Parental Cell Line (Ovary cells, <i>Cricetulus griseus</i> )	DiscoverX
One Shot® TOP 10 chemically competent <i>E. coli</i>	Life Technologies, C404010
1321N1 astrocytoma cells (Glial cells, <i>Homo sapiens</i> )	AK Prof. Dr. Müller, University of Bonn
3T3-L1 cells (Embryo fibroblast, <i>Mus musculus</i> )	ATCC®, CL-173™

### 2.2 Cell culture media

All the solutions used in the cells were already sterile or filtered using a 0.22 µM filter.

Bovine Calf Serum	Sigma-Aldrich, 12133C
DMEM/F-12, HEPES	Life Technologies, 31330038
DMEM	Life Technologies, 41966029; Sigma Aldrich, D5648
Fetal Bovine Serum (FBS)	Sigma-Aldrich, F0804
Ham's F-12 Nutrient Mix	Life Technologies, 21765037
Hygromycin B	Merck Millipore, 400052

Penicillin-Streptomycin

Life Technologies, 15140122;  
Sigma Aldrich, P3032, S66501

## 2.3 Enzymes

BamHI HF®

New England Biolabs®, R3136S

BglII

New England Biolabs®, R0144S

DNAse I

Sigma Aldrich, AMPD1-1KT

EcoRI HF®

New England Biolabs®, R3101S

HindIII HF®

New England Biolabs®, R3104S

NheI HF®

New England Biolabs®, R3131S

Q5®-High Fidelity DNA Polymerase

New England Biolabs®, M0491S

Trypsin

Lonza, 17-160;

Sigma Aldrich, T4799

T4-DNA Ligase

New England Biolabs®, M0202S

## 2.4 Kits

CloneJET PCR Cloning Kit

Thermo Scientific, K1231

DNA Clean & Concentrator™-25 Kit

Zymo Research, D4033

PathHunter® Detection Kit

DiscoverX, 93-0001L

PureLink® HiPure Plasmid Filter

Life Technologies, K2100-15

Midiprep Kit

Power SYBR® Green RNA-to-CT

Applied Biotechnology, 4389986

1-Step

Zymoclean™ Gel DNA Recovery Kit

Zymo Research, D4002

Zyppy™ Plasmid Miniprep Kit

Zymo Research, D4020

## 2.5 Material and equipment

Analytic balance	CP225D, Sartorius
Autoclave	Varioklav <sup>®</sup> Dampfsterileisator 75T, H+P, 3850; Phoenix, AV75
Automatic pipettes	0.5-10 µl, 2-20 µl, 20-200 µl, 100-1000 µl, Eppendorf; 0.2-2 µl, 2-20 µl, 20-200 µl, 100-1000 µl, ThermoFisher
Bacterial shaker	New Brunswick <sup>™</sup> Innova <sup>®</sup> 44 and Innova <sup>®</sup> 4200, Eppendorf
Balance	SBC 42, Scaltec; 440-47N, Kern
Cell incubator	Jouan IG 650, HERAc <sup>®</sup> ell, Heraeus; MCO-15AC, Sanyo
Centrifuge	Allegra <sup>™</sup> 21 R, Beckman Coulter; Avanti <sup>™</sup> J-201, Beckman; BIOFUGE pico, Heraeus; BR4i, Jouan; Mikro 200, Hettich; Rotofix 32, Hettich; Z 36 HK Hermle, Labortechnik
Drigalski spatula	Roth
Electrophoresis chamber	Schütt Labortechnik
Electrophoresis power supply	Power Pac 300, ELITE 300 Plus, Schütt Labortechnik
Fluorometer	FlexStation <sup>®</sup> 3 Multi-Mode Microplate Reader, Molecular Devices NOVOstar <sup>®</sup> , BMG Labtech

Gel photo documentor	Universal Hood II Geldoc, BioRad; Amersham Imager 600, GE
Heating block	Thermomixer comfort, Eppendorf
Laminar-Airflow bench	NUNC® Safe flow 1.2; NUNC® BIOFLOW; Bioseg 12 class II type A1, Veco
Magnetic stirrer with hot plate	RCT Basic, IKA Labortechnik
Microscope	Axiovert 25, Zeiss; Primo Vert, Zeiss
Microwave	Microwave 800, Severin
Multipipette	Multipette Plus, Eppendorf;
Neubauer counting chamber	Marienfeld Germany; Optik Labor
pH meter	691 pH Meter, Metrohm; Seven compact, Mettler-Toledo
Photometer	DU® 530, Beckman
Pipetboy	Pipettus Akku, Eppendorf; Accu Jet, Brand; Pipet-Aid, Drummond
Repeat dispenser	Ritips® professional 2.5 mL, 5mL, Labomedic
Spectrophotometer	Nano Vue Plus, GE Heathcare Beckham multimode DTX 800
Thermocycler	Px2 Thermal Cyclers, Thermo Scientific; StepOnePlus™ Real-Time PCR System, Applied Biosystems
Vortex	2x3, UniEquip; MS2 Minishaker, IKA Labortechnik; VV3, VWR

## 2.6 Nucleic acids

### 2.6.1 DNA Marker

Lambda DNA/EcoRI+HindIII Marker      Thermo Scientific, SM0191

### 2.6.2 Plasmids/vectors

PCMV-ProLink1	DiscoverX
PCMV-ProLink2	
PCMV-ProLink2-ARMS1	
PCMV-ProLink2-ARMS2	
pCMV6-Entry-FFAR4short	Origene
pJet1.2	CloneJet PCR Cloning Kit, Thermo Scientific

## 2.7 Reagents and solutions

Agarose	Roth, 2267
Ampicillin sodium salt	Roth, K029
Benarhodin A	AK Prof. Dr. Piel, University of Bonn
Bromophenol blue	Applichem, 3640
BSA/Albumin Fraction V	Roth, 8076
Calcium chloride dihydrate	Fluka, 21097
Copper(II) sulfate pentahydrate	Applichem, A1034
Coriolide	AK Prof. Dr. König, University of Bonn
D-(+)-glucose	Sigma-Aldrich, G8270
Disodium EDTA	Roth, X986
DMSO	AppliChem, A3608
	Sigma Aldrich, D8418

DMSO for cell culture	AppliChem, A3672
Drug library	AK Prof. Dr. Müller, University of Bonn
Epipyron	AK Prof. Dr. König, University of Bonn
Ethanol p.a.	Merck, 1.00983
Fluo4® AM	ThermoFischer, F14201
G418	Applichem, A2167
GelRed™	Biotrend, 41002
Glacial acetic acid	Merck, 1.00063.1011
Glycerol	Applichem, A1123
HEPES	Sigma-Aldrich, H3375
Hypoxanthine	Applichem, A0700
Infectopyrone	AK Prof. Dr. König, University of Bonn
Isopropanol	ZVE University of Bonn, 123903
Kanamycin sulfate	Roth, T832
LB Agar	Roth, X965
LB-medium	Roth, X968
Lipofectamine® 2000	Thermo Fischer, 11668
Magnesium chloride	Sigma, M8266
Magnesium sulfate	Sigma, M2643
Mycophenolic acid	Tocris, 1505
Oregon Green® 488 BAPTA-1, AM	Molecular Probes, O6807
Potassium chloride	Fluka, 60128
Potassium dihydrogen phosphate	Sigma-Aldrich, P9791
Pluronic® F-127	Sigma-Aldrich, P2443
Sodium bicarbonate	Sigma, S5761
Sodium chloride	Roth, 3957
Sodium dihydrogen phosphate	Applichem, A1938
Sodium hydroxide	Fluka, 71689
Stemphol	AK Prof. Dr. König, University of Bonn
Thiazolyl Blue Tetrazolium Bromide	Sigma Aldrich, M5655
Tris	Roth, AE15.3



Trypsin	Lonza, 17-160
Tryptone	Applichem, A1553
TUG-424	Sigma-Aldrich, T6829
TUG-891	Tocris, 4601
Water, purified, sterile	VWR, AX021403
Xanthine	Sigma-Aldrich, X7375
Yazh compounds	Synthesized by Dr. Thanigaimalai Pillaiyar, AK Prof. Dr. Müller, University of Bonn
Yeast extract	Applichem, A3732
4-butyl-3,5-dihydroxybenzoic acid	AK Prof. Dr. König, University of Bonn

## 2.8 Software and programs

BLAST®	National Center for Biotechnology Information, USA <a href="http://blast.ncbi.nlm.nih.gov/Blast.cgi">http://blast.ncbi.nlm.nih.gov/Blast.cgi</a>
Chromas Lite 2.1.1	Technelysium Pty Ltd.
Clone Manager 9	Scientific & Editorial Software
ClustalW2	EMBL-European Bioinformatics Institute, <a href="http://www.ebi.ac.uk/Tools/msa/clustalw2">http://www.ebi.ac.uk/Tools/msa/clustalw2</a>
DNATrans 2.5	Dr. Schiedel/J. Bosmann
EMBOSS Needle	EMBL-European Bioinformatics Institute, <a href="http://www.ebi.ac.uk/Tools/psa/emboss_needle">http://www.ebi.ac.uk/Tools/psa/emboss_needle</a>
Excel 2007	Microsoft®
MDL ISIS™/Draw 2.5	MDL Information Systems
OligoAnalyser 3.1	Integrated DNA Technologies, <a href="http://eu.idtdna.com/analyser/applications/oligoanalyser">http://eu.idtdna.com/analyser/applications/oligoanalyser</a>

Prism® 5.01	GraphPad
SoftMax® Pro Microplate	Molecular Devices
Data Acquisition & Analysis	
StepOne v2.1.	Applied Biosystems
Word 2007	Microsoft®

## 2.9 Solutions

### 2.9.1 Alternative lysis buffer for detection reagent

5 mM  $K_2HPO_4$ , 5 mM  $KH_2PO_4$ , 150 mM NaCl, 10 mM magnesium acetate, 2 % CHAPS (3-[(3-Cholamidopropyl)dimethylammonio]-1-propanesulfonate) were mixed, and pH was adjusted to 7.5. The solution was stored at 4 °C.

### 2.9.2 Cell dissociation buffer

2 mM EDTA and 10 mM glucose were dissolved in PBS, and the solution was autoclaved and stored at room temperature.

### 2.9.3 Dexamethasone solution

A stock solution of 10 mM in ethanol was prepared and stored at -20 °C. A work solution was made by diluting the stock solution of dexamethasone in PBS 1x for a final concentration of 1 mM. This solution was filtered in 0.22 µm membrane and stored at 4 °C.

### 2.9.4 Fluo4® AM

The Fluo4® AM was dissolved using 45.5 µL of DMSO and aliquoted (15 µL). The aliquots were stored protected from light at -20 °C.

### 2.9.5 HBSS-buffer

130 mM NaCl, 5.5 mM glucose, 5.4 mM KCl, 4.2 mM  $NaHCO_3$ , 1.25 mM  $CaCl_2$ , 1 mM  $MgCl_2$ , 0.8 mM  $MgSO_4$ , 0.44 mM  $KH_2PO_4$ , 0.34 mM  $Na_2HPO_4$ , 20 mM HEPES were dissolved in autoclaved water and pH was adjusted to 7.4. The solution was

stored at -20 °C.

#### 2.9.6 HXM-Medium (for GP<sup>+</sup>env AM-12-cells)

10 % FBS, 100 U/mL penicillin, 100 µg/mL streptomycin, 200 µg/mL hygromycin B, 15 µg/mL hypoxanthine, 250 µg/mL xanthine and 25 µg/mL mycophenolic acid were added to DMEM.

#### 2.9.7 Krebs-Hepes-buffer (KHB)

118.6 mM NaCl, 11.7 mM glucose, 10 mM HEPES, 4.7 mM KCl, 4.2 mM NaHCO<sub>3</sub>, 1.3 mM CaCl<sub>2</sub>, 1.2 mM MgSO<sub>4</sub> and 1.2 mM KH<sub>2</sub>PO<sub>4</sub> were dissolved in pure water and pH was adjusted to 7.4. The solution was stored at -20 °C.

#### 2.9.8 LB-medium/LB agar

Pre mixes were dissolved individually in pure water and autoclaved. After cooling down the solution to around 60 °C, sterile solution of 100 µg/mL ampicillin or 50 µg/mL kanamycin was added to the LB Agar. After the addition of the antibiotics, the LB agar was poured into plates. After solidification, the agar plates and the LB medium were stored at 4 °C and LB agar at RT.

#### 2.9.9 Maintenance medium for adipocytes

Complete DMEM was supplemented with insulin for a final concentration of 0.167 µM.

#### 2.9.10 MDI induction media to differentiate C3H/10T1/2 and 3T3-L1 cells into adipocytes

Methylisobutylxanthine (IBMX) 0.05 M, insulin 167 µM and dexamethasone 1mM was added to complete DMEM for final concentrations of 0.5 mM, 0.167 µM and 1 M, respectively.

#### 2.9.11 Medium for astrocytoma cells

DMEM was supplemented with 10 % FBS, 100 U/mL penicillin and 100 µg/mL streptomycin. After transfection of the cells, during the selection phase, 800 µg/mL of

geneticin (G418) was added to the standard medium. After this phase, the amount of antibiotic added to the medium was 400 µg/mL.

#### 2.9.12 Medium for CHO-K1 cells

DMEM/F-12 was supplemented with 10 % FBS, 100 U/mL penicillin and 100 µg/mL streptomycin. After transfection of the cells, 800 µg/mL G418 was added during the selection phase while for culture medium 200 µg/mL geneticin was used.

#### 2.9.13 Medium for PathHunter® CHO-K1 β-Arrestin cells

Ham's F-12 Nutrient Mix was supplemented with 10 % FBS, 100 U/mL penicillin, 100 µg/mL streptomycin and 300 µg/mL hygromycin B. After the transfection of the cells, 800 µg/mL of G418 was added to the standard medium.

#### 2.9.14 Medium for undifferentiated C3H/10T1/2 and 3T3-L1 cells

DMEM was supplemented with 10 % bovine calf serum (BCS), 100 U/mL penicillin and 100 µg/mL streptomycin.

#### 2.9.15 Methylisobutylxanthine (IBMX) solution

The solution was freshly prepared by dissolving IBMX in KOH 0.5 M for a final concentration of 0.0115 g/mL (0.05 M) and filtered in 0.22 µm membrane.

#### 2.9.16 Oregon Green®

50 µg Oregon Green® 488 BAPTA-1/AM was dissolved in 39.7 µL DMSO, and the final solution was aliquoted (3 µL) and stored protected from the light at -20 °C.

#### 2.9.17 PBS buffer

137 mM NaCl, 2.5 mM KCl, 7.5 mM Na<sub>2</sub>HPO<sub>4</sub>, 1.5 mM KH<sub>2</sub>PO<sub>4</sub> were dissolved in pure water and autoclaved. The solution was stored at room temperature.

#### 2.9.18 Pluronic®-F127

A 250 mg/mL Pluronic solution was produced and stored at room temperature in

brown flask.

#### 2.9.19 SOC medium

2 % tryptone, 0.5 % yeast extract, 8.6 mM NaCl, 2.5 mM KCl, 10 mM MgCl<sub>2</sub> were mixed and solubilized in pure water and autoclaved. Then a sterile 20 mM glucose solution was added, and the medium was stored at -20 °C.

#### 2.9.20 Trypsin

0.6 mM EDTA was added to the PBS buffer and autoclaved. After cooling down, sterile 0.05 % trypsin was added to the solution. The solution was stored at 4 °C.

#### 2.9.21 6x Loading dye

0.25 % bromophenol blue and 50 % glycerol were dissolved in pure water and stored at 4 °C.

#### 2.9.22 50x TAE-buffer

2 M Tris, 50 mM EDTA and 1 M glacial acetic acid were dissolved in ultrapure water and autoclaved. The stock solution buffer (50x) was diluted in pure water to create a 1x TAE-buffer.

### **2.10 Cloning of the human FFAR1 and FFAR4short receptors**

#### 2.10.1 Polymerase Chain Reaction (PCR)

To amplify the coding DNA sequences of the receptors a polymerase chain reaction was performed. Every reaction was performed using the PCR protocol for Q5<sup>®</sup> DNA polymerase (New England BioLabs, USA). This protocol consisted of a DNA template (~ 20 ng of plasmid, ~100 ng of cDNA or gDNA), f-primer and r-primer (5 µM, each), Q5<sup>®</sup> DNA polymerase (0.5 µL), dNTPs (5 mM), Q5<sup>®</sup> reaction buffer (5x) and sterile water to complete a final volume of 25 µL. With the aim to enhance the amplification, 5 % of DMSO (100 %) was added to the reaction. The PCR program used is shown below:

Step	Temperature	Time	No. of cycles
Initial denature	96 °C	30s	1
Denature	96 °C	15s	
Annealing	Tm minus 2-5 °C	25s	35
Extension	72 °C	40s	
Final extension	72 °C	5 min	1

### 2.10.2 Cloning of human FFAR1 cDNA into pCMV ProLink and pLXSN-Neo vectors

A nested polymerase chain reaction (nested PCR) was employed to amplify a fragment of FFAR1 cDNA. Therefore the following set of the primers was used:

Fish-Primer	f-hFFAR1-ATG 5'-ATGGACCTGCCCCCGCAGCTC-3'
	r-hFFAR1-TGA 5'-TTACTTCTGGGACTTGCCCCCTT-3'
pLXSN (EcoRI/BamHI):	f-hFFAR1-ATG-EcoRI 5'-CATAGAGAATTCACCATGGACCTGCCCCCGCAGCTC-3'
	r-hFFAR1-TGA-BamHI 5'-CATAGTGGATCCTTACTTCTGGGACTTGCCCCCTT-3'
ProLink-Vectors (BglII/HindIII):	f-hFFAR1-ATG-BglII 5'-GATAGAAGATCTACCATGGACCTGCCCCCGCAGCTC-3'
	r-hFFAR1-w/ostop-HindIII 5'-CATAGAAAGCTTGACTTCTGGGACTTGCCCCCTTGC-3'

### 2.10.2.1 CloneJet PCR Cloning Kit

The "CloneJET PCR Cloning Kit" (Thermo Scientific, USA) was used as suggested by the manufacturer's manual. Briefly, the blunting reaction was set with the addition of the DNA sample (~50 ng), reaction buffer (2x), DNA blunting enzyme and sterile water, and it occurred by a heat shock. The next step was the ligation of the DNA fragments through the addition of T4 DNA Ligase and pJET1.2/blunt Cloning Vector to the reaction, followed by 5 minutes incubation before transformation.

### 2.10.3 Cloning of human FFAR4short cDNA into PCMV ProLink and pLXSN-Neo vectors

The pCMV6-Entry-FFAR4short was used as DNA template for a PCR reaction. For this purpose the following sets of primers were used:

#### pLXSN

(EcoRI/BamHI): f-hFFAR4-ATG-EcoRI

5'-CATAGAGAATTCACCATGTCCCCTGAATGCGCGCGG-3'

r-hFFAR4-TGA-BamHI

5'-CATAGTGGATCCTTAGCCAGAAATAATCGACAAGTCATT

TTCTTTTGAC-3'

#### ProLink-Vectors

(NheI/HindIII): f-hFFAR4-ATG-NheI

5'-CATAGAGCTAGCACCATGTCCCCTGAATGCGCGCGG-3'

r-hFFAR4-w/ostop-HindIII

5'-

CATAGAAAGCTTGAGCCAGAAATAATCGACAAGTCATTTT

CTTTTGAC-3'

### 2.11 Agarose gel electrophoresis

The agarose powder was dissolved in 1x TAE buffer for a final concentration of 1 %. The solution was heated in a microwave to get a clear solution. The solution was briefly cooled before the addition of GelRed™ (dilution factor 1:20000). The solution was solidified with a comb to create wells in which the samples were

pipetted, after the coverage of the gel with 1x TAE buffer. The samples were mixed with 6x loading buffer before adding it to the gel. The electrophoresis was performed applying a voltage of 110V. The UV light was applied to check for the DNA bands in the gel and to verify the bands of the  $\lambda$  DNA marker was used.

## 2.12 DNA clean-up

To extract, purify and concentrate the DNA, two clean-up kits were used. For the DNA bands, which were cut from the agarose gel, the "Zymoclean™ Gel DNA Recovery Kit" (Zymo Research, USA) was applied, while the kit "DNA Clean & Concentrator" kit (Zymo Research, USA) was used for solutions containing DNA to be cleaned.

## 2.13 Restriction reaction

The restriction enzymes BamHI, BglIII, EcoRI, HindIII and NheI (New England BioLabs, USA) were used to create sticky or cohesive ends fragments, i.e. a "tail" with a single strand which is complementary to all other fragments generated by the same enzyme or other restriction enzymes generating the same kind of fragments. The receptors' cDNAs and plasmids were cut according to the primer sets used. The restriction reactions consisted of DNA (>100 ng of plasmid or >600 ng of PCR product), CutSmart® buffer, 0.5  $\mu$ L of each restriction enzyme and sterile water to complete a final volume of 10  $\mu$ L. As controls, the cDNAs were tested individually with each enzyme to evaluate their activity. After incubation at 37 °C for 60 minutes, the agarose gel was used to confirm if the cleavage was successful. The plasmids were cut using the following enzymes:

human FFAR1	pLXSN	EcoRI, BamHI
	pCMV ProLink vectors	BglIII, HindIII
human FFAR4short	pLXSN	EcoRI, BamHI
	pCMV ProLink vectors	NheI, HindIII



## 2.14 Ligation

The cut plasmid and insert were incubated with the enzyme T4 ligase (New England BioLabs, USA) for 30 min at room temperature to allow the ligation reaction of the complementary DNA overlaps at the end of both fragments. The reaction occurred by mixing the PCR product (~ 150 ng), the plasmid (~ 50 ng), T4 Ligase buffer, 0.5 µL of T4 ligase and sterile water to complete a final volume of 10 µL. The single plasmid was used as a control to see if religation occurs. Therefore, the cleaved insert and plasmid were ligated with the aim to construct the following clones:

human FFAR1	pLXSN-FFAR1
	pCMV-ProLink1-FFAR1
	pCMV-ProLink2-FFAR1
	pCMV-ProLink2-ARMS1-FFAR1
	pCMV-ProLink2-ARMS2-FFAR1
human FFAR4short	pLXSN-FFAR4
	pCMV-ProLink1-FFAR4
	pCMV-ProLink2-FFAR4
	pCMV-ProLink2-ARMS1-FFAR4
	pCMV-ProLink2-ARMS2-FFAR4

## 2.15 Transformation

The Top10 competent bacteria culture was removed from -80 °C freezer and was thawed on ice for around 30 minutes. After that, ~10 ng of the plasmid was pipetted to the culture and mixed carefully. The mixture was incubated for 30 min on ice and then a heat shock of 2:30 min at 37 °C was applied. The mixture was then incubated briefly on ice. Then 200 µL of LB medium was added to the bacterial mixture. The culture was incubated at 37 °C for 30 to 60 min at 300 rpm. After this, the culture was spread on a LB agar plate containing either kanamycin or ampicillin. The plates were incubated overnight at 37 °C. Single colonies were selected and

picked from the LB agar plate to culture in LB medium with the appropriate antibiotic and incubated overnight with shaking at 37 °C.

## 2.16 Extraction and purification of plasmid DNA from cell cultures of bacteria

Two kits were used to extract and purify the DNA from the bacteria. The “ZR Plasmid Miniprep Kit” (Zymo Research, USA) was used for small extractions, while for larger scale extractions were performed with the "PureLink® HiPure Plasmid Filter Midiprep Kit" (Invitrogen, USA). The process allows the extraction of the DNA and the removal of all contaminants based on the principle of alkaline lysis. An agarose gel was applied to evaluate the extraction and purification of plasmids.

## 2.17 Sanger sequencing reaction

The isolated plasmid DNAs were prepared for sequencing by dilution of 1000 ng in 30 µL of sterile water. DNA samples were sent to the company GATC Biotech (Konstanz, Germany), which performed the sequencing reactions.

## **2.18. Cell culture**

### 2.18.1 Thawing Cells

Cryopreserved cells were quickly thawed in a warm water bath and were added to a 175 cm<sup>2</sup> culture flask filled with 25 mL of cell medium. After adhesion of the cells, the flask was washed with PBS and medium was replaced with fresh medium.

### 2.18.2 Cell cultivation

The CHO, 3T3-L1 and C3H/10T1/2 cell lines were cultivated at 37 °C and 5 % CO<sub>2</sub>, while the astrocytoma cell lines at 37 °C and 10 % CO<sub>2</sub>. The passage of cells was performed when a confluence of around 90 % was reached. First, the medium of the cells was removed, and cells were washed with PBS. Then 0.05 % trypsin/0.6 mM EDTA solution was added to the cells. The cells were incubated for 2 minutes at 37 °C for better enzymatic activity. Subsequently, cell medium was added to the cells to stop the action of the trypsin, and a portion of the homogenized suspension was

placed in a new cell culture flask filled with fresh medium.

### 2.18.3 Cell counting

Cells were counted using a Neubauer chamber.

### 2.18.4 Cryoconservation

After reaching a high confluence, the cells were detached and centrifuged for 5 min at 200 x g. The pellet was resuspended in FCS and quickly transferred to cryovials filled with DMSO (final percentage of 10 %). The cells were cooled down slowly in a cell freezing container filled with isopropanol overnight at -80 °C. The cell lines were preserved in a -80 °C freezer for short time conservation while for long time preservation the cells were stored in liquid nitrogen.

### 2.18.5 Transfection of mammalian cells

#### 2.18.5.1 Generation of $\beta$ -arrestin cell lines

With the aim to create cell lines expressing the tagged receptors, the CHO-K1 PathHunter®  $\beta$ -arrestin cell line was used for transfection applying Lipofectamine® 2000. Therefore 1-2 x10<sup>6</sup> cells were seeded in a small cell culture flask one day before the assay. On the next day and couple of hours before the transfection, the medium of the cells was changed to 6.25 mL of medium without antibiotics. In a 15 mL falcon, 600  $\mu$ L of medium without supplements was mixed with 25  $\mu$ L of Lipofectamine® 2000, following of a 5 minutes incubation at RT. During this period, 10  $\mu$ g of the desired receptor DNA tagged with each of the pCMV-ProLink™ vectors were mixed with medium without supplements in a 15 mL falcon. Then the mixture containing Lipofectamine® was added carefully to the mixture with DNA and was incubated for 20 minutes at RT. After the incubation, the solution was added to the cells. One day after the transfection, the cells were transferred to a 175 cm<sup>2</sup> flask and cultivated with standard medium with antibiotics. On the day after, the medium was replaced to a selection medium with 800  $\mu$ g/mL of gentamicin (G418), a selective antibiotic. The cells were selected for approximately 10 days, and after this period, the cells could be used to perform in vitro assays. Even after the end of the

selection phase, the cells were cultivated in medium supplemented with G418.

#### 2.18.5.2 Retroviral transfection of mammalian cells

The retroviral transfection had the final purpose of transfecting CHO-K1 and astrocytoma cells with human FFAR1 or FFAR4short receptor expressing vector pLXSN, which were used in calcium mobilization assays.

##### 2.18.5.2.1 Virus production

The GP<sup>+</sup>env AM-12 packaging cells were counted to an amount of  $1.5 \times 10^5$  cells and were grown in a small cell culture flask filled with 5 mL of medium without xanthine, hypoxanthine and mycophenolic acid. On the day after, one hour prior the transfection, the medium of the cells was replaced with 6.25 mL of DMEM supplemented with 10 % FBS and ultraglutamine but without antibiotics. The transfection was performed with Lipofectamine® 2000. To transfect a small cell culture flask, 6.25 µg of the vector pLXSN with the desired receptor cDNA (human FFAR1 or human FFAR4short) and 3.75 µg of VSV-G protein DNA were used. In a falcon 600 µL of DMEM without supplements was mixed with 25 µL of Lipofectamine® 2000 and incubated for 5 minutes. In the meanwhile, the receptor DNA/VSV-G protein mixture was pipetted into another centrifuge tube and filled up with 625 µL of DMEM. Both mixtures were placed together and incubated for 20 minutes, and then poured on the packaging cells. The medium was replaced with 3 mL of null medium (DMEM, FBS, penicillin and streptomycin) around 12-15 hours after transfection. With the aim to increase the virus production, by stabilisation of the proteins of the virus, 30 µL of sterile sodium butyrate solution (500 mM in water) was added to the transfected cells. The cells were then incubated for 48h at 32 °C.

##### 2.18.5.2.2 Infection of the target cells

$3 \times 10^5$  CHO-K1 cells and  $5 \times 10^5$  1321N1 astrocytoma cells were seeded separately in 25 cm<sup>2</sup> cell culture flasks and incubated at 37 °C/5% CO<sub>2</sub> (CHO-K1 cells) and 37 °C/10 % CO<sub>2</sub> (astrocytoma cells). On the day after, 3 mL of the medium of the packaging cells were filtered using a 45 µm filter and was added to the target

cells, in addition to 6  $\mu\text{L}$  of polybrene solution (4 mg/mL in water), with the aim to enhance the efficiency of the retroviral infection. After incubation of 2.5 hours, this medium was replaced with 5 mL of null medium. After two days, the cells were transferred to a big cell culture flask, and they were cultured with a selection medium (addition of 800  $\mu\text{g}/\text{mL}$  of G418). Every two days, for one week, the medium was exchanged. The untransfected CHO-K1 and 1321N1 astrocytoma cell lines were used as control. After this phase, the cells were cultured using a selection medium supplemented with 200  $\mu\text{g}/\text{mL}$  (CHO cells) and 400  $\mu\text{g}/\text{mL}$  (astrocytoma cells) of G418.

## **2.19. Pharmacological experiments**

### **2.19.1 $\beta$ -arrestin recruitment assay**

The PathHunter®  $\beta$ -Arrestin GPCR assay (DiscoverX, USA) allows the measurement of a ligand's potency, based on the recruitment of  $\beta$ -arrestin in a G protein-independent signalling mechanism. In this assay, the GPCR, which is fused to a  $\beta$ -galactosidase fragment called ProLink, and is co-expressed in cells stably expressing  $\beta$ -arrestin with an N-terminal deletion mutant of  $\beta$ -galactosidase. The activation of the receptor promotes binding of  $\beta$ -arrestin to the ProLink-tagged GPCR resulting in enzyme complementation. Subsequently, enzyme activity can be measured using a chemiluminescence detection system. Additionally, an alternative lysis buffer for the  $\beta$ -arrestin assay was tested, and signalling was compared to the available commercial reagent (DiscoverX, USA).

#### **2.19.1.2 Agonist screening**

On the day before the assay, the cells were detached using a trypsin-free dissociation buffer and  $3 \times 10^4$  cells were plated per well in a 96-well cell culture white plate. The cells were incubated at 37 °C and 5 %  $\text{CO}_2$ . On the next day and four hours before the assay, the supplemented medium of the cells was replaced with one without FCS. For the assay 10  $\mu\text{L}$  of an agonist solution in F12 medium (10 % DMSO) was added to each well and the same volume of buffer was used as negative control. As positive control, 10  $\mu\text{L}$  of the standard agonist was added to the

cells (TUG-424, final concentration of 10  $\mu$ M for human FFAR1. TUG-891, final concentration of 30  $\mu$ M for human FFAR4short). After the addition of the compounds, plates were incubated for 90 minutes at 37 °C. The detection was made by adding 50  $\mu$ L of detection reagent (alternative lysis buffer, Emerald™ and Galacton Star®) to each well. The plates were then incubated for 60 minutes at room temperature protected from light. The chemiluminescence activity was measured using a luminescence counter (Topcount NXT™). The signals were normalised by the standard agonist signal, and GraphPad Prism® software was employed to analyse the results. The assays were performed in duplicate and replicated at least three times.

#### 2.19.1.3 Antagonist screening

To measure the antagonistic activity at the receptor, each compound was tested at a concentration of 10  $\mu$ M versus 4  $\mu$ M of the standard agonist ( $\sim$ EC<sub>80</sub> of TUG-891). Cells were first incubated for 30 minutes in the presence of the compounds to be tested. After that, the standard agonist was added to each well and incubated for 1.5 hours. Except these variations the  $\beta$ -arrestin assay was performed as previously described. The assays were performed in duplicate and replicated three times.

#### 2.19.1.4 Validation of the ProLink® sequences

With the aim to know which ProLink-tagged sequence would best suit for the  $\beta$ -arrestin assays, the known agonists for FFAR1 (TUG-424, final concentration of 10  $\mu$ M) and for FFAR4 (TUG-891, final concentration of 30  $\mu$ M) were tested in the transfected cells. Higher signalling would indicate better recruitment of the  $\beta$ -arrestin molecule and then, a better suited sequence for the assays.

#### 2.19.1.5 Monoclonal cell culture

The transfected  $\beta$ -arrestin cell lines were seeded in a 96-well plate for a density of one cell per well. Cells were propagated, and after verification of monoclonal origin, the cell lines were used to perform  $\beta$ -arrestin assays, employing

the adapted detection reagent previously described. Cell lines were tested by their signal induction when using 10  $\mu\text{M}$  of TUG-424 and 30  $\mu\text{M}$  of TUG-891 for hFFAR1-tagged and hFFAR4s-tagged cell lines, respectively. The monoclonal cell lines were named by their positions in the 96-well plate (from 1A to 12H).

#### 2.19.1.5.1 Protocol validation for $\beta$ -arrestin assays using monoclonal cells

To determine signal-to-background ratios TUG-424 was first tested at a concentration of 30  $\mu\text{M}$  and TUG-891 at a concentration of 100  $\mu\text{M}$  and compared to respective buffer values. The assay was performed using monoclonal CHO cells expressing ProLink2-ARMS2-tagged hFFAR1, ProLink2-ARMS1-tagged hFFAR4s and ProLink2-ARMS2-tagged hFFAR4s under two different conditions explained below. Except these deviations, the assays were performed as previously described. The assays were performed in duplicate and replicated at least two times.

Standard condition (condition I)	30000 cells/well were plated in 90 $\mu\text{L}$ F12 medium (Gibco®, Life Technologies, USA) supplemented with 10 % fetal bovine serum, 300 $\mu\text{g}/\text{mL}$ hygromycin and G418. The medium was exchanged for medium without FBS 4h after cell plating. For the treatment, 10 $\mu\text{L}$ of agonist solution (10 % DMSO, 90 % F12 medium) was used.
Condition II	Supplemented F12 medium (10 % fetal bovine serum, 300 $\mu\text{g}/\text{mL}$ hygromycin and G418) was exchanging for 99 $\mu\text{L}$ medium without FBS 4h after cell plating (30000 cells/well), and the treatment was made by addition of 1 $\mu\text{L}$ of agonist solution in pure DMSO.

#### 2.19.1.6 Protocol validation for $\beta$ -arrestin assays using polyclonal cells

The two reference compounds (TUG-424 and TUG-891) were first tested at a concentration of 100  $\mu\text{M}$  at polyclonal CHO cells expressing ProLink2-ARMS2-tagged hFFAR1, ProLink2-ARMS1-tagged hFFAR4s and ProLink2-ARMS2-tagged

hFFAR4s. The assay was performed under standard conditions previously described.

#### 2.19.1.6.1 $\beta$ -arrestin assays to determine concentration-response curves

TUG-891 was tested at concentrations of 0.01-100  $\mu$ M and polyclonal CHO cells stably expressing ProLink2-ARMS1-tagged hFFAR4s were used. The medium was exchanged according to the three different assay conditions described below with the aim to find a stable assay condition. Apart from the differences reported, the  $\beta$ -arrestin assay was performed as previously described.

Standard condition	as described in item 2.19.1.5.1
Condition III	Complete F12 medium was exchanged four hours before the assay for one without FBS and cells were treated with 10 $\mu$ L of agonist solution (10 % DMSO, 90 % F12 medium).
Condition IV	The cell medium was exchanged for 90 $\mu$ L/well of HBSS four hours before the assay and the treatment was performed by adding 10 $\mu$ L of agonist solution (10 % DMSO, 90 % F12 medium) to the cells.

#### 2.19.1.7 Compound screening

The Yazh compounds, as well infectopyrone, 4-butyl-3,5-dihydroxybenzoic acid, coriolide, stemphol, epipyron, benarhodin A, were initially tested at a concentration of 10  $\mu$ M at the receptors in all the assays. Additionally, a library of commercial compounds (Drug library) was tested for agonist screening at the receptor FFA4 at an initial concentration of 10  $\mu$ M in  $\beta$ -arrestin assays. Compounds with effects > 50 % would be considered as hits. The possible hits were then used to reach a dose-response curve, aiming to determine the compounds' EC<sub>50</sub> or IC<sub>50</sub> value, depending on the type of the assay (agonist or antagonist assay,



respectively).

### 2.19.2 Calcium mobilization assay

The calcium mobilization assay was performed for the compounds screening at the FFAR1 receptor. Calcium mobilization assays are functional assays to measure the calcium flux associated with  $G_q$  protein-coupled receptor activation or inhibition. For this assay, a calcium-sensitive fluorescent dye is used. It binds to the calcium ions released into the cytoplasm and upon binding calcium ions its fluorescence intensity increases. Since the  $G_q$  protein activation mechanism is associated with calcium release to the cytoplasm via PLC activation, the fluorescence intensity is directly correlated to the ligand activation of the receptor of interest.

#### 2.19.2.1 Protocol with non-adherent cells using NOVOSTar® fluorometer

TUG-424 was tested at concentrations of 30 to 0,0003  $\mu\text{M}$  at four cell lines (CHO-K1, null-astrocytoma, astrocytoma expressing human FFAR1 receptor and CHO expressing human FFAR1). Cells were shortly trypsinised and resuspended in 30 mL of medium in a falcon, which was incubated for 45 minutes at 37 °C. After this, cells were centrifugated at 1200 rpm for 5 min and resuspended with 994  $\mu\text{L}$  of 1x Krebs-HEPES buffer (KHB buffer). The suspension was transferred to a reaction tube filled with 3  $\mu\text{L}$  of Oregon Green® BAPTA-1/AM and 3  $\mu\text{L}$  of the Pluronic® F127 solution. The reaction tube was incubated in a spinning wheel and protected from the light for 1 hour at RT. Afterwards, centrifugation at 2500 rpm for 12 s was made, and the supernatant was removed. The pellet was washed and resuspended in 994  $\mu\text{L}$  of KHB buffer twice. Subsequently, the cells were poured in a glass tank filled with 20 mL of KHB buffer and were constantly homogenised while 180  $\mu\text{L}$  of the suspension was pipetted per well into a black, clear flat bottom 96-well plate. The plate was incubated for 20 minutes in the dark before the measurement of the cells to take place at the bottom. In the meanwhile, a reagent plate was prepared with agonist solution (10 % DMSO in KHB) in different concentrations and was placed in the fluorometer, as well the plate with cells. As positive controls carbachol (100  $\mu\text{M}$ ) and

ATP (100  $\mu\text{M}$ ) were tested, while the buffer was used as negative control. 20  $\mu\text{L}$  of the solution was added from the reagent plate to the cells, and the measurement was made by NOVOStar® Fluorometer. The parameters of the measurement were the fluorescence intensity measured during a period of 120 s, excitation wavelength = 485 nm, emission wavelength = 520 nm, 60 measuring points, interval time = 0.4 s. The assays were performed in duplicate and repeated at least three times, independently. The signals were normalised by the signal of carbachol 100  $\mu\text{M}$ , and the GraphPad Prism® was employed to analyse the data.

#### 2.19.2.2 Protocol with adherent cells using Flexstation® fluorometer

Additionally, the Flexstation® protocol was chosen to perform calcium assays at human FFAR1. Aiming to determine the  $\text{EC}_{50}$ , TUG-424 was tested at concentrations of 30 to 0.0003  $\mu\text{M}$  at FFAR1 transfected astrocytoma cells. One day before the assay, the astrocytoma cells with the confluence of around 80-90 % were shortly trypsinised and  $5 \times 10^4$  cells were plated per well in a Corning® 3340 black 96 well-plate. The cells were incubated overnight at standard conditions. On the next day, the medium of the cells was removed by inversion and 40  $\mu\text{L}$  of the dye solution (per plate: 4970  $\mu\text{L}$  of Hank's Balanced Salt Solution (HBSS), 15  $\mu\text{L}$  of Fluo4® AM and 15  $\mu\text{L}$  Pluronic®, vortexed briefly and protected from light) was added to each well. The cells were incubated for 1 hour at 37 °C. After this period, the dye solution was removed by inversion, and 190  $\mu\text{L}$  of HBSS was added to each well. At the Flexstation® fluorometer, 10  $\mu\text{L}$  of the agonist solution (final concentration of DMSO equal to 0.5 %, different concentrations) was pipetted to the cells. As negative control, 10  $\mu\text{L}$  of buffer was added while as positive control, 10  $\mu\text{L}$  of the standard agonist was pipetted (TUG-424, final concentration of 10  $\mu\text{M}$ ). The solutions were taken from a previously prepared reagent plate and added automatically to the respective well of the Corning® 3340 96 well-plate by the fluorometer. The fluorescence intensity was measured for a period of 120 s (measurement parameters were 94 measuring points, interval time 1.28 s, minimum run time 36 s, excitation wavelength 485 nm, emission wavelength 515 nm). The signals were normalised to that induced by 10  $\mu\text{M}$  of TUG-424. The experiments were performed

independently three times in triplicate. The data was analysed by GraphPad Prism® software.

#### 2.19.2.2.1 Antagonist screening

The cells were first incubated for 30 minutes at room temperature in the presence of 10 µM of each compound to be tested after the standard step of dye removal. After incubation, 1 µM of the standard agonist (~EC<sub>80</sub> of TUG-424) was pipetted by the fluorometer to each well right before the measurement. The buffer and 1 µM of TUG-424 were used as controls. The rest of the assay was performed as previously described. The possible hits were tested to get dose-response curves with the aim to determine the IC<sub>50</sub> value of the compounds. The assays were performed in triplicate and replicated three times.

#### 2.20. Cell Viability Assay

3 x 10<sup>4</sup> undifferentiated C3H/10T1/2 and 3T3-L1 cells were plated in 96-well cell culture plate. The day after, the medium was replaced, and treatments were added (1 % DMSO, final concentration). Cells were then incubated at 37 °C/5 % CO<sub>2</sub> for 24 h prior the addition of 50 µg of 3-(4,5-dimethylthiazol-2-yl)-2,5-diphenyltetrazolium bromide (MTT). The reagent MTT was allowed in contact with the cells for 4 h. After this period, the medium was gently removed from wells. Pure DMSO was added to the cells, and the plates were shaken protected from the light until complete solubilization of formazan crystals. The absorbance (λ 570 nm) was measured in a spectrophotometer (Beckham multimode DTX 800). The cell viability was calculated by the equation: mean OD treatment / mean OD control \*100, where OD means absorbance. GraphPad Prism® was employed to plot the data.

#### 2.21. Differentiation assay to adipocytes

Undifferentiated C3H/10T1/2 and 3T3-L1 cells were seeded in 6-well cell culture plates and maintained at 37 °C/5 % CO<sub>2</sub> until full confluence was reached. Two days after the confluence (considered as Day 0), the differentiation was initiated by addition of the MDI induction media to the cells, as well as the proposed

treatments (1  $\mu\text{M}$  rosiglitazone; 100  $\mu\text{M}$  TUG-891; Yazh 3, Yazh 4, Yazh 16, Yazh 357, digitonin, 10  $\mu\text{M}$  each) and vehicle (DMSO, 10 %). From Day 2 the media was replaced to one supplemented with 10 % FBS and 0.17  $\mu\text{M}$  insulin. The media and treatments/vehicle were refreshed every 48 hours until the third (initial differentiation) or tenth day (complete differentiation).

#### 2.22. Oil Red O staining (ORO)

Aiming to dye the cytoplasmic lipid droplets of the adipocytes, cells were washed three times with PBS 1 x and then were fixed with formalin 4 % for 40 minutes. The formalin was removed, and cells were washed once with PBS before a 5 minutes incubation with 60 % isopropyl alcohol. Cells were stained by incubation of 1 mL/well of Oil Red O for 1 h at room temperature. The Oil Red O was then removed, and cells were washed three times with 1 mL of distilled water before photo documenting at 20 x magnification.

#### 2.23. RNA extraction and purification

To quantify the gene expression, the mRNA was extracted from the cells. After the differentiation of adipocytes, the medium was removed from cells, and they were washed with PBS 1x. The total RNA was collected using TRI Reagent® (Sigma Aldrich, USA). The samples were centrifuged at 14000 rpm for 10 min at 4 °C. After the addition of 200  $\mu\text{L}$  of chloroform, samples were incubated for 3 min at RT and centrifuged at 14000 rpm / 4 °C for 15 minutes. It was added 500  $\mu\text{L}$  of isopropyl alcohol to the upper phase and samples were let at RT for 10 min. The samples were pelleted by cooled centrifugation at 14000 rpm for 10 min. The pellet was washed with 1 mL of cooled ethanol 75 % and then was air-dried, solubilised with RNA free water and RNA yield was determined using Nano Vue Plus (GE, England). Remains of DNA were removed from the samples by treatment with DNase I, as suggested by the fabricant (Sigma Aldrich, USA).

## 2.24. Real-time quantitative polymerase chain reaction with reverse transcriptase (RT - qPCR)

To amplify and quantify the expression of reference and target genes a quantitative polymerase chain reaction with reverse transcriptase was applied. The Power SYBR® Green RNA-to-CT 1-Step protocol (Applied Biosystems, USA) was performed using a 96-well plate (MicroAmp Optical, Applied Biosystems). Every reaction consisted of 10 ng of RNA template, 200 nM of each f-primer and r-primer, reverse transcriptase (RT) enzyme mix (125x), Power SYBR® Green RT-PCR Mix (2x) and nuclease free water for a final volume of 10 µL. The results were analysed with the Software StepOne v2.1. The PCR program used is described as follows:

Step	Temperature	Time	No. of cycles
Reverse transcription	48 °C	30 min	1
Initial denature	95 °C	10 min	1
Denature	95 °C	15s	} 40
Annealing/extension	60 °C	60s	

### 2.24.1 Validation of primers

Prior the gene expression analysis the set of primers to be used was validated. The primer validation aims to demonstrate the equivalence of efficiency between the reference and target genes' primers, as well as the specificity of the PCR reaction. For this purpose, a serial RNA dilution curve was made (25, 5, 1, 0.2, 0.04 ng RNA; dilution factor = 5). The analysis were made applying the equation:

$$\Delta Ct = Ct_{\text{target}} - Ct_{\text{reference}},$$

where Ct (cycle threshold) is the number of cycles for the fluorescence signal to cross the threshold value, i.e. the number of PCR cycles needed for exponential amplification. The curve was represented by the  $\Delta Ct$  values about the log of the correspondent dilution, to create a linear semi-log regression. For equivalence, the "a" value ( $y = ax + b$ ) should be  $< 0.1$  and  $> -0.1$ .

#### 2.24.1.1 Primers dissociation curve (Melting curve)

The dissociation curves were made for every pair of primers to verify their specificity, confirming the absence of unspecific amplification products and dimers. The melting curves were generated in the thermocycler after the RT - qPCR, by increasing the temperature (0.3 °C) gradually from 60 °C to 95 °C. As the temperature is raised, the SYBR® Green fluorescence decreases and the point which corresponds to the fastest fluorescence decay is called melting temperature (T<sub>m</sub>). The T<sub>m</sub> determines the temperature at which half of DNA is denatured, and it is specific to each amplified DNA sequence. Therefore one may expect a single detected dissociation peak for each set of primers applied in the RT - qPCR. The data was given by the ratio between the fluorescence derivative and the temperature derivative (dF / dT) in relation to the temperature.

#### 2.24.2 Relative quantification of target genes

The RT - qPCR reactions were made using the set of primers to amplify the reference and target genes shown below. The Ct value of the samples was normalised by the reference gene' Ct (ΔCt) and the quantification of the relative gene expression was given by the equation  $2^{-\Delta\Delta Ct}$ , where  $\Delta\Delta Ct = \Delta Ct_{\text{treated samples}} - \Delta Ct_{\text{vehicle}}$ .

Reference gene

*Actb* (β-actina)

f-5'-GTGACGTTGACATCCGTAAG-3'

r-5'-GCCGGACTCATCGTACTCC-3'

Target genes

*Fabp4*

f-5'-ACACCGAGATTTCCCTTCAAAGT-3'

r-5'-CCATCTAGGGTTATGATGCTCTTCA-3'

*Ffar4*

f-5'-GTGCCGGGACTGGTCATTGTG-3'

r-TTGTTGGGACACTCGGATCTGG-3'

*Ppar-γ*

f-5'-TTTTCCGAAGAACCATCCGAT-3'

r-5'-ATGGCATTGTGAGACATCCCC-3'

## **2.25. Statistics**

For  $\beta$ -arrestin and calcium mobilization assays, the dose-response curves were achieved by plotting the luminescence or fluorescence signals against the compounds concentrations. Results were fitted by nonlinear regression parameters, and the sigmoidal dose-response equation was chosen to estimate EC<sub>50</sub>/IC<sub>50</sub> values.

For gene expression levels, the effect of ligands versus vehicle was compared using the analysis of variance ANOVA, followed by the Bonferroni's Multiple Comparison test ( $p < 0.05$ ). All the statistical analysis were performed by the GraphPad Prism® Software, version 5.01).

### 3. RESULTS AND DISCUSSION

#### Part 1. Screening of compound libraries at human FFAR1 and FFAR4 and SAR of ligands

The results described in this first part have partially been published (PILLAIYAR et al., 2017, 2018).

#### 3.1. Cloning of the human FFAR1 and FFAR4short receptors

##### 3.1.1 Cloning of FFAR1 into pCMV ProLink vectors and pLXSN-Neo applying nested PCR

A fragment of the FFAR1 cDNAs was amplified employing Q5® Polymerase, and the genomic DNA (gDNA) of 1321N1 astrocytoma cells (Dr. Dominik Thimm, AK Müller, University of Bonn) was used as a template. However this attempt to amplify the human FFAR1 showed many non-specific bands, one of which showed an exceptionally high yield (about 800 bp length) (Figure 4).

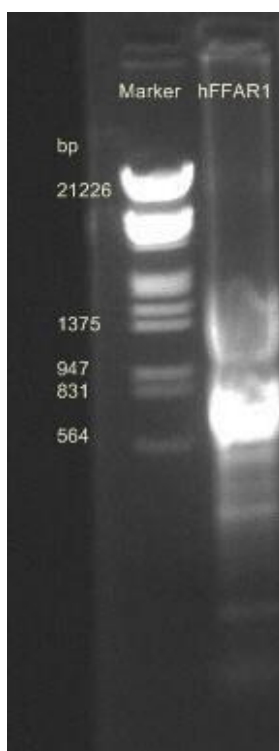


Figure 4. Agarose gel electrophoresis after amplification of the human FFAR1 cDNA.



Therefore it was decided to employ a nested polymerase chain reaction (nested PCR). This modified PCR has the goal to reduce non-specific products due to the amplification of fragments yielded by primers binding to unspecific sites. It is performed in two consecutive polymerase chain reactions and involves two sets of primers. In the first run, a primer set is used to amplify a bigger fragment, while the second run in this process has the purpose of amplifying a specific target sequence within the first fragment, using the first PCR product as template.

After the processing, one band was seen in the region of about 800 bp (Figure 5), suggesting an amplified product smaller than the expected fragment of human FFAR1, which consist of around 900 bp. One possible explanation would be the high amount of DNA loaded, which could shift the amplified DNA towards the anode. Nevertheless, this cDNA was inserted into pJet1.2 vector, followed by transformation and plasmid isolation ("miniprep").

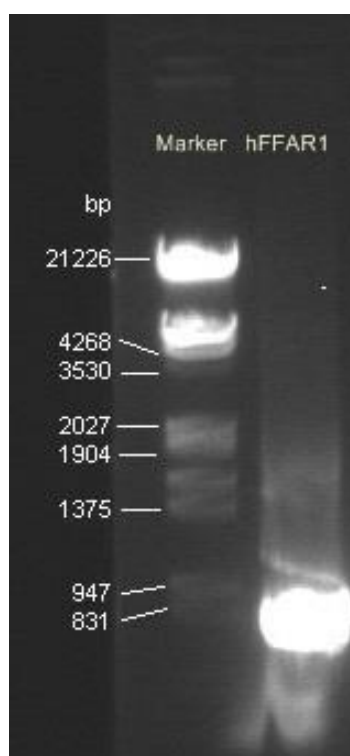


Figure 5. Agarose gel electrophoresis after Nested PCR of human FFAR1. The amplified product is seen in the region of about 800 bp.

The analysis of the clone sequence showed a point mutation leading to an

amino acid exchange in position 211 (dbSNP cluster id rs2301151). This mutation naturally occurs as a single nucleotide polymorphism with an allele frequency of 12.04 % of the population (KALIS et al., 2007). As the wild-type receptor cDNA was desired, another clone was sent for sequencing reaction, which was shown to represent the wild type sequence.

Another PCR was performed using the previously sequenced clone as template, with the aim to insert the receptor cDNA into pCMV ProLink vectors and the pLXSN-Neo vector. After the isolation of the recombinant plasmids, an agarose gel electrophoresis was performed to evaluate the clones. They showed a bigger size in comparison to the empty plasmids (pLXSN-Neo and ProLink vector), suggesting the successful insertion of desired fragments into the vectors. The analysis of the Sanger sequencing indicated that cDNA fragments were properly inserted into each plasmid. Subsequently plasmid-carrying bacteria were propagated to isolate plasmids in a midiprep scale.

### 3.1.2. Cloning of FFAR4-receptor into pCMV ProLink vectors and pLXSN Neo

The PCR reaction was successful as shown by agarose gel electrophoresis (fragment of 1000 bp in length) (Figure 6, with the  $\lambda$  DNA marker (lane 1), the control pCMV-Entry-FFAR4short (2), PCR products (FFAR4short cDNA) flanked by cleavage sites EcoRI (5') and BamHI (3') (lane 3 and 4) or NheI (5') and HindIII (3', stop codon was deleted) (lane 5)).

After transformation and miniprep, one clone of each plasmid was selected for sequencing, which confirmed a correct insertion of the FFAR4short cDNA in the plasmid. Plasmid-carrying bacteria were propagated and plasmids were purified in a midiprep scale.

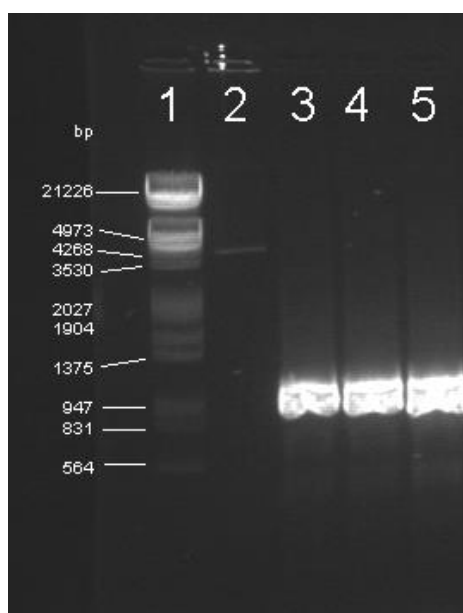


Figure 6. Agarose gel electrophoresis after amplification of human FFAR4short. The amplified cDNA can be seen in the lanes 3 to 8, while the controls  $\lambda$  DNA marker and pCMV-Entry-FFAR4short can be seen in the lanes 1 and 2, respectively.

### 3.2. Biological assays

#### 3.2.1 Validation of the ProLink sequences in $\beta$ -arrestin recruitment assay

CHO cells were transfected with the amplified plasmids applying the Lipofectamine® 2000 reagent (ThermoFisher Scientific, USA) to create the following stable transfected cell lines: ProLink1-, ProLink2-, ProLink2-ARMS1- and ProLink2-ARMS2-tagged human FFAR1. The transfected cells lines were then tested aiming to find the best-suited one for compound screening. Statistical analysis were not performed for validation experiments.

The CHO cells expressing the ProLink2-ARMS2-tagged human FFAR1 showed the highest signal and best signal:background ratio using 10  $\mu$ M of TUG-424 (Figure 7). These data suggest more efficient recruitment of  $\beta$ -arrestin in this cell line in comparison to the other ProLink-tagged cell lines, indicating that the CHO cells expressing the ProLink2-ARMS2-tagged FFAR1 are best suited for this assay system. The ARMS (Arrestin Recruitment Modulating Sequence) is a sequence of 18 to 21 amino acid containing GRK phosphorylation sites (DiscoverX, USA). As the binding of  $\beta$ -arrestin to the receptor is GRK-dependent, better  $\beta$ -arrestin recruitment

has been demonstrated when applying this vector; therefore it can improve low signal:background ratios (DiscoverX, USA).

The signal-to-background ratio of the other cell lines appears not to be sufficient. This result was reproducible also when using an adapted detection reagent (Figure 7, B). A reduction in the relative luminescence unit (RLU) was seen with the use of the adapted detection reagent. However there was no change in the signal-to-background ratio of the cell lines.

For CHO cells expressing the ProLink2-ARMS2 tagged FFAR1 the signal-to-background ratio using the commercially available and adapted detection reagent was 2.25 and 1.99, respectively. As the ratio for both treatments was comparable, the two detection reagents are interchangeable (Figure 7, C).

When performing the same tests at human FFAR4short, the best-suited cell lines for  $\beta$ -arrestin assays was shown to be the ProLink2-ARMS1-tagged and ProLink2-ARMS2-tagged FFAR4short (Figure 8). However, when comparing both, the ProLink2-ARMS1 cell line showed the best signal-to-background ratio. The same reduction in the RLU signal profile was demonstrated using the adapted detection reagent but without a change in the signalling background, as occurred with human FFAR1.

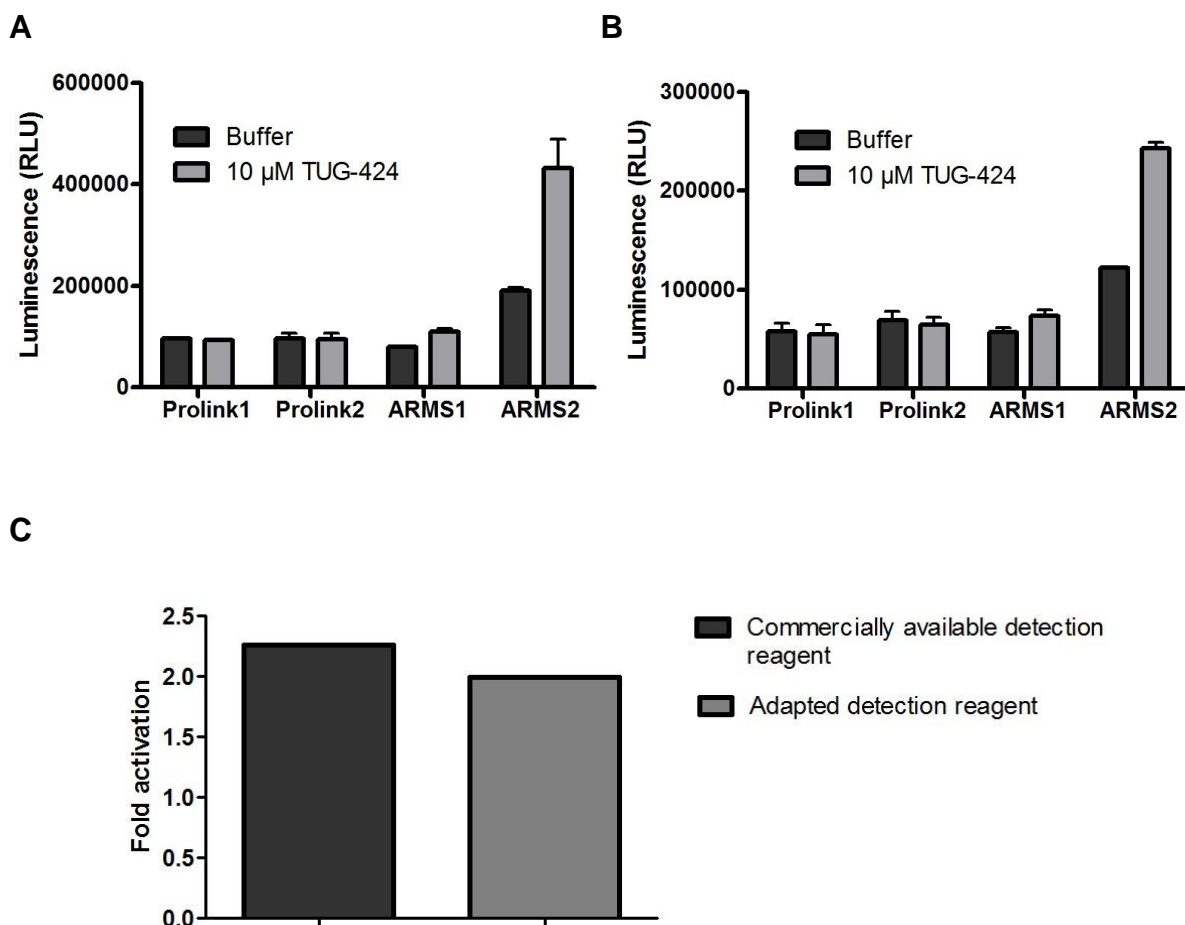


Figure 7.  $\beta$ -arrestin recruitment assays at human FFAR1, performed with commercially available (A) and adapted detection reagent (B). 10  $\mu$ M of TUG-424 was used to induce the signals. (C) The ratio of CHO cells expressing ProLink2-ARMS2 tagged human FFAR1 in the presence of 10  $\mu$ M of TUG-424 when comparing a commercially and an adapted detection reagent. Results are seen as mean  $\pm$  SEM (A, B) and mean values (C) from a single experiment performed in duplicate.

The signal-to-background ratio for CHO cells expressing the ProLink2-ARMS1-tagged FFAR4s using the commercially available and adapted detection reagent was 9.12 and 8.46, respectively (Figure 8, C). For CHO cells expressing the ProLink2-ARMS2-tagged FFAR4s using the commercially available and adapted detection reagent the ratio was 3.50 and 3.21, respectively. This data confirms that CHO cells expressing the ProLink2-ARMS1-tagged FFAR4s exhibit a better signal-to-background ratio using both commercially and adapted detection reagent.

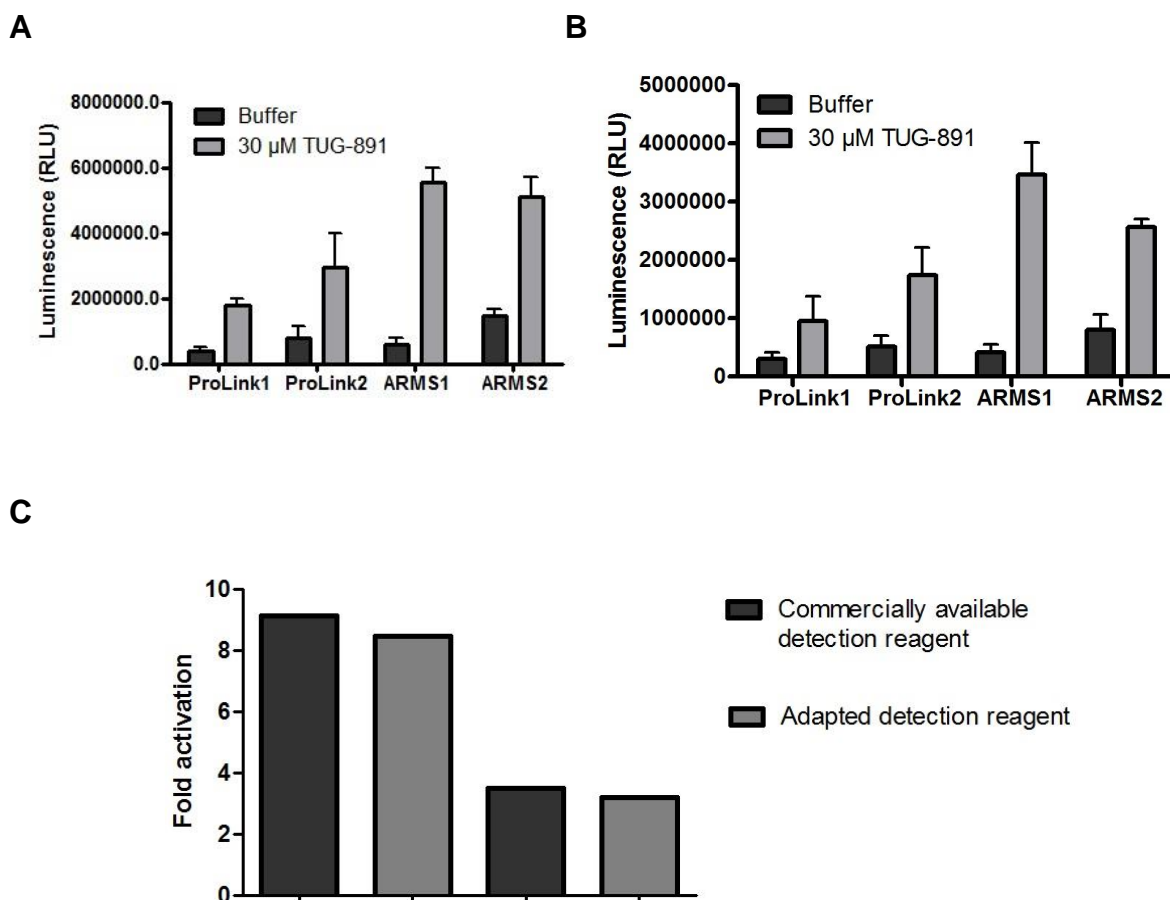


Figure 8.  $\beta$ -arrestin recruitment assays at human FFAR4s, performed with commercially available (A) and adapted detection reagent (B). The signals were induced by 30  $\mu$ M of TUG-891. (C) The ratio of ProLink2-ARMS1-tagged and ProLink2-ARMS2-tagged FFAR4s in the presence of 30  $\mu$ M of TUG-891, when comparing both commercially and adapted detection reagent. Results are seen as mean  $\pm$  SEM (A, B) and mean values (C) from a single experiment performed in duplicate.

### 3.2.1.2 Monoclonal cell cultures

Monoclonal cell cultures are composed of cells derived from a single cell of a polyclonal culture. Whereas for a polyclonal cell line one may observe changes in pharmacological responses in respective assays over time, this occurs less frequently using monoclonal cell lines. This effect may be due to a selective pressure on the polyclonal culture that could reduce the transgene expression over time, as the lower expressing cells may proliferate faster. Instead, the monoclonal cell culture is more likely to stabilize the transgene expression. Therefore these cell lines were chosen aiming to get better-suited cell lines, with a high signal and a better signal-to-

background ratio.

### 3.2.1.2.1. Evaluation of monoclonal cell lines signalling

#### 3.2.1.2 1.1 Human FFAR1

The monoclonal cell line 1C showed a higher signal and great signalling-to-background in the presence of 10  $\mu\text{M}$  of TUG-424, when compared to the other monoclonal cell lines (4B, 6G, 6H, and 10H) and also with the pooled cells (PC), indicating a well-suited cell line for the  $\beta$ -arrestin recruitment assay. The signal of the monoclonal cell lines 4B, 6G, 6H, and 10H, appeared not to be sufficient. Results are shown in Figure 9 (A). For the pooled cells and monoclonal cell line 1C the signal-to-background ratio was 2.30 and 4.22, respectively, confirming the monoclonal cell line 1C as the best-suited cell line for the  $\beta$ -arrestin assays (Figure 9, B).

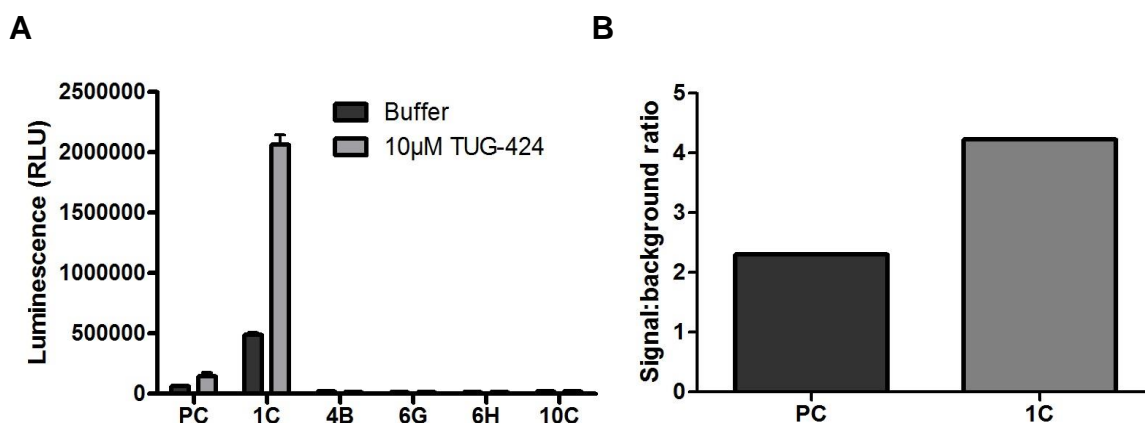


Figure 9.  $\beta$ -arrestin recruitment assays at human FFAR1 using (A) monoclonal cell lines (1C, 4B, 6G, 6H, 10C) and (B) signal-to-background ratio of the cell lines expressing ProLink2-ARMS2-tagged human FFAR1. PC: pooled cells. Signals were induced by 10  $\mu\text{M}$  of TUG-424. Results are seen as mean  $\pm$  SEM (A) and mean values (B) from a single experiment performed in duplicate.

#### 3.2.1.2.1.2 Human FFAR4s

##### 3.2.1.2.1.2.1 CHO cells expressing ProLink2-ARMS1-tagged human FFAR4short

Four monoclonal cell lines showed a high signal in the presence of 30  $\mu\text{M}$  of TUG-891 when compared to the other monoclonal cell lines (3A, 3C, 3F, 4A, 4C, 5D, and 5F) and also with the pooled cells (Figure 10, A).

Especially the monoclonal cell lines 4B and 4G appeared to have a better

signal:background ratios. For the pooled cells, monoclonal cells 4B and monoclonal cells 4G the signal-to-background ratio was 9.2, 3.8, and 9.9, respectively (Figure 10, B). Thereby the monoclonal cell line 4G appeared to be the best-suited even with a slightly lower signal in comparison with the monoclonal cell line 4B.

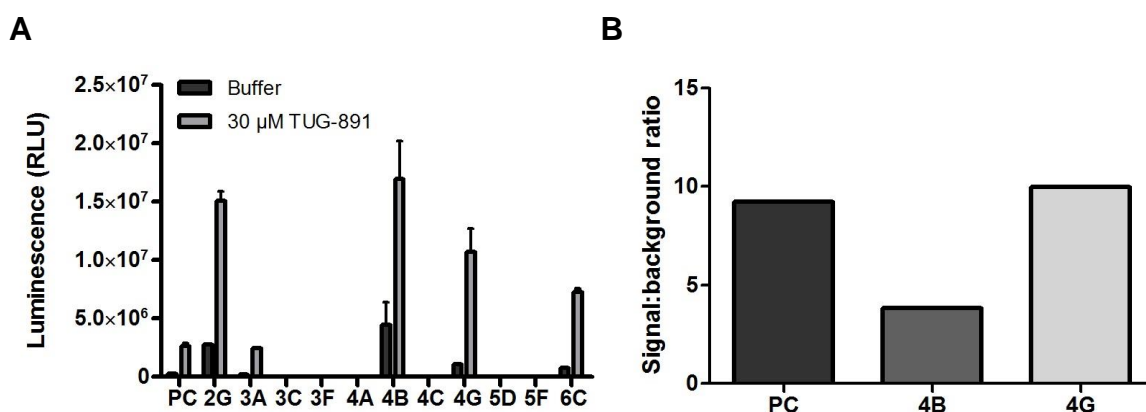


Figure 10.  $\beta$ -arrestin recruitment assays using (A) monoclonal cell lines expressing ProLink2-ARMS1-tagged human FFAR4s. (B) Signal-to-background ratio of the cell lines expressing ProLink2-ARMS1-tagged human FFAR4s. PC: pooled cells. Signals were induced by 30  $\mu$ M of TUG-891. Results are seen as mean  $\pm$  SEM (A) and mean values (B) from a single experiment performed in duplicate.

### 3.2.1.2.1.2.2 CHO cells expressing ProLink2-ARMS2-tagged human FFAR4short

For assays using CHO cells expressing ProLink2-ARMS2-tagged FFAR4s, three monoclonal cell lines showed a sufficient signal when compared to the pooled cells. However, only the monoclonal cell lines 4B and 4D demonstrated a higher signal than the pooled cells. The monoclonal cell lines 2F, 3F, 4C, 5A, 5D, and 6H had no sufficient signal. Results are shown in Figure 11 (A).

For the pooled cells, monoclonal cells 4B and monoclonal cells 4D the signal-to-background ratio was 4.33, 2.14 and 4.83, respectively (Figure 11, B). This data confirms the monoclonal cell line 4D as the better-suited cell line to perform  $\beta$ -arrestin assays.



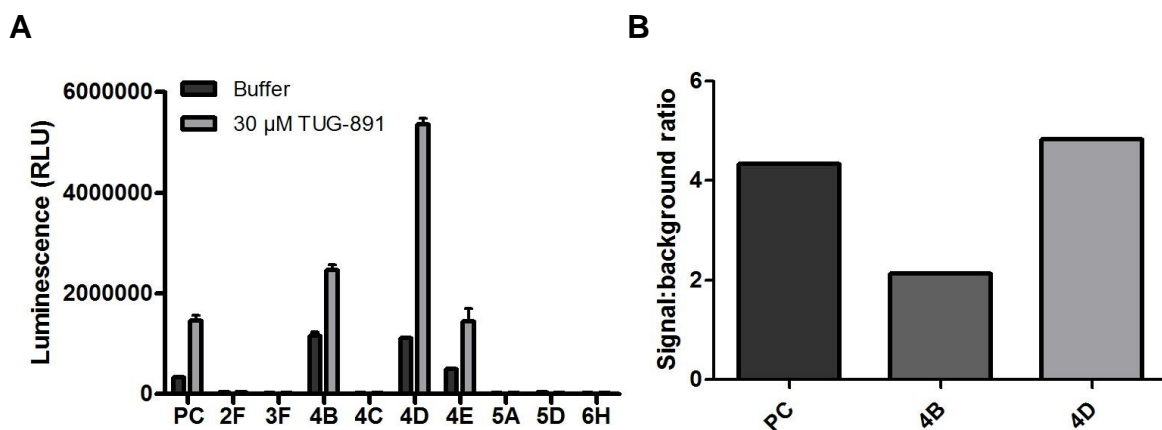


Figure 11.  $\beta$ -arrestin recruitment assays using (A) monoclonal cell lines expressing human FFAR4s tagged with ProLink2-ARMS2. (B) Signal:background ratio of monoclonal cell lines. PC: pooled cells. Signals were induced by 30  $\mu$ M of TUG-891. Results are seen as mean  $\pm$  SEM (A) and mean values (B) from a single experiment performed in duplicate.

Although the ProLink2-ARMS1 tagged human FFAR4s showed a better signal-to-background ratio and a higher absolute signal, the signals induced by activation of the ProLink2-ARMS2-tagged receptor appeared to be more stable. Therefore the generated monoclonal cell lines for hFFAR1 and hFFAR4s, which showed excellent signal-to-background ratios and high absolute signals, were chosen for the determination of concentration dose-response curves to show which ProLink tag would be better suited for performing the  $\beta$ -arrestin assays.

### 3.2.1.2.2 Dose-response curves using monoclonal cells

#### 3.2.1.2.2.1 Human FFAR1

The monoclonal cells were tested under different conditions, with the purpose to find the best assay protocol. Briefly, 30000 cells / well were plated, and the medium was replaced by medium without FBS 4 hours after cell plating. In the standard condition, cells were treated by addition of 10  $\mu$ L of agonist solution (10 % DMSO, 90 % F12 medium), while in the condition II, 1  $\mu$ L of agonist solution in pure DMSO was used. The final volume in both conditions was 100  $\mu$ L / well.

When testing both conditions, the monoclonal cell line 1C showed not adequate results and even at the highest agonist concentration, the concentration-response curve did not reach a plateau (Figure 12).

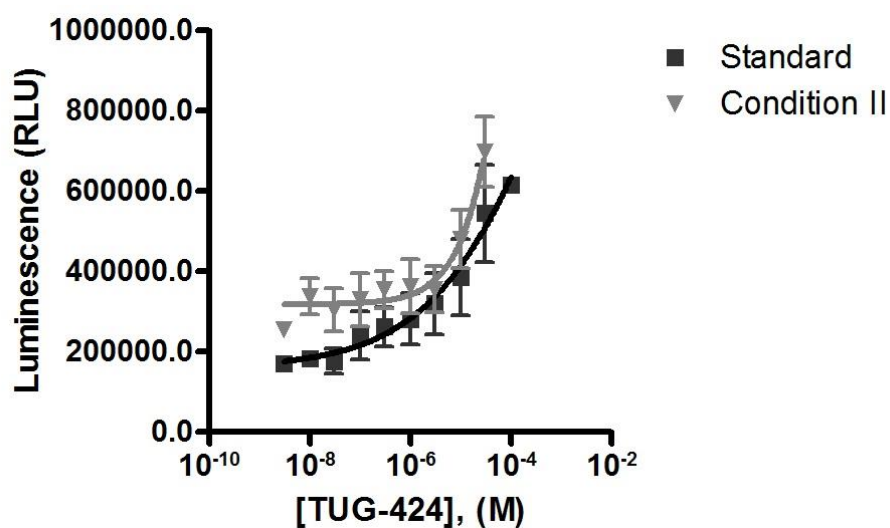


Figure 12.  $\beta$ -arrestin recruitment assay at human FFAR1, performed under different conditions. Under the standard condition, 10  $\mu$ L of agonist solution (10 % DMSO, 90 % F12 medium) was used. The treatment in the condition II was made by addition of 1  $\mu$ L of agonist solution in pure DMSO. For both conditions, the medium was added to complete a final volume of 100  $\mu$ L / well. Results are seen as mean  $\pm$  SEM from a single experiment performed in duplicate.

### 3.2.1.2.2.2. Human FFAR4s

#### 3.2.1.2.2.2.1 CHO cells expressing ProLink2-ARMS1-tagged human FFAR4s

The concentration-response curves using CHO cells expressing ProLink2-ARMS1-tagged human FFAR4s showed a similar profile as with CHO cells expressing ProLink2-ARMS2-tagged hFFAR1. Again, even in the presence of a high concentration of the agonist (100  $\mu$ M), for none of the curves, a plateau could be reached (Figure 13). This suggests that this cell line is not suitable to perform  $\beta$ -arrestin assays for compound screening, especially since a plateau could previously be reached for polyclonal cell line and the reference agonist has been described as potent in the literature ( $EC_{50}$  0.1  $\mu$ M) (HUDSON et al., 2013; SHIMPUKADE et al., 2012).

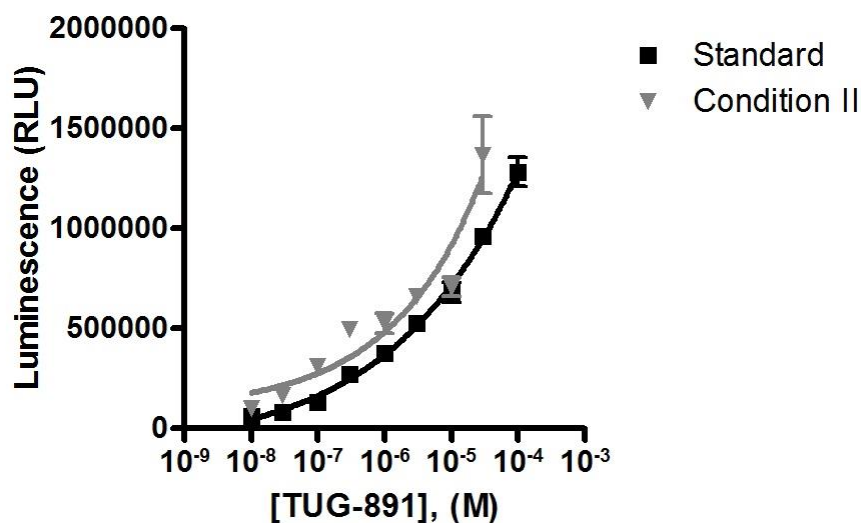


Figure 13.  $\beta$ -arrestin recruitment assays at human FFAR4s, performed under two different conditions. In the standard condition, 10  $\mu$ L of agonist solution (10 % DMSO, 90 % F12 medium) was used, while the treatment in the condition II was made by addition of 1  $\mu$ L of agonist solution in pure DMSO. For both conditions, the final volume was 100  $\mu$ L / well. Data was plotted as mean  $\pm$  SEM from a single experiment performed in duplicate.

#### 3.2.1.2.2.1 CHO cells expressing ProLink2-ARMS2-tagged human FFAR4s

The monoclonal CHO cells expressing ProLink2-ARMS2-tagged human FFAR4s 4D showed the best results of the three monoclonal cell lines. Under condition II a sigmoid curve could be determined which barely reached a plateau. Nevertheless, the results were unsatisfactory, as shown in Figure 14.

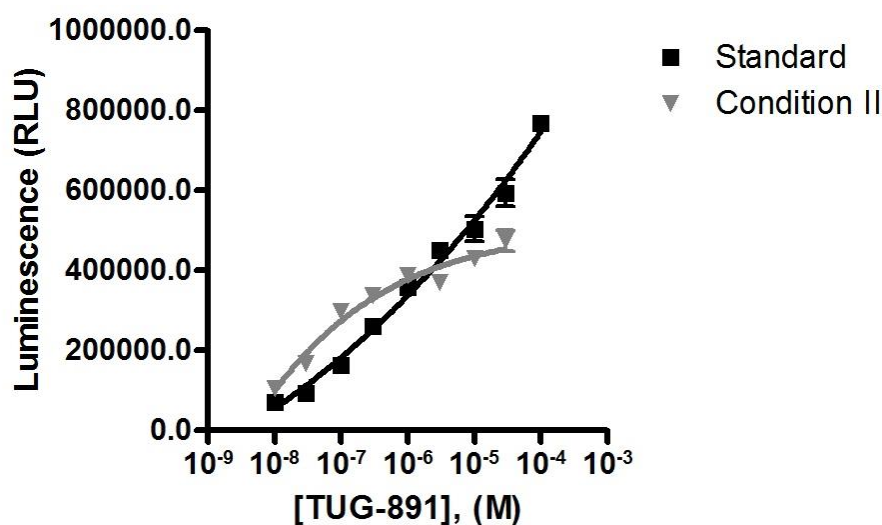


Figure 14.  $\beta$ -arrestin recruitment assays at ProLink2-ARMS2-tagged human FFAR4s, performed under standard condition (10  $\mu$ L of agonist solution in 10 % DMSO / 90 % F12 medium) and condition II (1  $\mu$ L of agonist solution in pure DMSO), for a final volume of 100  $\mu$ L / well. Results are shown as mean  $\pm$  SEM from a single experiment performed in duplicate.

### 3.2.2 Evaluation of polyclonal cell lines signalling

Despite the excellent signal-to-background ratio of the previously described monoclonal cell lines, satisfactory results in concentration-response curves could not be archived using these cells. Therefore polyclonal cells were used to perform  $\beta$ -arrestin recruitment assays.

A concentration-response curve could not be determined using the polyclonal CHO cells stably expressing ProLink2-ARMS2-tagged human FFAR1. The assay using this cell line appeared not to be stable and reproducible which can be observed when the results of two independent experiments are compared (Figure 15, A). The lack of response in this assay could be explained by the TUG-424's biased agonism. This was also reported for TAK-875, which showed to be partially Gq-dependent (MANCINI et al., 2015). Biased agonism has been referred as the capability of chemical structures of specific ligands to stabilize the conformation of a receptor, influencing its affinity for one signalling pathway over another (RANKOVIC; BRUST; BOHN, 2016). Therefore, the agonism of TUG-424 at FFAR1 may display a higher affinity for other effectors such as G $\alpha_{q/11}$  than for the  $\beta$ -arrestin pathway.

Therefore a different assay system must be used for screening compounds at this receptor, such as the calcium mobilization assay, as the FFAR1 was also described to be Gq-coupled (BRISCOE et al., 2003; ITOH et al., 2003).

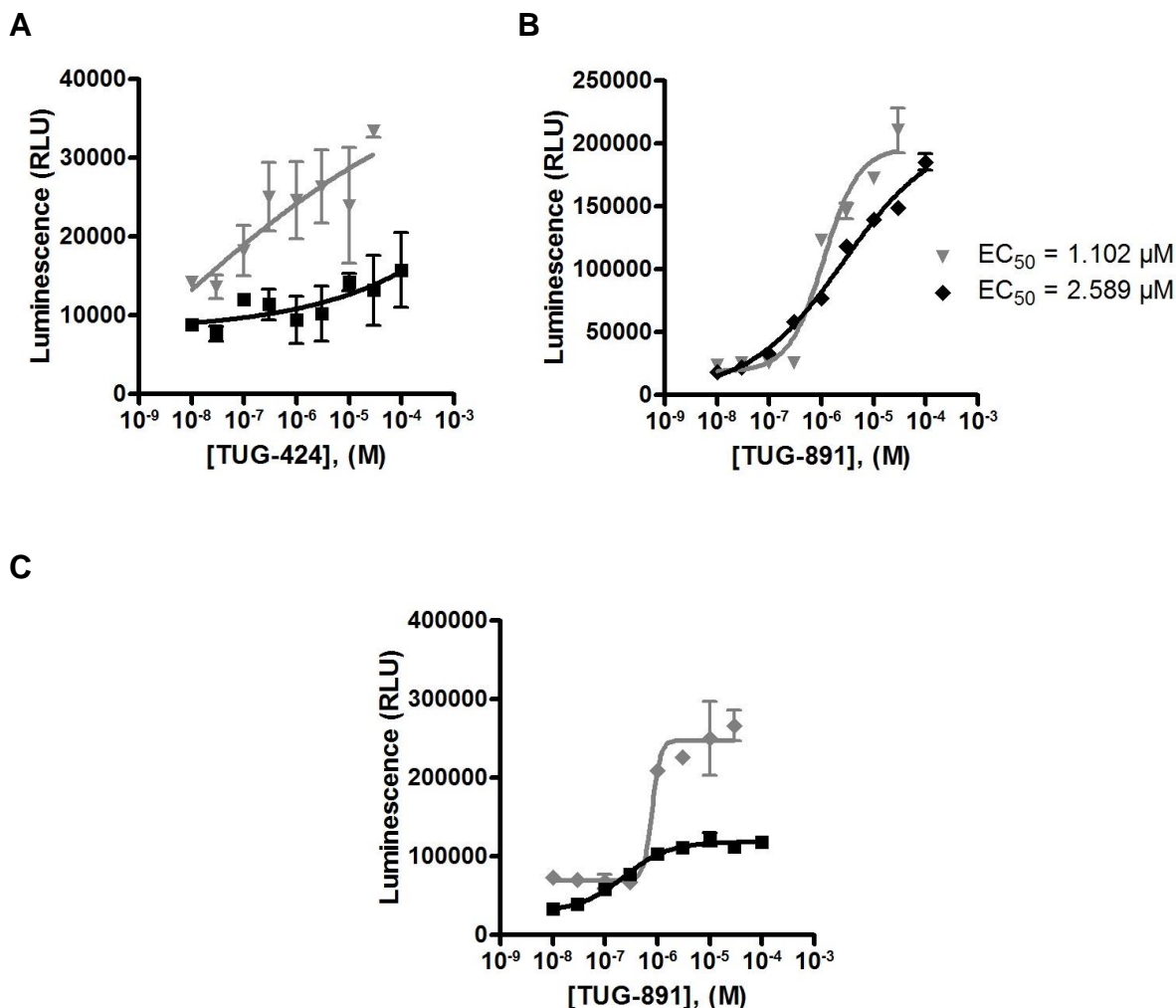


Figure 15.  $\beta$ -arrestin recruitment assays using polyclonal CHO cell line transfected with human (A) FFAR1, (B) FFAR4s tagged ProLink2-ARMS1, (C) FFAR4s tagged ProLink2-ARMS2. Results of two independent assays were plotted for curve comparison.

In contrast to the human FFA1 receptor, a concentration-response curve could be determined using CHO cells expressing ProLink2-ARMS1-tagged human FFAR4s (Figure 15, B). This result could be confirmed in a second independent assay. There was no significant change in the EC<sub>50</sub> value of both curves, suggesting this cell line as the better suited for  $\beta$ -arrestin recruitment assays with human FFAR4s.

Even though a concentration-response curve could be determined in the first assay using ProLink2-ARMS2-tagged hFFAR4s cells, a lack of reproducibility could be observed (Figure 15, C). Therefore, the ProLink2-ARMS1-tagged human FFAR4s cell line is the best-suited cell line for screenings, reinforcing the results shown previously.

Since better results were achieved using CHO cells expressing ProLink2-ARMS1-tagged human FFAR4s, the cells were tested for the best assay condition (Figure 16). The transfected CHO cells preincubated with HBSS (condition IV) showed a higher absolute signal when compared to the same cell line preincubated with F12 medium (condition III). However, the condition III showed a better signal-to-background ratio, appearing then to be the better-suited for performing  $\beta$ -arrestin recruitment assays with ProLink2-ARMS1-tagged human FFA4s receptor. When compared with condition II (See Figure 14) both conditions III and IV showed a better curve profile and signal-to-background ratio, confirming them as better-suited for screening.

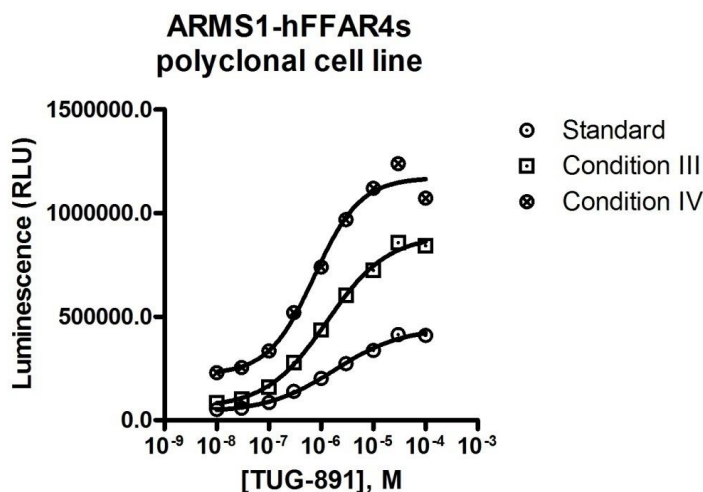


Figure 16.  $\beta$ -arrestin recruitment assays at ProLink2-ARMS1-tagged human FFAR4s performing under three different conditions. In standard condition, the medium was exchanged for 90  $\mu$ L / well free serum media 4 h after cell plating, while in condition III medium was exchanged 4h before the assay. In condition IV the medium was replaced with 90  $\mu$ L / well of HBSS 4 h before the assay. For all the conditions the treatment was made by addition of 10  $\mu$ L of agonist solution (10 % DMSO, 90 % F12 medium). Data is shown as mean values of a single experiment performed in duplicate.

Therefore a dose-response curve for TUG-891 at ProLink2-ARMS1 tagged human FFAR4s was determined using the third assay condition (Figure 17). The  $EC_{50}$  of TUG-891 was found to be 1.83  $\mu$ M, and it differed approximately 10-fold to the one reported by HUDSON et al. (2013) in a BRET  $\beta$ -arrestin 1 recruitment assay. However, such differences in the  $EC_{50}$  value have been reported regarding the respective assay system (HUDSON et al., 2013; SHIMPUKADE et al., 2012).

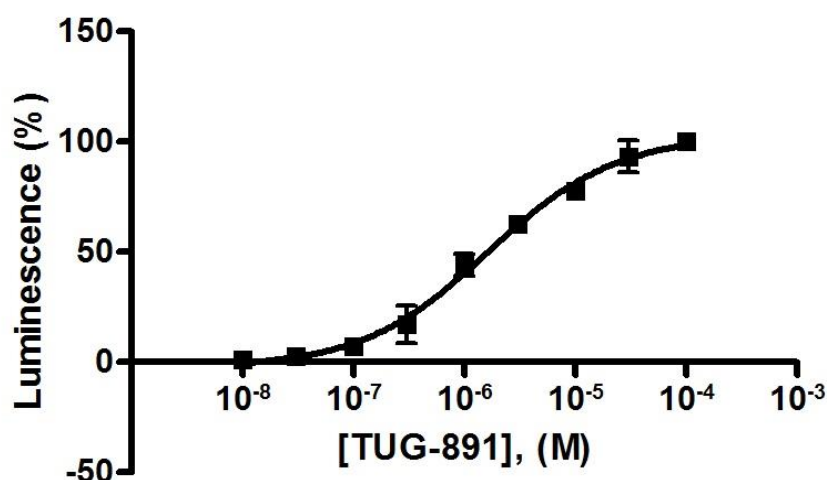


Figure 17. Dose-response curve of TUG-891 in  $\beta$ -arrestin recruitment assay performed with CHO cells expressing human FFAR4s. TUG-891 was tested at concentrations from 100 to 0.01  $\mu$ M.  $EC_{50}$  1.83  $\pm$  0.43  $\mu$ M. Mean values  $\pm$  SEM from three independent experiments performed in duplicates are shown.

### 3.2.2 Calcium mobilization assay

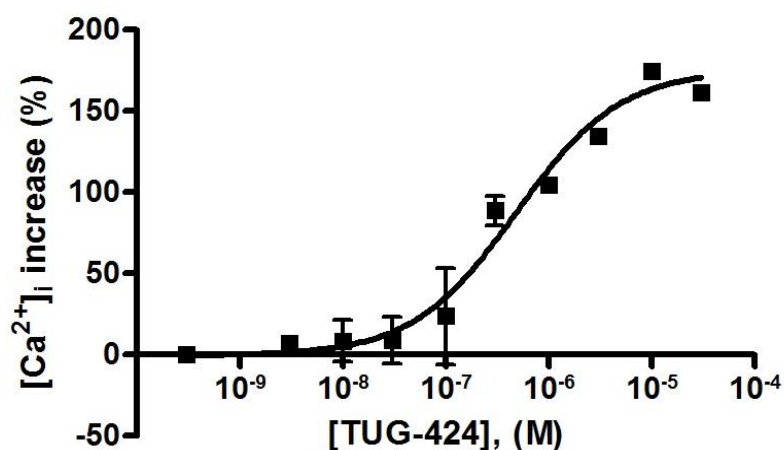
Since the  $\beta$ -arrestin assays at the human FFAR1 were irreproducible and inconclusive, calcium mobilization assays were chosen to characterize this receptor. Studies have been linking this type of assay to GPCRs (CAERS et al., 2014; SCHNELL; SCHAEFER; SCHÖFL, 2007), which would be an advantage when comparing the obtained results with the ones from literature.

To check the inherent activation of the non-transfected cell lines, TUG-424 was tested, and it did not induce any effect in neither native CHO-K1 cell or untransfected 1321N1 astrocytoma cells. Therefore, we can presume that there is no unspecific background in these cells.

For the transfected CHO cells, the results were not adequate and

reproducible, invalidating this cell line for compound screening. This also could be observed for other receptors in the working group, possibly due to low expression levels of suitable Gq proteins in this cell line. In contrast, transfected 1321N1 astrocytoma cells showed a reproducible response to the agonist TUG-424. An  $EC_{50}$  value of 0.495  $\mu$ M could be determined (Figure 18).

**A**



**B**

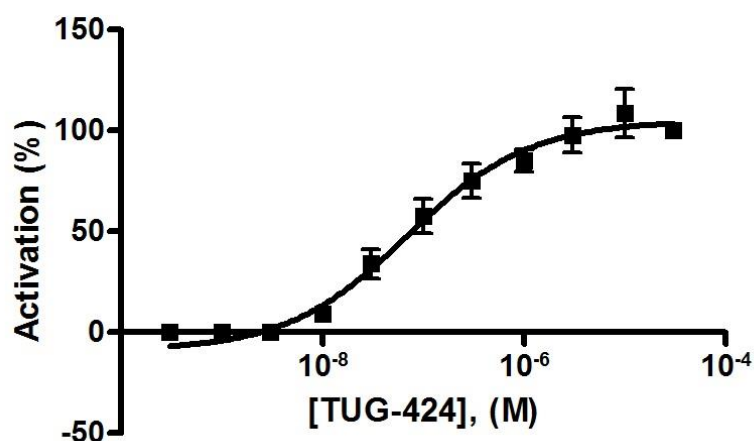


Figure 18. Dose-response curves of TUG-424 in calcium mobilization assays performed with 1321N1 astrocytoma cells expressing human FFAR1. **(A)** Applying the NOVOSTar® Fluorometer.  $EC_{50}$   $0.495 \pm 0.076$   $\mu$ M. Signal was normalized to effects of 100  $\mu$ M carbachol. Results are shown as mean  $\pm$  SEM from two independent experiments performed in duplicates. **(B)** Using the FlexStation® Fluorometer.  $EC_{50}$   $0.144 \pm 0.048$   $\mu$ M. Mean values  $\pm$  SEM from four independent experiments performed in triplicates are shown.



However, the assay system appeared not to be stable enough since in some assays no signals could be detected, not even by the assay standard agonist carbachol. In this way, another calcium mobilization assay protocol at this receptor was performed, i.e., with adherent cells using a different dye (Fluo-4) and the Flexstation® fluorometer, to provide results with higher reproducibility.

Using the Flexstation® Fluorometer, the EC<sub>50</sub> of TUG-424 previously obtained was confirmed by a concentration-response curve, staying roughly at similar molar range (Figure 18, B) (CHRISTIANSEN et al., 2008; SHIMPUKADE et al., 2012). The assay showed to be steady with high reproducibility, enforcing it as a suited calcium mobilization platform for the compound screening.

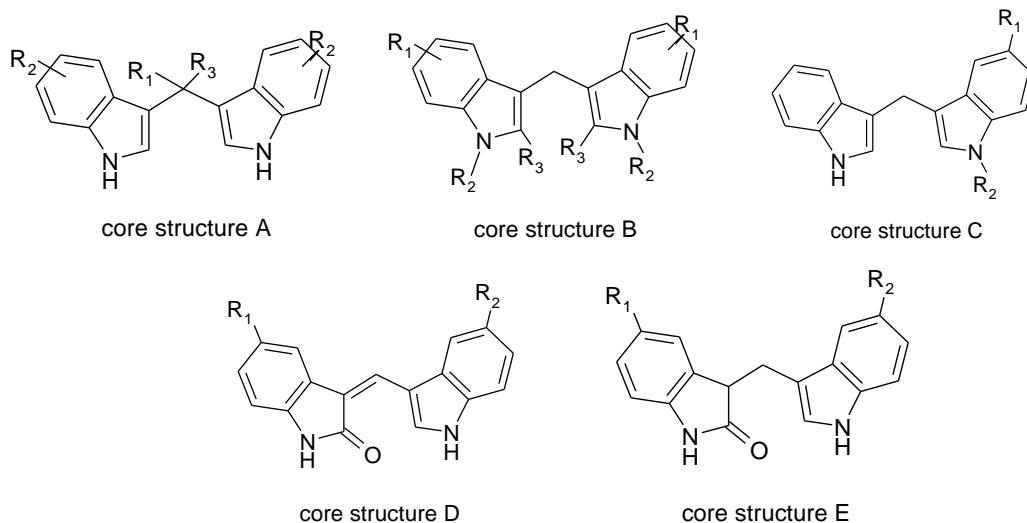
### 3.3 Compound screening

After establishing transfected cell lines and assay system protocols, the compounds could be screened at the receptors. Initially, the compounds were tested at a concentration of 10 µM, and the signals were normalized by the signal of 10 µM of TUG-424 (for FFAR1) and 30 µM of TUG-891 (for FFAR4) in agonist screening. For antagonist assays compounds were screened versus 1 µM of TUG-424 (for FFAR1) and 4 µM of TUG-891 (for FFAR4). Dose-response curves were made for compounds showing effects or inhibitions of more than 50 % and EC<sub>50</sub> or IC<sub>50</sub> were calculated.

#### 3.3.1 Screening of diindolylmethane derivatives (Yazh library, AK Prof. Dr. Müller) at human FFA1 receptor and human FFAR4short

The diindolylmethane derivatives were screened at the receptors FFAR1 and FFAR4, once 3,3'-diindolylmethane was found as an agonist at GPR84, another free fatty acid receptor sharing similar endogenous ligand preference (TAKEDA et al., 2003). None of the diindolylmethane derivatives were found to have agonist effects at the receptors FFAR1 and FFAR4. Also, none of the derivatives could inhibit FFAR4 activity. However, four ligands were found to antagonize FFAR1. 10-ethyl- (**Yazh 16**), 10-propyl- (**Yazh 4**), 10-isopropyl- (**Yazh 3**) and 4,4'-difluoro-3,3'-diindolylmethane (**Yazh 357**) could inhibit the human FFAR1 moderately. Results are shown in Table 5.

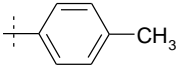
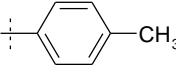
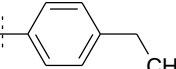
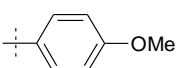
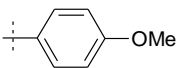
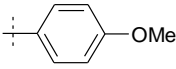
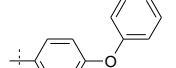
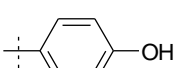
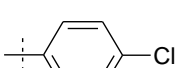
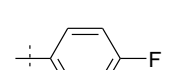
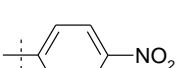
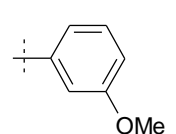
**Table 5. Potency of diindolylmethane derivatives (Yazh library) at the human FFAR1 and FFAR4.**



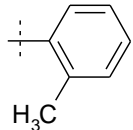
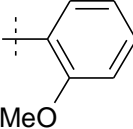
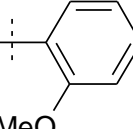
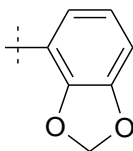
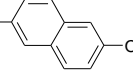
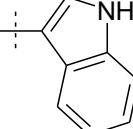
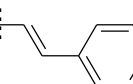
(Table to be continued)

Ligand	Structure	FFAR1		FFAR4s			
		Agonist screening <sup>a</sup> EC <sub>50</sub> ± SEM (μM)	Antagonist screening <sup>a</sup> IC <sub>50</sub> ± SEM (μM)	Agonist screening <sup>c</sup> EC <sub>50</sub> ± SEM (μM)	Antagonist screening <sup>c</sup> (% inhibition ± SEM) <sup>d</sup>		
TUG-424		<b>0.144 ± 0.048</b>	-	-	-		
TUG-891		-	-	<b>1.83 ± 0.43</b>	-		
Core Structure A							
Yazh	R1	R2	R3	Agonist screening <sup>a</sup> EC <sub>50</sub> ± SEM (μM)	Antagonist screening <sup>a</sup> IC <sub>50</sub> ± SEM (μM)	Agonist screening <sup>c</sup> EC <sub>50</sub> ± SEM (μM)	Antagonist screening <sup>c</sup> (% inhibition ± SEM) <sup>d</sup>
16		H	-	(8 ± 3)	<b>1.76 ± 0.33</b>	(7 ± 3)	(32 ± 15)
04		H	-	(-0 ± 6)	<b>8.81 ± 0.16</b>	(2 ± 1)	(15 ± 22)
02		H	-	(1 ± 2)	(14 ± 2)	(0 ± 0)	(22 ± 11)
05		H	-	(0 ± 1)	(19 ± 8)	(-0 ± 0)	(14 ± 11)

(Table continued)

Yazh	R1	R2	R3	FFAR1		FFAR4s	
				Agonist screening <sup>a</sup>	Antagonist screening <sup>a</sup>	Agonist screening <sup>c</sup>	Antagonist screening <sup>c</sup>
				EC <sub>50</sub> ± SEM (μM)	IC <sub>50</sub> ± SEM (μM)	EC <sub>50</sub> ± SEM (μM)	Antagonist screening <sup>c</sup> (% inhibition ± SEM) <sup>d</sup>
				(% effect ± SEM) <sup>b</sup>	(% inhibition ± SEM) <sup>b</sup>	(% effect ± SEM) <sup>d</sup>	
103		5-OCH <sub>3</sub>	-	(0 ± 6)	(18 ± 8)	(- 0 ± 1)	(29 ± 5)
86		H	CH <sub>3</sub>	(-2 ± 4)	(11 ± 14)	(- 0 ± 0)	(35 ± 9)
15		H	-	(2 ± 2)	(32 ± 10)	(0 ± 0)	(39 ± 5)
10		H	-	(6 ± 2)	(26 ± 6)	(- 0 ± 1)	(21 ± 10)
104		5-OCH <sub>3</sub>	-	(-4 ± 1)	(4 ± 7)	(1 ± 0)	(27 ± 16)
83		H	CH <sub>3</sub>	(12 ± 15)	(13 ± 11)	(- 0 ± 1)	(32 ± 18)
11		H	-	(6 ± 1)	(30 ± 9)	(1 ± 1)	(26 ± 12)
20		H	-	(0 ± 6)	(21 ± 14)	(2 ± 1)	(29 ± 7)
1		H	-	(3 ± 3)	(47 ± 7)	(3 ± 1)	(18 ± 9)
21		H	-	(-1 ± 3)	(26 ± 5)	(0 ± 0)	(43 ± 8)
06		H	-	(2 ± 1)	(22 ± 6)	(0 ± 1)	(24 ± 12)
77		H	-	(0 ± 2)	(19 ± 6)	(0 ± 1)	(10 ± 10)

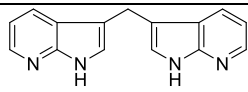
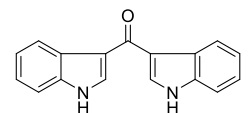
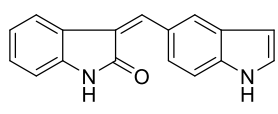
(Table continued)

Yazh	R1	R2	R3	FFAR1		FFAR4s	
				Agonist screening <sup>a</sup>	Antagonist screening <sup>a</sup>	Agonist screening <sup>c</sup>	Antagonist screening <sup>c</sup>
				EC <sub>50</sub> ± SEM (μM)	IC <sub>50</sub> ± SEM (μM)	EC <sub>50</sub> ± SEM (μM)	EC <sub>50</sub> ± SEM (μM)
				(% effect ± SEM) <sup>b</sup>	(% inhibition ± SEM) <sup>b</sup>	(% effect ± SEM) <sup>d</sup>	(% inhibition ± SEM) <sup>d</sup>
79		H	-	(-4 ± 4)	(5 ± 8)	(0 ± 2)	(43 ± 21)
76		H	-	(8 ± 10)	(11 ± 11)	(0 ± 1)	(27 ± 10)
80		H	CH <sub>3</sub>	(5 ± 3)	(17 ± 5)	(-0 ± 1)	(19 ± 12)
19		H	-	(-3 ± 6)	(27 ± 13)	(1 ± 0)	(35 ± 8)
22		H	-	(5 ± 3)	(28 ± 6)	(0 ± 0)	(24 ± 15)
09		H	-	(7 ± 2)	(38 ± 9)	(0 ± 0)	(13 ± 10)
12		H	-	(14 ± 3)	(29 ± 3)	(1 ± 0)	(15 ± 24)

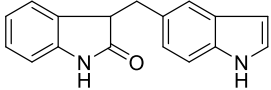
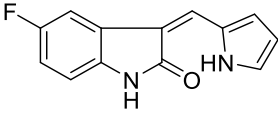
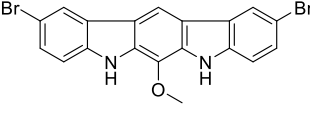
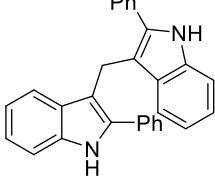
(Table continued)

Core structure B							
Yazh	R1	R2	R3	FFAR1		FFAR4s	
				<u>Agonist screening</u> <sup>a</sup> (% effect ± SEM) <sup>b</sup>	<u>Antagonist screening</u> <sup>a</sup> IC <sub>50</sub> ± SEM (μM) (% inhibition ± SEM) <sup>b</sup>	<u>Agonist screening</u> <sup>c</sup> (% effect ± SEM) <sup>d</sup>	<u>Antagonist screening</u> <sup>c</sup> (% inhibition ± SEM) <sup>d</sup>
25	H	H	H	(-0 ± 3)	(27 ± 5)	(2 ± 1)	(19 ± 6)
143	H	CH <sub>3</sub>	H	(-0 ± 2)	(9 ± 12)	(0 ± 1)	(33 ± 1)
27	H	H	CH <sub>3</sub>	(-3 ± 4)	(-14 ± 2)	(0 ± 0)	(40 ± 6)
456	4-CH <sub>3</sub>	H	H	(-4 ± 2)	(49 ± 16)	(3 ± 0)	(-7 ± 8)
176	4-OCH <sub>3</sub>	H	H	(-5 ± 6)	(9 ± 8)	(-1 ± 2)	(28 ± 3)
357	4-F	H	H	(1 ± 1)	<b>6.49 ± 1.84</b>	(2 ± 1)	(44 ± 5)
457	4-Cl	H	H	(1 ± 1)	(50 ± 13)	(4 ± 0)	(-12 ± 4)
417	4-NO <sub>2</sub>	H	H	(1 ± 6)	(20 ± 10)	(0 ± 1)	(15 ± 3)
131	5-CH <sub>3</sub>	H	H	(-7 ± 5)	(4 ± 14)	(-5 ± 4)	(40 ± 4)
105	5-OCH <sub>3</sub>	H	H	(1 ± 1)	(18 ± 8)	(1 ± 1)	(22 ± 5)
160	5-F	H	H	(-2 ± 3)	(49 ± 12)	(-2 ± 3)	(32 ± 3)
130	5-Cl	H	H	(3 ± 0)	(8 ± 15)	(-1 ± 2)	(38 ± 5)
116	5-Br	H	H	(0 ± 1)	(1 ± 9)	(-1 ± 3)	(33 ± 8)
185	5-CN	H	H	(4 ± 4)	(46 ± 10)	(7 ± 0)	(24 ± 1)
297	5-NO <sub>2</sub>	H	H	(10 ± 7)	(33 ± 7)	(3 ± 1)	(34 ± 3)
151	5-COOCH <sub>3</sub>	H	H	(-2 ± 2)	(5 ± 13)	(3 ± 0)	(23 ± 4)
232	5-CHO	H	H	(-0 ± 1)	(46 ± 13)	(2 ± 1)	(22 ± 7)
159	5-COOH	H	H	(-2 ± 1)	(-35 ± 18)	(2 ± 1)	(19 ± 5)
117	5-OCH <sub>2</sub> Ph	H	H	(3 ± 4)	(-9 ± 9)	(-2 ± 1)	(30 ± 6)
106	6-CH <sub>3</sub>	H	H	(-4 ± 5)	(7 ± 16)	(-1 ± 2)	(30 ± 2)
165	6-OCH <sub>3</sub>	H	H	(-5 ± 4)	(14 ± 11)	(0 ± 0)	(27 ± 5)
358	6-F	H	H	(4 ± 1)	(22 ± 21)	(5 ± 1)	(33 ± 4)
428	6-Cl	H	H	(11 ± 14)	(40 ± 11)	(21 ± 5)	(11 ± 6)
175	7-OCH <sub>3</sub>	H	H	(-4 ± 7)	(-6 ± 13)	(-1 ± 1)	(28 ± 4)
381	7-F	H	H	(2 ± 2)	(21 ± 13)	(0 ± 1)	(33 ± 3)
118	4,6-Cl	H	H	(-7 ± 8)	(9 ± 6)	(-1 ± 2)	(38 ± 4)
383	5-F, 6-Cl	H	H	(3 ± 3)	(47 ± 6)	(12 ± 7)	(9 ± 6)
582	4,5-F	H	H	(7 ± 5)	(27 ± 12)	(2 ± 1)	(-8 ± 9)
586	5,6-F	H	H	(3 ± 2)	(35 ± 18)	(10 ± 5)	(10 ± 13)
413	Ph	H	H	(5 ± 7)	(21 ± 6)	(-0 ± 0)	(12 ± 3)

(Table continued)

Core structure C						
Yazh	R1	R2	FFAR1		FFAR4s	
			Agonist screening <sup>a</sup> EC <sub>50</sub> ± SEM (μM)	Antagonist screening <sup>a</sup> IC <sub>50</sub> ± SEM (μM)	Agonist screening <sup>c</sup> EC <sub>50</sub> ± SEM (μM)	Antagonist screening <sup>c</sup> (% inhibition ± SEM) <sup>d</sup>
242	H	CH <sub>3</sub>	(2 ± 4)	(4 ± 8)	(- 2 ± 3)	(12 ± 10)
184	OCH <sub>3</sub>	H	(7 ± 1)	(13 ± 6)	(- 1 ± 0)	(29 ± 0)
244	F	H	(8 ± 3)	(46 ± 11)	(2 ± 0)	(35 ± 5)
195	COOCH <sub>3</sub>	H	(-4 ± 1)	(4 ± 8)	(- 0 ± 1)	(35 ± 5)
198	COOH	H	(4 ± 4)	(-0 ± 22)	(- 0 ± 0)	(14 ± 2)
Core structure D						
Yazh	R1	R2	(% effect ± SEM) <sup>b</sup>	(% inhibition ± SEM) <sup>b</sup>	(% effect ± SEM) <sup>d</sup>	(% inhibition ± SEM) <sup>d</sup>
260	H	H	(-2 ± 3)	(37 ± 13)	(- 6 ± 5)	(51 ± 4)
250	H	F	(4 ± 1)	(38 ± 10)	(- 5 ± 3)	(42 ± 3)
236	H	OCH <sub>3</sub>	(-7 ± 4)	(47 ± 9)	(- 4 ± 4)	(45 ± 4)
247	F	F	(5 ± 2)	(19 ± 6)	(- 5 ± 3)	(42 ± 3)
246	F	OCH <sub>3</sub>	(5 ± 4)	(13 ± 6)	(- 4 ± 3)	(40 ± 3)
Core structure E						
Yazh	R1	R2	(3 ± 6)	(28 ± 5)	(- 4 ± 3)	(28 ± 6)
237	H	OCH <sub>3</sub>	(3 ± 6)	(28 ± 5)	(- 4 ± 3)	(28 ± 6)
248	F	F	(-5 ± 1)	(16 ± 8)	(- 3 ± 3)	(25 ± 5)
249	F	OCH <sub>3</sub>	(-6 ± 8)	(32 ± 12)	(- 4 ± 3)	(27 ± 6)
Other derivatives structures						
Yazh	Structure		(-6 ± 0)	(12 ± 11)	(2 ± 1)	(20 ± 7)
186			(-6 ± 0)	(12 ± 11)	(2 ± 1)	(20 ± 7)
359			(4 ± 3)	(9 ± 1)	(1 ± 1)	(26 ± 8)
238			(-8 ± 2)	(32 ± 13)	(- 4 ± 3)	(43 ± 6)

(Table concluded)

Yazh	Structure	FFAR1		FFAR4s	
		Agonist screening <sup>a</sup> EC <sub>50</sub> ± SEM (μM) (% effect ± SEM) <sup>b</sup>	Antagonist screening <sup>a</sup> IC <sub>50</sub> ± SEM (μM) (% inhibition ± SEM) <sup>b</sup>	Agonist screening <sup>c</sup> EC <sub>50</sub> ± SEM (μM) (% effect ± SEM) <sup>d</sup>	Antagonist screening <sup>c</sup> (% inhibition ± SEM) <sup>d</sup>
239		(-6 ± 4)	(17 ± 5)	(- 2 ± 2)	(27 ± 5)
261		(4 ± 8)	(-3 ± 10)	(- 7 ± 4)	(42 ± 3)
107		(3 ± 6)	(3 ± 12)	(- 3 ± 4)	(26 ± 8)
414		(6 ± 11)	(37 ± 12)	(- 2 ± 1)	(27 ± 8)

<sup>a</sup> Screening of diindolylmethane derivatives was performed at a concentration of 10 μM at human FFAR1 receptor. For [Ca<sup>2+</sup>] mobilization assays the receptor was expressed in an astrocytoma cell line.

<sup>b</sup> Effects were normalized to 10 μM (agonist screening) and 1 μM (~ EC<sub>80</sub>, antagonist screening) of TUG-424.

<sup>c</sup> Screening of diindolylmethane derivatives was performed at a concentration of 10 μM at human FFA4short receptor. For β-arrestin assays the receptor was expressed in a CHO β-arrestin cell line which is part of an open assay system (PathHunter®, DiscoverX).

<sup>d</sup> Effects were normalized to 30 μM (agonist screening) and 4 μM (~ EC<sub>80</sub>, antagonist screening) of TUG-891.

Whereas the simple and prototypic compound **Yazh 25** was virtually inactive, the introduction of an ethyl substituent (**Yazh 16**) was shown to be very beneficial for antagonistic potency (IC<sub>50</sub> value 1.76 μM). However further elongation of the introduced alkyl chain (**Yazh 4**) or introducing branched substituents (**Yazh 3**) resulted in a reduction in potency (IC<sub>50</sub> values of 8.81 and 8.89 μM, respectively).

The introduction of even longer (e.g. like in **Yazh 2**) and higher (e.g. as in **Yazh 5**) residues rendered the compounds inactive. Thus any further spatial extension in this region of the molecule appears to be disadvantageous. Therefore an ethyl substituent seems to be most beneficial for the compounds potency, possibly by perfectly filling out the receptor's binding pocket. However it would be interesting to also test a methylated compound in the future.

Also the introduction of fluorine substituents in 4 position of each distal aromatic system of compound **Yazh 357** increased the compounds potency ( $IC_{50}$  6.49  $\mu$ M) compared to the inactive compound **Yazh 25**. The fact that a chlorination (**Yazh 457**) in the same position has a weaker effect indicates either that a higher spatial extension or a less electronegative substituent are less beneficial. Also the location of the fluorination appears to be crucial as a fluorination in 5, 6 or 7 position are far less beneficial than in 4 position (compare **Yazh 357** with **Yazh 160**, **358** and **381**). For future optimization it would be interesting to synthesize a fluorinated compound with an ethylated methylene linker, thus combining the two beneficial substitution patterns.



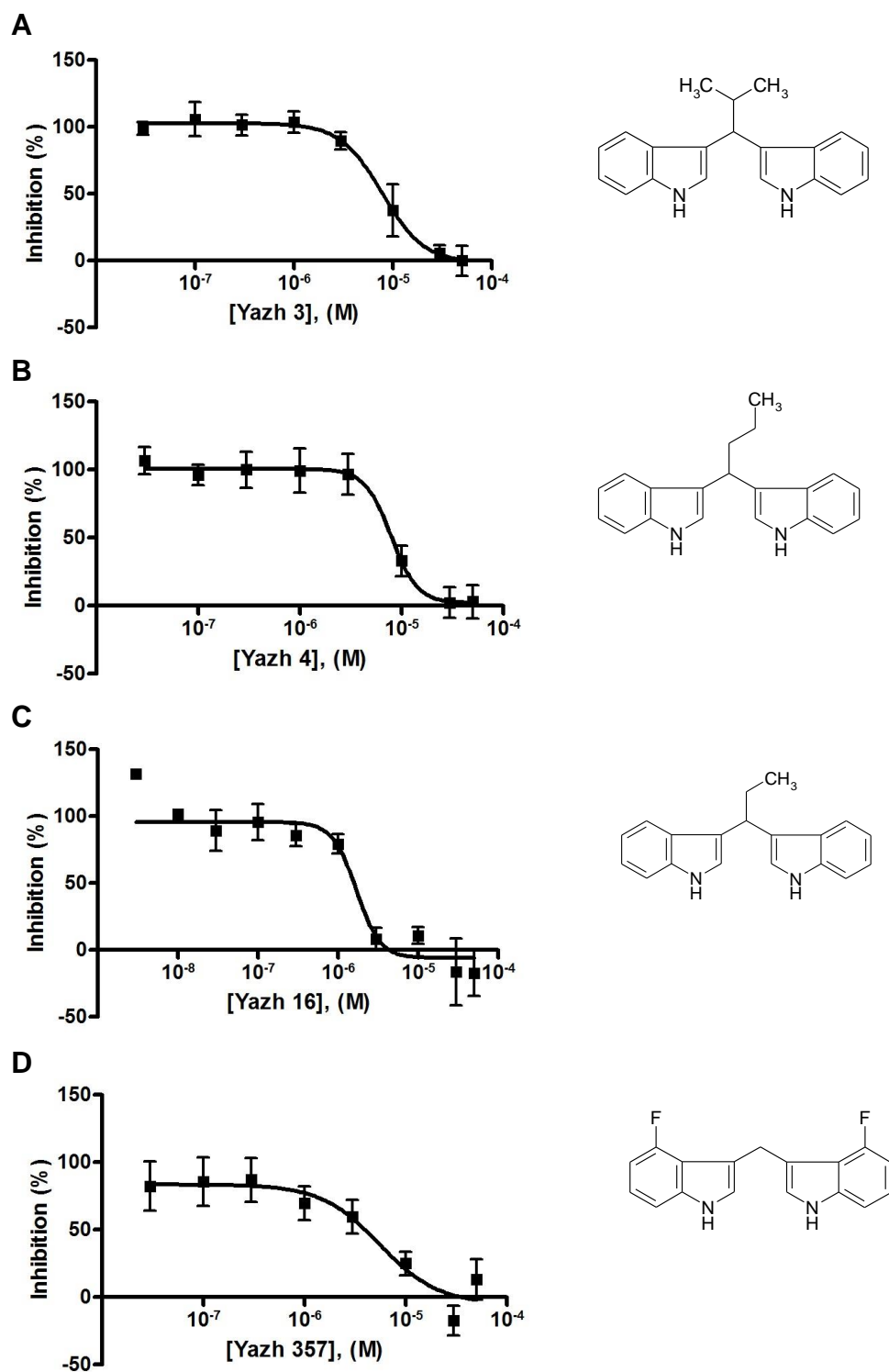


Figure 19. Dose-response curves of diindolylmethane derivatives (Yazzh library) with antagonist activity at human FFAR1. **(A)** Yazzh 3 ( $IC_{50}$  8.89  $\mu$ M). **(B)** Yazzh 4 ( $IC_{50}$  8.81  $\mu$ M). **(C)** Yazzh 16 ( $IC_{50}$  1.76  $\mu$ M). **(D)** Yazzh 357 ( $IC_{50}$  6.49  $\mu$ M). Mean values  $\pm$  SEM from three to five independent experiments performed in triplicates are shown.

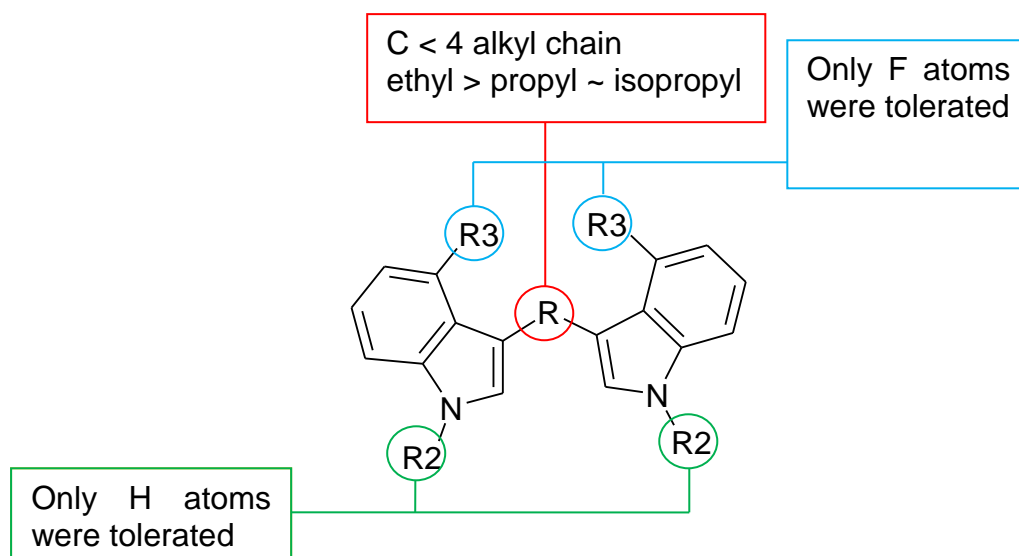
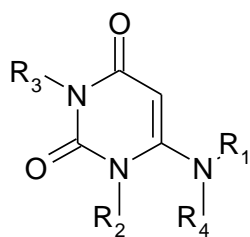


Figure 20. Structure-activity relationship of diindolylmethane derivatives for antagonist activity at human FFAR1.

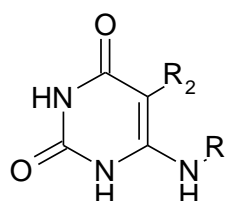
### 3.3.2 Screening of uracil derivatives (Yazh library, AK Müller) at human FFA1 receptor and human FFAR4short

Due to structural similarity to free fatty acids, uracil derivatives were also screened at human FFAR1 and FFAR4 short. Recently, PILLAIYAR, et al. discovered that some of these compounds could activate the human GPR84, which shares ligand preference for medium-chain free fatty acids (PILLAIYAR et al., 2018). However, they were shown to be inactive at both human FFAR1 and FFAR4. Results are shown in Table 6.

Table 6. Potency of uracil derivatives (Yazh library, AK Müller) at the human FFAR1 and FFAR4.



core structure F



core structure G

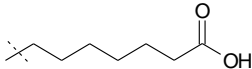
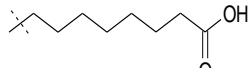
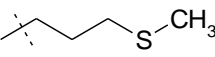
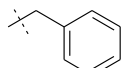
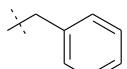
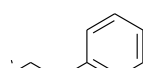
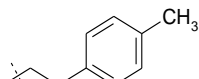
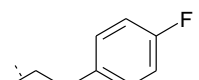
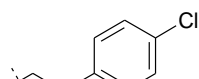
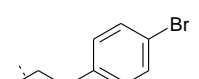
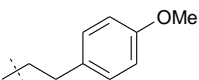
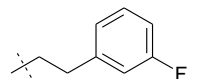
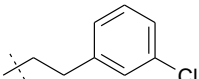
(Table to be continued)

Ligand	Structure	FFAR1		FFAR4s				
		Agonist screening <sup>a</sup> EC <sub>50</sub> ± SEM (μM)	Antagonist screening <sup>a</sup> IC <sub>50</sub> ± SEM (μM)	Agonist screening <sup>c</sup> EC <sub>50</sub> ± SEM (μM)	Antagonist screening <sup>c</sup>			
		(% effect ± SEM) <sup>b</sup>	(% inhibition ± SEM) <sup>b</sup>	(% effect ± SEM) <sup>d</sup>	(% inhibition ± SEM) <sup>d</sup>			
TUG-424		<b>0.144 ± 0.048</b>	-	-	-			
TUG-891		-	-	<b>1.83 ± 0.43</b>	-			
Core structure F								
Yazh	R1	R2	R3	R4				
102		H	H	H	(9 ± 10)	(-16 ± 6)	(1 ± 0)	(13 ± 2)
84		H	H	H	(11 ± 11)	(1 ± 5)	(0 ± 0)	(21 ± 3)
91		H	H	H	(4 ± 3)	(-9 ± 5)	(2 ± 1)	(20 ± 2)
88		H	H	H	(-3 ± 4)	(5 ± 10)	(1 ± 0)	(23 ± 6)
87		H	H	H	(-6 ± 3)	(-16 ± 6)	(0 ± 0)	(24 ± 8)
92		H	H	H	(2 ± 2)	(-0 ± 4)	(1 ± 0)	(18 ± 5)

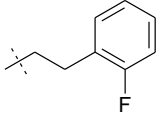
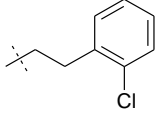
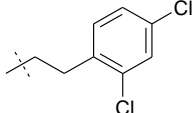
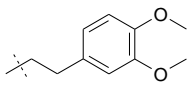
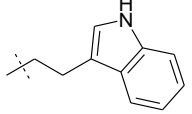
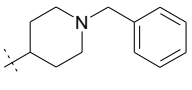
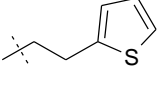
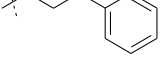
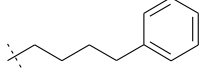
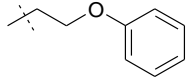
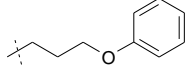
(Table continued)

Yazh	R1	R2	R3	R4	FFAR1		FFAR4s	
					Agonist screening <sup>a</sup>	Antagonist screening <sup>a</sup>	Agonist screening <sup>c</sup>	Antagonist screening <sup>c</sup>
					EC <sub>50</sub> ± SEM (μM)	IC <sub>50</sub> ± SEM (μM)	EC <sub>50</sub> ± SEM (μM)	EC <sub>50</sub> ± SEM (μM)
					(% effect ± SEM) <sup>b</sup>	(% inhibition ± SEM) <sup>b</sup>	(% effect ± SEM) <sup>d</sup>	(% inhibition ± SEM) <sup>d</sup>
94		H	H	H	(3 ± 4)	(8 ± 9)	(1 ± 0)	(17 ± 1)
205		H	H	H	(5 ± 4)	(-0 ± 11)	(-2 ± 2)	(11 ± 2)
363		H	H	CH <sub>3</sub>	(7 ± 3)	(1 ± 9)	(1 ± 0)	(16 ± 13)
277		CH <sub>3</sub>	H	H	(6 ± 4)	(-2 ± 5)	(-3 ± 3)	(19 ± 7)
229		H	H	H	(-3 ± 4)	(10 ± 8)	(-1 ± 1)	(13 ± 6)
96		H	H	H	(-2 ± 3)	(-1 ± 9)	(0 ± 0)	(18 ± 1)
254		H	H	H	(3 ± 3)	(6 ± 10)	(-3 ± 2)	(21 ± 5)
584		H	H	H	(-6 ± 5)	(15 ± 16)	(-1 ± 0)	(-13 ± 7)
39		H	H	H	(-5 ± 3)	(-4 ± 5)	(-1 ± 0)	(22 ± 9)
364		H	H	CH <sub>3</sub>	(5 ± 1)	(-1 ± 10)	(1 ± 0)	(22 ± 2)
40		H	CH <sub>3</sub>	H	(4 ± 3)	(8 ± 4)	(-1 ± 0)	(20 ± 19)
278		CH <sub>3</sub>	H	H	(5 ± 11)	(2 ± 6)	(-1 ± 1)	(25 ± 9)
85		CH <sub>3</sub>	CH <sub>3</sub>	H	(2 ± 7)	(9 ± 25)	(1 ± 0)	(30 ± 3)
97		H	H	H	(-5 ± 2)	(1 ± 2)	(-1 ± 0)	(26 ± 2)
100		H	CH <sub>3</sub>	H	(-8 ± 2)	(-3 ± 5)	(0 ± 0)	(17 ± 2)
98		H	H	H	(5 ± 14)	(-8 ± 9)	(-0 ± 0)	(32 ± 9)
101		H	CH <sub>3</sub>	H	(3 ± 7)	(-19 ± 9)	(-0 ± 1)	(15 ± 1)
202		H	H	H	(3 ± 2)	(2 ± 7)	(1 ± 0)	(13 ± 1)
203		H	H	H	(6 ± 2)	(12 ± 5)	(0 ± 0)	(11 ± 2)
206		H	H	H	(3 ± 3)	(1 ± 8)	(0 ± 0)	(16 ± 2)

(Table continued)

Yazh	R1	FFAR1			FFAR4s			
		R2	R3	R4	Agonist screening <sup>a</sup>	Antagonist screening <sup>a</sup>	Agonist screening <sup>c</sup>	Antagonist screening <sup>c</sup>
					EC <sub>50</sub> ± SEM (μM)	IC <sub>50</sub> ± SEM (μM)	EC <sub>50</sub> ± SEM (μM)	(% inhibition ± SEM) <sup>d</sup>
					(% effect ± SEM) <sup>b</sup>	(% inhibition ± SEM) <sup>b</sup>	(% effect ± SEM) <sup>d</sup>	
207		H	H	H	(-1 ± 2)	(11 ± 7)	(0 ± 1)	(18 ± 5)
208		H	H	H	(-3 ± 2)	(-10 ± 3)	(0 ± 0)	(23 ± 7)
89		H	H	H	(2 ± 3)	(-11 ± 3)	(-0 ± 0)	(25 ± 10)
82		H	H	H	(2 ± 5)	(2 ± 8)	(-0 ± 0)	(37 ± 5)
37		H	CH <sub>3</sub>	H	(-3 ± 0)	(3 ± 9)	(-0 ± 0)	(11 ± 7)
352		H	H	H	(10 ± 2)	(6 ± 13)	(2 ± 1)	(21 ± 9)
433		H	H	H	(-2 ± 1)	(5 ± 10)	(1 ± 1)	(15 ± 6)
480		H	H	H	(25 ± 14)	(-2 ± 6)	(2 ± 1)	(11 ± 3)
434		H	H	H	(1 ± 2)	(15 ± 11)	(0 ± 0)	(10 ± 4)
365		H	H	H	(-2 ± 4)	(6 ± 13)	(0 ± 1)	(17 ± 3)
410		H	H	H	(-7 ± 1)	(8 ± 12)	(-0 ± 0)	(14 ± 5)
408		H	H	H	(1 ± 3)	(4 ± 12)	(0 ± 0)	(11 ± 5)
406		H	H	H	(-1 ± 5)	(9 ± 7)	(1 ± 1)	(7 ± 5)

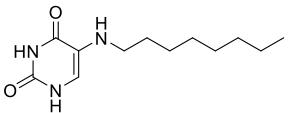
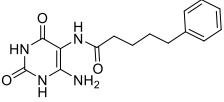
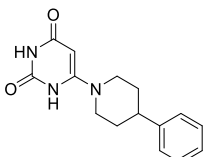
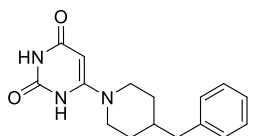
(Table continued)

Yazh	R1	R2	R3	R4	FFAR1		FFAR4s	
					Agonist screening <sup>a</sup>	Antagonist screening <sup>a</sup>	Agonist screening <sup>c</sup>	Antagonist screening <sup>c</sup>
					EC <sub>50</sub> ± SEM (μM)	IC <sub>50</sub> ± SEM (μM)	EC <sub>50</sub> ± SEM (μM)	EC <sub>50</sub> ± SEM (μM)
					(% effect ± SEM) <sup>b</sup>	(% inhibition ± SEM) <sup>b</sup>	(% effect ± SEM) <sup>d</sup>	(% inhibition ± SEM) <sup>d</sup>
409		H	H	H	(0 ± 7)	(21 ± 9)	(1 ± 1)	(15 ± 4)
407		H	H	H	(6 ± 8)	(-2 ± 6)	(0 ± 0)	(9 ± 2)
478		H	H	H	(19 ± 11)	(16 ± 10)	(1 ± 1)	(6 ± 6)
477		H	H	H	(15 ± 6)	(10 ± 9)	(1 ± 0)	(-1 ± 8)
481		H	H	H	(23 ± 16)	(17 ± 9)	(1 ± 0)	(14 ± 6)
493		H	H	H	(11 ± 10)	(17 ± 10)	(1 ± 1)	(29 ± 4)
492		H	H	H	(14 ± 9)	(7 ± 6)	(1 ± 1)	(-19 ± 8)
347		H	H	H	(1 ± 4)	(2 ± 8)	(1 ± 0)	(14 ± 16)
253		H	H	H	(8 ± 6)	(1 ± 12)	(-3 ± 2)	(21 ± 3)
90		H	H	H	(8 ± 7)	(-24 ± 4)	(-0 ± 0)	(27 ± 6)
283		H	H	H	(7 ± 8)	(4 ± 13)	(-2 ± 2)	(16 ± 6)

(Table continued)

Yazh	R1	R2	R3	R4	FFAR1		FFAR4s	
					Agonist screening <sup>a</sup>	Antagonist screening <sup>a</sup>	Agonist screening <sup>c</sup>	Antagonist screening <sup>c</sup>
					EC <sub>50</sub> ± SEM (μM)	IC <sub>50</sub> ± SEM (μM)	EC <sub>50</sub> ± SEM (μM)	IC <sub>50</sub> ± SEM (μM)
					(% effect ± SEM) <sup>b</sup>	(% inhibition ± SEM) <sup>b</sup>	(% effect ± SEM) <sup>d</sup>	(% inhibition ± SEM) <sup>d</sup>
99		H	H	H	(2 ± 10)	(-2 ± 7)	(2 ± 0)	(15 ± 2)
574		H	H	H	(14 ± 5)	(5 ± 12)	(1 ± 0)	(5 ± 16)
571		H	H	H	(5 ± 4)	(-7 ± 8)	(0 ± 0)	(-10 ± 7)
575		H	H	H	(11 ± 7)	(8 ± 9)	(-1 ± 1)	(-8 ± 12)
Core structure G								
Yazh	R1	R2						
372		Br	(7 ± 13)	(14 ± 10)	(-0 ± 0)	(6 ± 4)		
343		N=O	(0 ± 3)	(3 ± 12)	(1 ± 1)	(13 ± 3)		
348		N=O	(14 ± 8)	(0 ± 7)	(-0 ± 0)	(27 ± 5)		
373		Br	(13 ± 17)	(7 ± 6)	(-0 ± 1)	(14 ± 3)		
349		N=O	(6 ± 2)	(2 ± 11)	(-0 ± 1)	(26 ± 4)		
353		N=O	(11 ± 1)	(10 ± 8)	(1 ± 1)	(19 ± 8)		
370		Br	(2 ± 5)	(-3 ± 11)	(-0 ± 0)	(14 ± 5)		
374		Br	(-5 ± 4)	(2 ± 5)	(-0 ± 0)	(14 ± 1)		
351		N=O	(7 ± 2)	(-1 ± 6)	(1 ± 1)	(15 ± 12)		

(Table concluded)

Other derivatives structures		FFAR1		FFAR4s	
Yazh	Structure	Agonist screening <sup>a</sup>	Antagonist screening <sup>a</sup>	Agonist screening <sup>c</sup>	Antagonist screening <sup>c</sup>
		EC <sub>50</sub> ± SEM (µM)	IC <sub>50</sub> ± SEM (µM)	EC <sub>50</sub> ± SEM (µM)	EC <sub>50</sub> ± SEM (µM)
		(% effect ± SEM) <sup>b</sup>	(% inhibition ± SEM) <sup>b</sup>	(% effect ± SEM) <sup>d</sup>	(% inhibition ± SEM) <sup>d</sup>
129		(-6 ± 4)	(-29 ± 7)	(-3 ± 1)	(38 ± 4)
300		(18 ± 3)	(1 ± 11)	(1 ± 1)	(17 ± 4)
572		(15 ± 2)	(8 ± 9)	(0 ± 0)	(-12 ± 6)
573		(14 ± 5)	(9 ± 13)	(0 ± 1)	(-13 ± 7)

<sup>a</sup> Screening of Yazh compounds was performed at a concentration of 10 µM at human FFAR1 receptor. For [Ca<sup>2+</sup>] mobilization assays the receptor was expressed in an astrocytoma cell line.

<sup>b</sup> Effects were normalized to 10 µM (agonist screening) and 1 µM (~ EC<sub>80</sub>, antagonist screening) of TUG-424.

<sup>c</sup> Screening of Yazh compounds was performed at a concentration of 10 µM at human FFA4short receptor. For β-arrestin assays the receptor was expressed in a CHO β-arrestin cell line which is part of an open assay system (PathHunter®, DiscoverX).

<sup>d</sup> Effects were normalized to 30 µM (agonist screening) and 4 µM (~ EC<sub>80</sub>, antagonist screening) of TUG-891.

### 3.3.3 Screening of natural products at human FFAR1 and FFAR4s

Selected natural products from other libraries (AK König and AK Piel, University of Bonn) were also tested for their activity at both receptors. Some of these compounds either were previously tested at other GPCRs or share structural

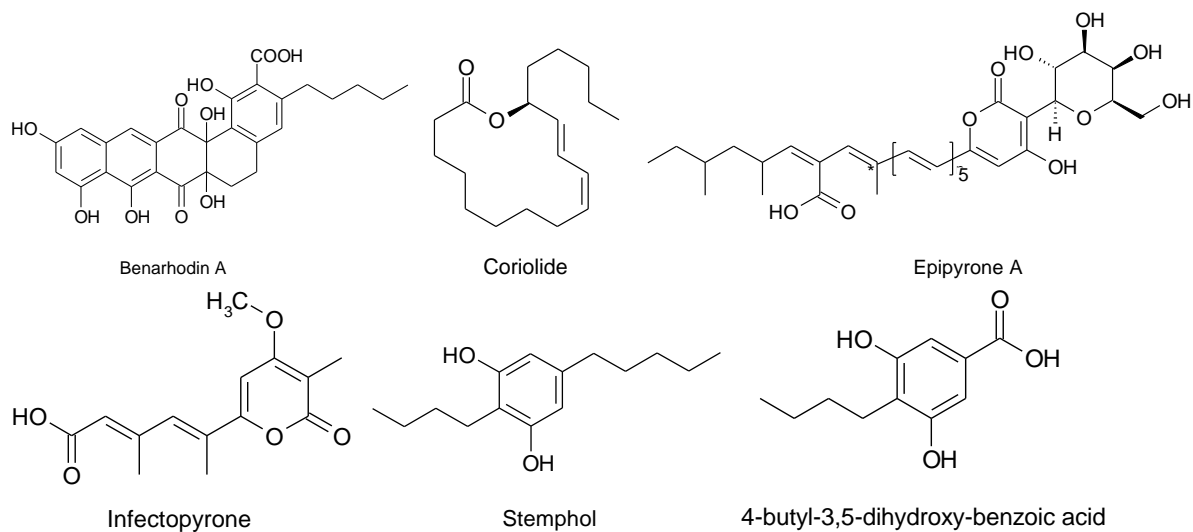


similarity to the FFAR1 and FFAR4 ligands. Among the tested products, none could activate or inhibit the human FFAR4short. Also, none of them was found to inhibit the human FFAR1. Only stemphol was identified as a human FFAR1 partial agonist. Results are shown in Table 7. Stemphol exhibited a moderate potency at FFAR1 ( $EC_{50}$  1.76  $\mu$ M, Figure 21). Interestingly the compound also showed a high inhibition percentage at the receptor ( $86 \pm 5$ , Table 7), however characterizing rapid desensitization through activation of the receptor.

Stemphol (2-butyl-5-pentylbenzene-1,3-diol) is a mycotoxin first isolated from *Stemphylium majusculum* but also produced by other *Stemphylium* species (STODOLA; WEISLEDER; VESONDER, 1973). It has been found in some contaminated plants such as tomatoes and rapeseed (ANDERSEN; FRISVAD, 2004; SOLFRIZZO et al., 1994). Studies have shown the potential antibiotic activity of this compound against some species of fungus, yeast and pathogenic bacteria (ACHENBACH; KOHL, 1979; ZHOU et al., 2015). The compound was also linked to a cytotoxicity activity against several human cancer cell lines (ZHOU et al., 2015).

Recently, stemphol was predicted as an agonist of the cannabinoid type 1 receptor ( $CB_1$ ) (FERREIRA et al., 2017). This receptor has been described as the target for the effects of the drug marijuana, derived from *Cannabis sativa*. Among dozens of cannabinoids found in this plant,  $\Delta^9$  - tetrahydrocannabinol ( $\Delta^9$  - THC) is the main component responsible for the psychoactive effects and a potent  $CB_1$  agonist. So far there are no effective approved medicines for the *C. sativa* withdrawal syndrome and  $CB_1$  agonists have been suggested as possible pharmacological tools to attenuate the symptoms of cannabis use disorders (VANDREY; HANEY, 2009). In the same manner as FFAR1,  $CB_1$  is a rhodopsin-like (Class A) GPCR. However they share protein similarity of only about 24 %. Therefore the computational prediction of stemphol at  $CB_1$  should be further confirmed in experimental analysis such as in  $[Ca^{2+}]$  mobilization assays.

**Table 7. Potency of AK König and AK Piel library compounds at the human FFAR1 and FFAR4s.**



Ligand	FFAR1		FFAR4s	
	<u>Agonist screening</u> <sup>a</sup> <b>EC<sub>50</sub> ± SEM (μM)</b> (% effect ± SEM) <sup>b</sup>	<u>Antagonist screening</u> <sup>a</sup> (% inhibition ± SEM) <sup>b</sup>	<u>Agonist screening</u> <sup>c</sup> <b>EC<sub>50</sub> ± SEM (μM)</b> (% effect ± SEM) <sup>d</sup>	<u>Antagonist Screening</u> <sup>c</sup> (% inhibition ± SEM) <sup>d</sup>
TUG-424	<b>0.144 ± 0.048</b>	-	-	-
TUG-891	-	-	<b>1.83 ± 0.43</b>	-
Benarhodin A	(3 ± 0)	(37 ± 17)	(-1 ± 2)	(5 ± 1)
Coriolide	(19 ± 18)	(21 ± 6)	(-1 ± 3)	(-5 ± 3)
Epipyron	(9 ± 5)	(35 ± 17)	(1 ± 2)	(19 ± 14)
Infectopyrone	(2 ± 5)	(-8 ± 6)	(-0 ± 1)	(-10 ± 4)
Stemphol	<b>1.76 ± 0.26</b>	(86 ± 5)	(2 ± 1)	(19 ± 10)
4-butyl-3,5-dihydroxy-benzoic acid	(4 ± 4)	(12 ± 14)	(0 ± 3)	(0 ± 9)

<sup>a</sup> Screening of the compounds was performed at a concentration of 10 μM at human FFAR1 receptor. For Calcium mobilization assays the receptor was expressed in an astrocytoma cell line.

<sup>b</sup> Effects were normalized to 10 μM (agonist screening) and 1 μM (~ EC<sub>80</sub>, antagonist screening) of TUG-424.

<sup>c</sup> Screening of the compounds was performed at a concentration of 10 μM at human FFAR4short receptor. For β-arrestin assays the receptor was expressed in a CHO β-arrestin cell line which is part of an open assay system (PathHunter®, DiscoverX).

<sup>d</sup> Effects were normalized to 30 μM (agonist screening) and 4 μM (~ EC<sub>80</sub>, antagonist screening) of TUG-891.

Considering the SAR of the natural products at FFAR1, the structural similarity of stemphol and 4-butyl-3,5-dihydroxybenzoic acid is notable. A brief analysis shows that the carboxylation at 5-position lead to the abolishment of the activity of 4-butyl-3,5-dihydroxybenzoic acid, suggesting that a certain level of hydrophobicity in this region of the molecule is necessary for agonistic effects at FFAR1.

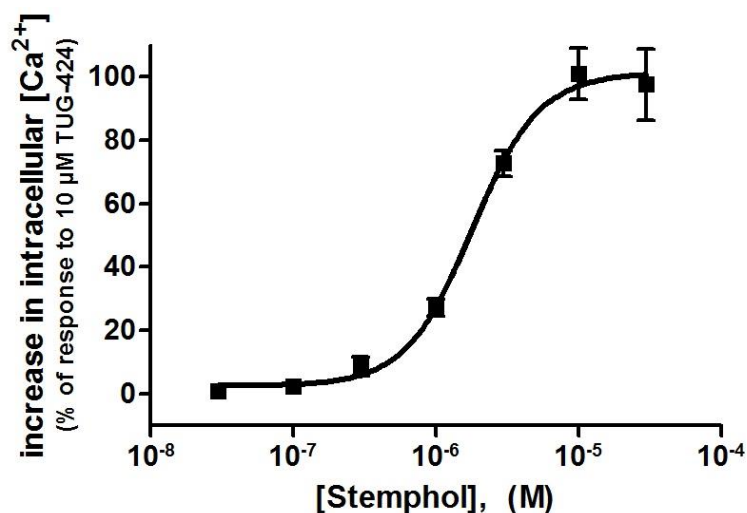


Figure 21. Dose-response curve of stemphol at human FFAR1.  $EC_{50}$   $1.76 \pm 0.26 \mu\text{M}$ . Results are shown as mean values  $\pm$  SEM from three independent experiments performed in triplicates.

#### 3.3.4 Screening of Drug library at human FFAR4short

A library of about four hundred commercially available compounds (Drug library, AK Müller, University of Bonn) was also tested in agonist screening with the aim to find possible hits at human FFAR4. The characterization of this receptor was done by performing  $\beta$ -arrestin recruitment assays with transfected CHO cells. The signals were normalized to that induced by 30  $\mu\text{M}$  TUG-891, which represents the maximal effect.

Only digitonin was found to activate the receptor moderately ( $EC_{50}$  3.78  $\mu\text{M}$ , Figure 22, A). Digitonin is a saponin extracted from the plant *Digitalis purpurea*. It may usually be mistaken with digoxin (Figure 22, B) once they both share same origin and similar structure, however while digoxin is a cardiac glycoside to treat heart failure, digitonin has been applied as a mild non ionic detergent (FAN; HEERKLOTZ, 2017). As seen in Figure 22 (B), the digitonin structure is composed of a sterol tail

followed by a sugar head consisting of galactose, glucose, and xylose. In this way, digitonin can bind to the membrane cholesterol allowing the formation of digitonin-cholesterol complexes, which create pores in the cellular membrane (NISHIKAWA et al., 1984). As a consequence, it has been widely used on several biological assays, for example, to permeabilize cell membranes to peptides (GEELEN, 2005) and to isolate cellular components as mitochondria (MOREADITH; FISKUM, 1984). Besides, its detergent activity depends on the digitonin concentration as well on the cholesterol content in membrane (FAN; HEERKLOTZ, 2017).

Regarding to membrane receptors, digitonin could solubilize and extract without loss of function several GPCRs such as purinergic P2Y receptors (BODOR et al., 2004),  $\beta$ 2 adrenergic receptor ( $\beta$ 2AR), the muscarinic acetylcholine receptor M2 (M2), the neurotensin receptor (NTR) (ISHIHARA et al., 2005), as well as the free fatty acid receptor 4 (FFAR4) (MIYAUCHI et al., 2009). Interestingly, JONES et al. (2010) suggested the use of digitonin as a positive control in aequorin functional assays to evaluate GPCRs  $[Ca^{2+}]$  release signal using transfected CHO cells. However its activity was not receptor-dependent, but due the high  $[Ca^{2+}]$  influx caused by membrane permeabilization.

Up to date, no evidence was found in literature of digitonin directly binding to a receptor or activating a receptor in  $\beta$ -arrestin recruitment assays. Since this assay platform creates less unspecific signals, we are under the impression that digitonin could somehow allow the enzyme complementation and further signalling. Therefore the agonist activity of digitonin at human FFAR4s should be confirmed and elucidate in other assay systems.

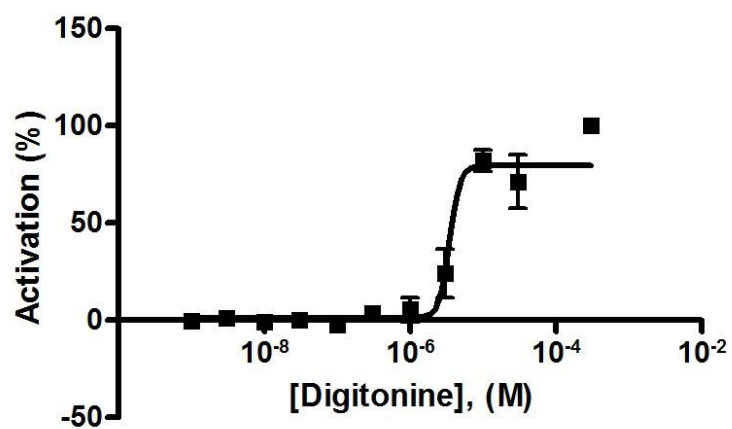
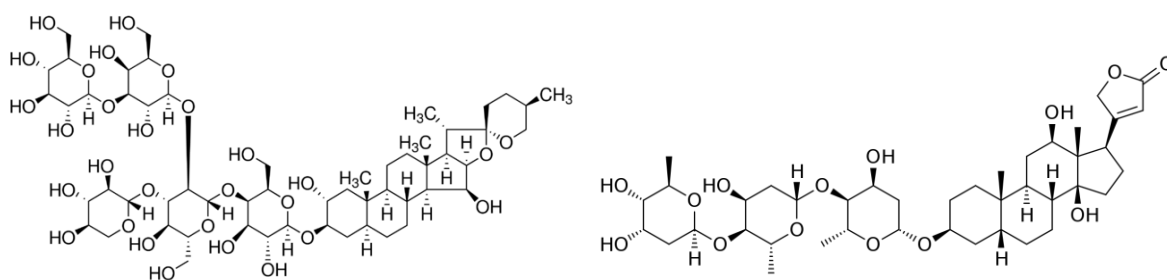
**A****B**

Figure 22. Dose-response curve of digitonin at human FFAR4s (A)  $\beta$ -arrestin recruitment assay performed with CHO stably expressing human FFAR4short.  $EC_{50}$   $3.78 \pm 0.36$   $\mu$ M. Results are shown as mean values  $\pm$  SEM from five independent experiments performed in duplicates. (B) Digitonin and digoxin structures (PubChem CID 25444 and 2724385, respectively).

## **Part 2. Adipogenic activity of ligands**

Once FFAR4 has been found highly expressed in mature adipocytes, it would be interesting to check the adipogenic activity of digitonin. Besides, the investigation of the diindolylmethane derivatives Yazh 3, Yazh 4 and Yazh 357 in the adipocyte differentiation is also intriguing since it has been demonstrated that 3,3'-diindolylmethane could inhibit adipogenesis in 3T3-L1 cells and *in vivo* (LEE et al., 2017).

### **3.4. Cell viability assay**

Up to date, there is no evidence of the found ligands being tested in mice pre-adipocytes 3T3-L1 and mesenchymal C3H/10T1/2 cells. Additionally, TUG-891 has not yet been tested in C3H/10T1/2 cell line. Therefore, it would be interesting to check whether these compounds would interfere with the cell lines viability. At the concentration of 10  $\mu$ M, none of the ligands decreased the viability of both cell lines below 70 % (Figure 23 and 24). Consequently, this concentration was chosen for further assays at the cell lines.

It is interesting to note that digitonin has been related in literature as a positive cytotoxic control in cytotoxicity assays (FAKHRUDIN et al., 2014). This natural product has been used for this purpose in a nanomolar range (JOHANSSON et al., 2001). However, in MTT cell viability assay, we found that digitonin could reduce the viability of 3T3-L1 and C3H/10T1/2 only up to a concentration of 50  $\mu$ M (Figure 23 and 24).

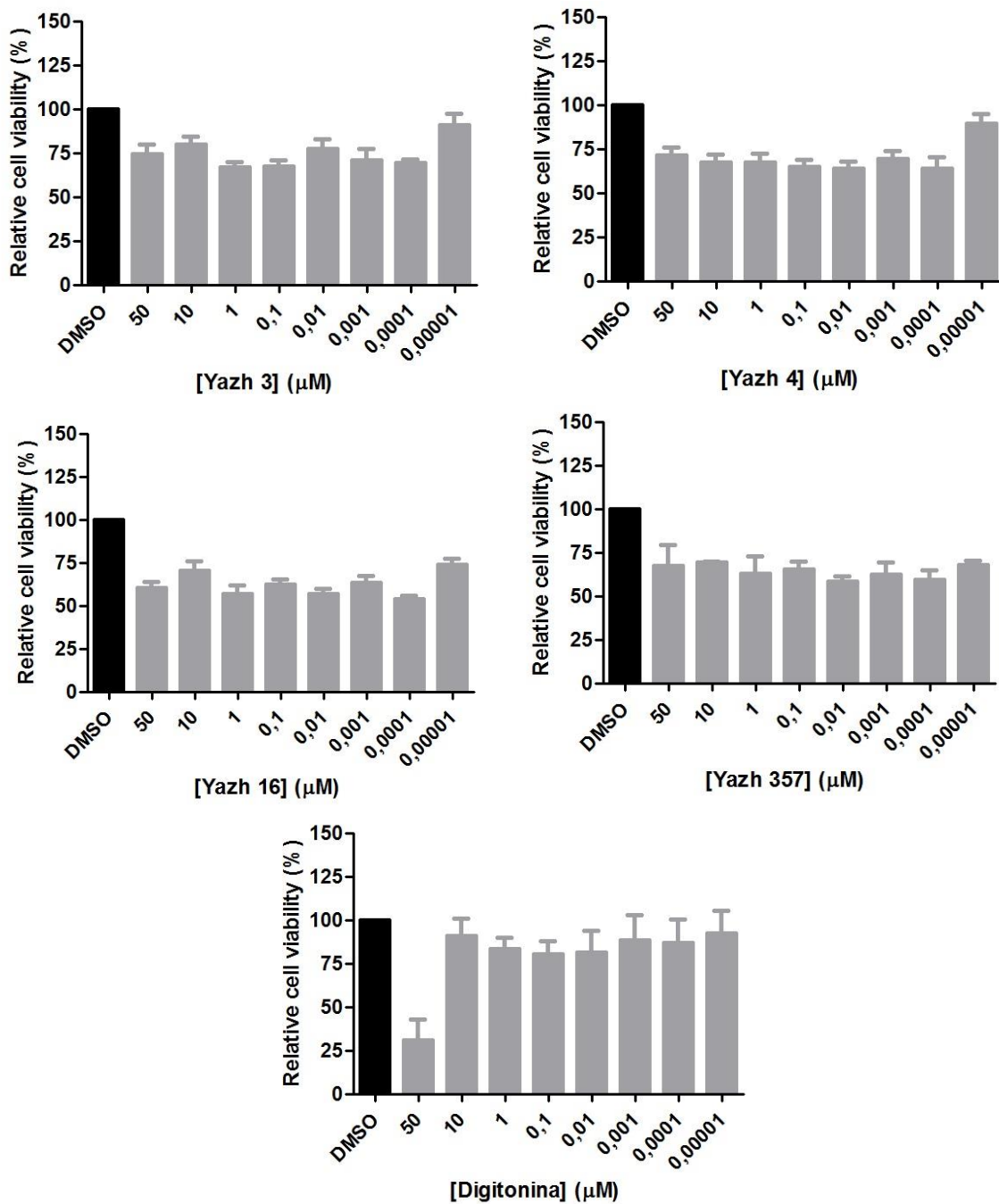


Figure 23. Relative cell viability using MTT. 3T3-L1 cells were treated with crescent concentrations of different compounds for 24 hours. After this period, MTT was added to the cells before an incubation time of 4 hours. The reduced MTT crystals were solubilized with pure DMSO, and the absorbance was measured at 570 nm. Results are shown as mean (SD) from three independent experiments performed in duplicate.

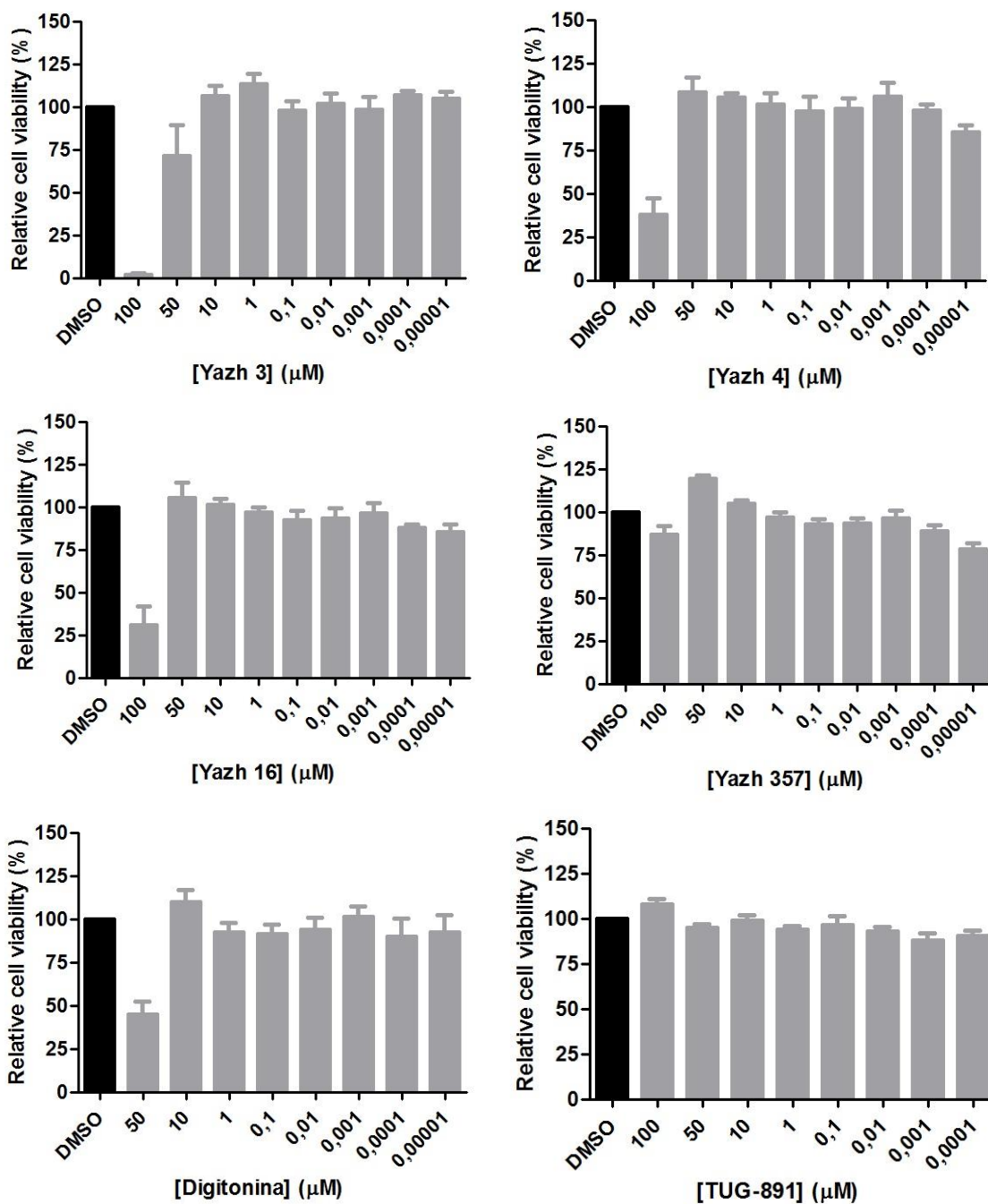


Figure 24. Relative cell viability using MTT. C3H/10T1/2 cells were treated with crescent concentrations of different compounds for 24 hours. After this period, MTT was added to the cells before an incubation time of 4 hours. The reduced MTT crystals were solubilized with pure DMSO, and the absorbance was measured at 570 nm. Results are shown as mean (SD) from three independent experiments performed in duplicate.



### **3.5. Differentiation assay into adipocytes**

#### **3.5.1 Oil Red O staining to validate the protocol for adipogenesis**

Oil Red O staining was used to evaluate the protocol for adipogenesis, as it can dye cytoplasmic lipid droplets. Briefly, cells were plated, and two days after confluence, they were induced with MDI containing IBMX (0.5 mM), insulin (0.167  $\mu$ M) and dexamethasone (1 M). After 48h, MDI was exchanged for medium containing insulin (0.167  $\mu$ M) until the end of the process. Initially, the protocol for differentiation was validated by testing the vehicle and standard agonists for 10 days using 3T3-L1 and C3H/10T1/2 cells. However, C3H/10T1/2 cells could not promote adipogenesis properly. Therefore 3T3-L1 cell line was chosen for the differentiation experiments.

As seen in Figure 25 (A and B), cells treated with the standard PPAR- $\gamma$  agonist rosiglitazone showed more intense coloration macroscopically in comparison to the vehicle and undifferentiated cells. Accordingly, cells treated with rosiglitazone showed higher cytoplasmic lipid accumulation than the cells treated with DMSO (Figure 25, C), confirming the protocol as a suitable one to evaluate the effect of the ligands of FFAR1 and FFAR4.

Surprisingly the synthetic agonist at FFAR4 showed a weak adipogenic effect at 3T3-L1 cells on my hands even at high concentrations. This result disagrees with the study of SONG et al. (2016), in which TUG-891 could increase the cytoplasmic lipid accumulation in 3T3-L1 cells in a concentration manner. However, due to lack of availability of another FFAR4 selective agonist, we performed the experiments applying rosiglitazone as the main positive control for adipogenesis.

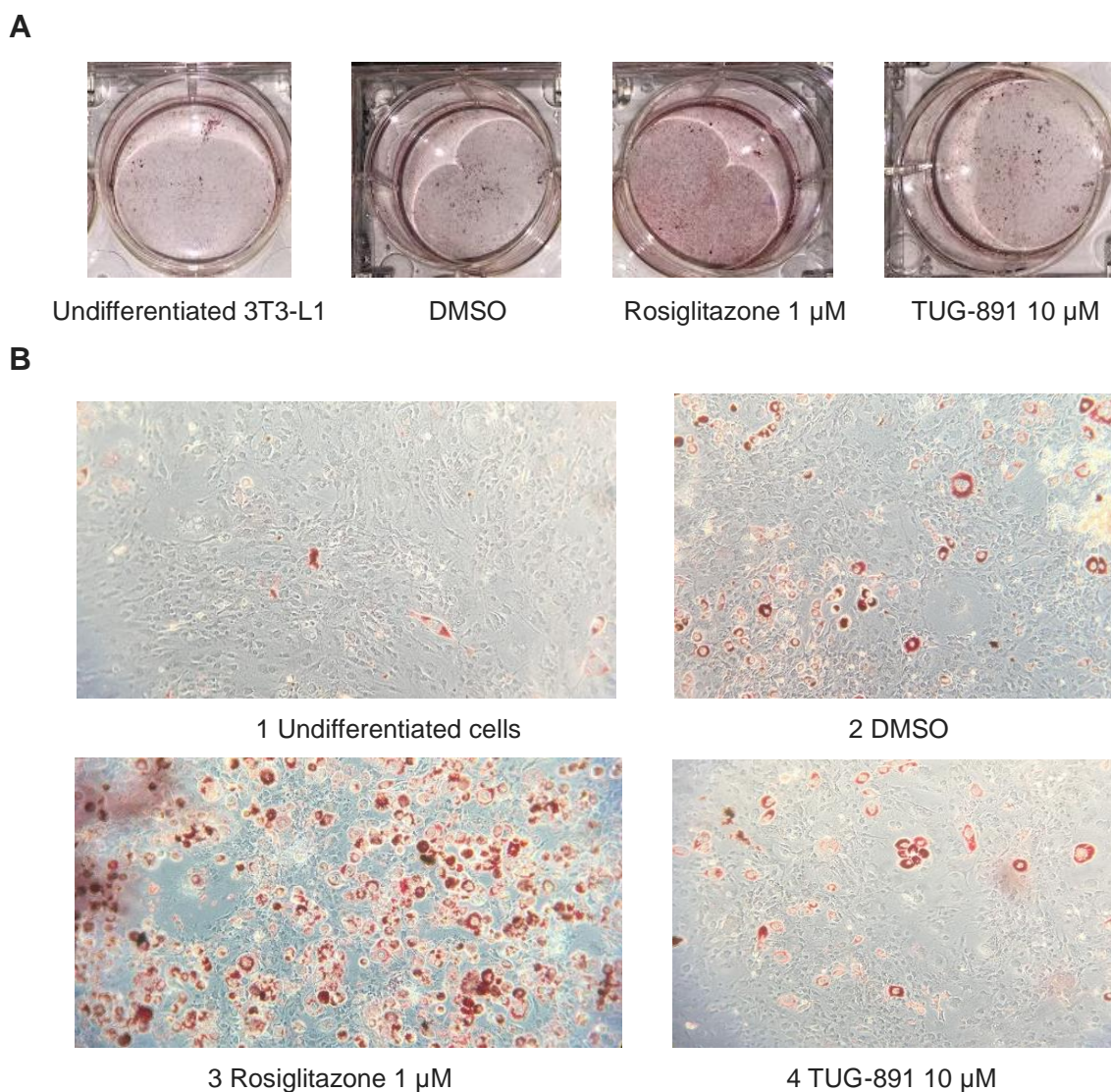


Figura 25. Differentiation assay to adipocytes using Oil Red O staining. Two days after reaching confluence, 3T3-L1 cells were induced to differentiate into adipocytes with MDI (DMEM, 10 % SFB, 1  $\mu\text{M}$  dexamethasone, 0.5 mM IBMX, 0.17  $\mu\text{M}$  insulin) for 2 days, and then with medium supplemented with SFB and 0.17  $\mu\text{M}$  insulin for more 8 days. After differentiation process, cells were dyed using Oil Red O and were photographed (**A**) macroscopically and (**B**) microscopically with 20 x magnification.

### 3.5.2 Gene expression during adipogenesis

To evaluate the changes in gene expression in the 3T3-L1 cells promoted by the test compounds, real-time PCR was applied. Previous study conducted by MILTON et al. (2015) showed that adipogenic genes such as *Fabp4* and *Adipoq* are highly expressed in the initial phase of the differentiation process. Based on this, the

effect of digitonin, Yazh 3, Yazh 4, Yazh 16 and Yazh 357 on the expression of adipocyte marker *Fabp4* genes was evaluate initially on the 3rd day of adipogenesis. Results are seen in Figure 26.

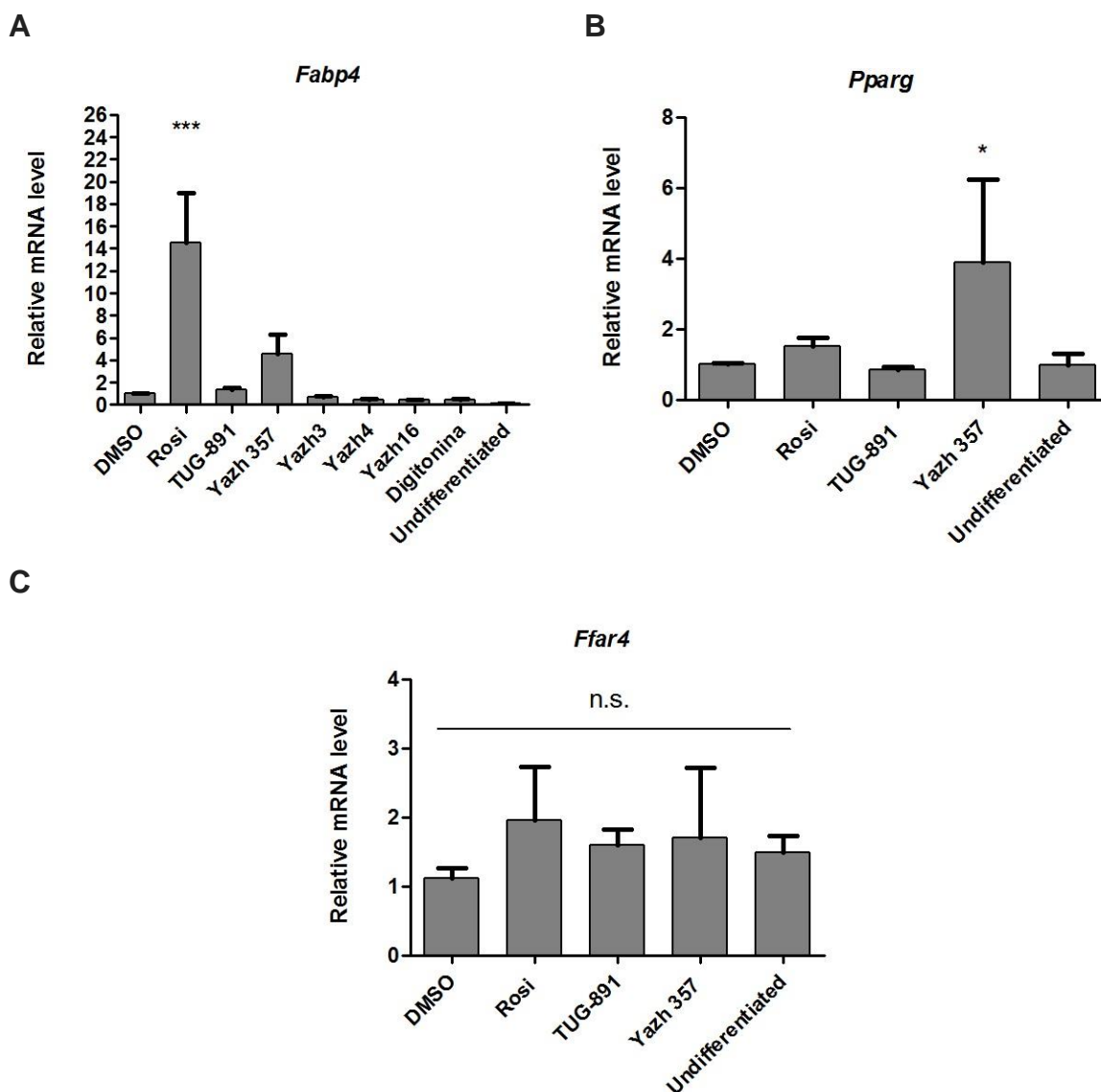


Figure 26. Relative mRNA expression of genes involved in adipogenesis on the third day of differentiation. 3T3-L1 cells were induced to differentiate with supplemented media and treated with vehicle (DMSO), 1  $\mu$ M Rosi, and 10  $\mu$ M of the other compounds. RNA was collected on the 3rd day of adipogenesis, and RT-qPCR was performed. The relative mRNA level of (A) *Fabp4*, (B) *Pparg* and (C) *Ffar4* were normalized by the expression of  $\beta$ -actin. \*\*\*  $p < 0.001$ , \*  $p < 0.05$ , vs vehicle DMSO. n.s. non significant. These results are representative of at least five independent experiments in triplicate and show the mean  $\pm$  SD

On the day-3, only rosiglitazone 1  $\mu$ M could significantly increase the mRNA expression of the adipocyte marker *Fabp4* (Figure 26, A). Also, an increase in *Fabp4* expression was seen when cells were treated with Yazh 357. Consistent with the results for *Fabp4*, treatment with 10  $\mu$ M of Yazh 357 promoted the expression of *Pparg* in mice cells significantly when compared to the vehicle (Figure 26, B). This effect of Yazh 357 was not expected, considering its inhibitory activity at FFAR1 and inactivity at FFAR4.

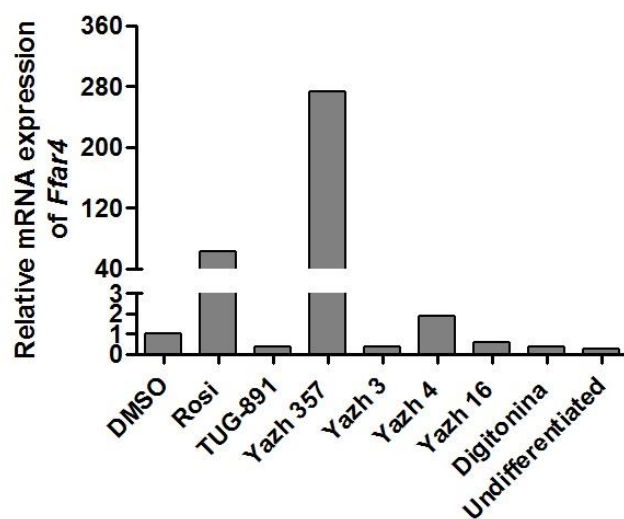
In concordance with our prior results applying ORO staining, TUG-891 was unable to advocate an increase in mRNA levels of adipogenic genes, contrasting with findings in literature (SONG et al., 2016). However, it is worth noting that the effect of TUG-891 on the expression of *Pparg* and *Fabp4* in the study of SONG et al. (2016) was still discrete, although significant in comparison to the vehicle.

Moreover, the treatment with the other diindolylmethane derivatives did not show any effect in *Fabp4* expression; therefore their effects on the other adipogenic genes were not investigated. Unexpectedly digitonin was also inactive in the differentiation process, although we found this compound as a FFAR4 agonist in  $\beta$ -arrestin assays.

Besides, the overall low level of *Ffar4* mRNA on the third day of differentiation (Figure 26, C) is in agreement with the findings that the expression of this gene is poorly found in preadipocytes and increases over the course of differentiation, being highly expressed in mature adipocytes (GOTOH et al., 2007).

To assess the expression of *Ffar4* and *Pparg* in mature adipocytes, RT-qPCR was performed after 10 days of differentiation in a single experiment due to lack of the ligand Yazh 357 (Figure 27).

A



B

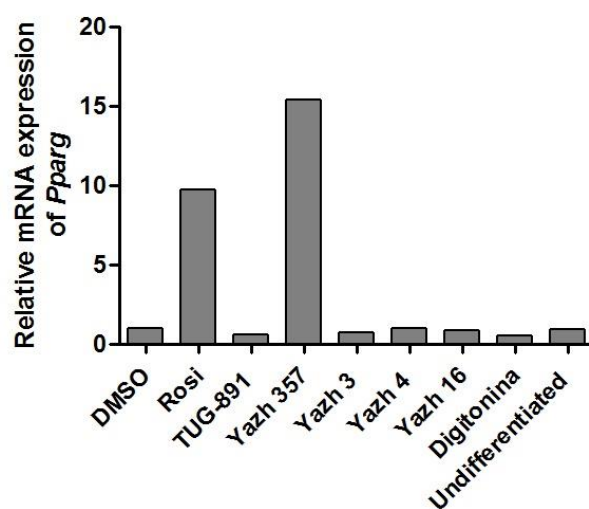


Figure 27. Relative mRNA expression of genes involved in adipogenesis on the tenth day of differentiation. 3T3-L1 cells were induced to differentiate with supplemented media and treated with vehicle (DMSO), Rosi (1  $\mu$ M) and ligands (10  $\mu$ M). RNA was collected on the 10th day of the adipocyte differentiation, and RT-qPCR was performed. The relative mRNA level of (A) *Ffar4* and (B) *Pparg* were normalized by the expression of  $\beta$ -actin. These results are representative of a single experiment in triplicate and show the mean  $\pm$  SD.

Unlike the initial phase of the adipocyte differentiation, FFAR4 mRNA was found abundantly in mature adipocytes, as seen in cells exposed to rosiglitazone (Figure 27, A). Additionally, 3T3-L1 cells treated with Yazh 357 highly expressed the free fatty acid receptor 4, indicating an adipogenic activity of this derivative. Therefore

FFAR4 could also be used as a marker of mature adipocytes. As expected, none of the other ligands showed any effect on the differentiation of 3T3-L1 cells.

High levels of PPAR- $\gamma$  mRNA was found in mature adipocytes treated with 10  $\mu$ M of Yazh 357 (Figure 27, B), confirming the gene expression on the 3rd day of adipogenesis. The PPAR- $\gamma$  is the master regulator in the process of adipogenesis, and without this transcription factor, preadipocytes are unable to differentiate (ROSEN et al., 2002). Taken together, these findings imply that Yazh 357 may play a role in the adipocyte maturation.

It is interesting to mention that a recent study showed the reduction of lipid accumulation in 3T3-L1 cells treated with 3,3'-diindolylmethane (LEE et al., 2017). The treatment could also suppress the expression of *Pparg* and *Fabp4*. These results suggest that slight changes in the structure of 3,3'-diindolylmethane could evoke opposite effects in adipogenesis; considering that Yazh 357 differs from 3,3'-diindolylmethane by the addition of 4,4'-fluorine atoms.

## Perspectives

Since Yazh 357 increased the expression of PPAR- $\gamma$  in adipogenesis through 3T3-L1, we evaluated whether this ligand could activate the receptor in a reporter gene platform (Figure 28). In short, HeLa cells were co-transfected with the human PPAR- $\gamma$ , and the peroxisome proliferator-activated receptor response element (PPRE) fused with the luciferase gene reporter using Lipofectamine® 2000 (Invitrogen). Six hours after transfection, cells were treated either with vehicle, Rosi (10  $\mu$ M) or Yazh 357 (10  $\mu$ M), and the luminescence activity was detected 24h after treatment by addition of luciferin. Due to a lack of available reagent, this experiment was performed only a single time in triplicate.

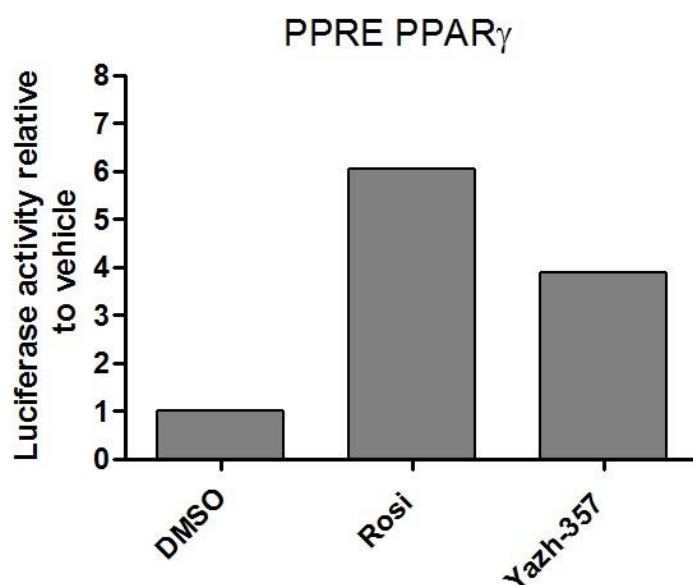


Figure 28. Activity of Yazh 357 at human PPAR- $\gamma$ . HeLa cells were transiently co-transfected with the human PPAR- $\gamma$  and with the PPRE fused with the luciferase reporter gene. Cells were treated with DMSO, rosiglitazone (10  $\mu$ M) and Yazh 357 (10  $\mu$ M). Results are seen as mean values from a single experiment performed in triplicate.

As seen in Figure 28, Rosi could activate PPAR- $\gamma$  circa 6 times more than the vehicle DMSO. Additionally, Yazh 357 could induce the transcriptional activity of PPAR- $\gamma$  partially when compared to rosiglitazone. This result should be confirmed in other biological replicates. However it corroborates to a possibly PPAR- $\gamma$ -related

adipogenic effect of Yazh 357, and suggests this ligand as a possible PPAR- $\gamma$  partial agonist.

Therefore, it would be interesting to check the effect of Yazh 357 on the expression and activation of other effectors in the adipogenic differentiation, such as the CCAAT-enhancer-binding proteins C/EBP, specially the ones directly involved in the promotion of PPAR- $\gamma$  activation and expression. Also, other diindolylmethane derivatives could also be tested for their activity at the nuclear receptor PPAR- $\gamma$ .



#### 4. CONCLUSION

During screening with diindolylmethane derivatives, four compounds were found to moderately antagonize the activity of FFAR1 (Yazh 3, Yazh 4, Yazh 16 and Yazh 357).

The natural product stemphol was found to moderately activate FFAR1.

For FFAR4, digitonin was the only compound which could have an effect on the activation of the receptor.

Yazh 357 could promote the adipocyte differentiation using the 3T3-L1 cell line model.

Yazh 357 may activate the PPAR- $\gamma$  receptor partially when compared to the effects of rosiglitazone (10  $\mu$ M).

## 5. REFERENCES

- ACHENBACH, H.; KOHL, W. Untersuchungen an Stoffwechselprodukten von Mikroorganismen, XVIII. Zur Konstitutionsaufklärung der Pigmente vom Flexirubin-Typ — Massenspektrometrische Untersuchungen. **Chemische Berichte**, v. 112, n. 1, p. 209–217, jan. 1979.
- ADAMS, G. L. et al. Discovery of Chromane Propionic Acid Analogues as Selective Agonists of GPR120 with *in Vivo* Activity in Rodents. **ACS Medicinal Chemistry Letters**, v. 8, n. 1, p. 96–101, 2017.
- AGARWAL, S. et al. Identification of an Orally Efficacious GPR40/FFAR1 Receptor Agonist. **ACS Medicinal Chemistry Letters**, v. 7, n. 12, p. 1134–1138, 2016.
- AHRÉN, B. Islet G protein-coupled receptors as potential targets for treatment of type 2 diabetes. **Nature Reviews Drug Discovery**, v. 8, n. 5, p. 369–385, 2009.
- AIZAWA, F. et al. GPR40/FFAR1 deficient mice increase noradrenaline levels in the brain and exhibit abnormal behavior. **Journal of Pharmacological Sciences**, v. 132, n. 4, p. 249–254, 2016.
- AMMÄLÄ, C.; ASHCROFT, F. M.; RORSMAN, P. Calcium-independent potentiation of insulin release by cyclic AMP in single beta-cells. **Nature**, v. 363, n. 6427, p. 356–8, 1993.
- ANDERSEN, B.; FRISVAD, J. C. Natural Occurrence of Fungi and Fungal Metabolites in Moldy Tomatoes. **Journal of Agricultural and Food Chemistry**, v. 52, n. 25, p. 7507–7513, dez. 2004.
- ATAK, J.; LAVREYSEN, H. Agonist. In: STOLERMAN, I. P. (Ed.). **Encyclopedia of Psychopharmacology**. Berlin, Heidelberg: Springer Berlin Heidelberg, 2010. p. 45.
- ATTWOOD, T. K.; FINDLAY, J. B. C. Fingerprinting G-protein-coupled receptors. v. 7, n. 2, p. 195–203, 1994.
- AUGUSTE, S. et al. Central Agonism of GPR120 Acutely Inhibits Food Intake and Food Reward and Chronically Suppresses Anxiety-Like Behavior in Mice. **International Journal of Neuropsychopharmacology**, v. 19, n. 7, p. 1–10, 2016.
- AZEVEDO, C. M. G. et al. Non-Acidic Free Fatty Acid Receptor 4 Agonists with Antidiabetic Activity. **Journal of Medicinal Chemistry**, v. 59, n. 19, p. 8868–8878, 2016.
- BJARNADÓTTIR, T. K. et al. Comprehensive repertoire and phylogenetic analysis of the G protein-coupled receptors in human and mouse. **Genomics**, v. 88, n. 3, p. 263–273, 2006.
- BODOR, E. T. et al. Delineation of ligand binding and receptor signaling activities of purified P2Y receptors reconstituted with heterotrimeric G proteins. **Purinergic Signalling**, v. 1, n. 1, p. 43–49, 2004.
- BRISCOE, C. P. et al. The orphan G protein-coupled receptor GPR40 is activated by medium and long chain fatty acids. **Journal of Biological Chemistry**, v. 278, n. 13,

p. 11303–11311, 2003.

BRISCOE, C. P. et al. Pharmacological regulation of insulin secretion in MIN6 cells through the fatty acid receptor GPR40: identification of agonist and antagonist small molecules. **British Journal of Pharmacology**, v. 148, n. 5, p. 619–628, 2006.

CAERS, J. et al. Characterization of G Protein-coupled Receptors by a Fluorescence-based Calcium Mobilization Assay. **Journal of Visualized Experiments**, n. 89, p. 1–10, 2014.

CALANNA, S. et al. Secretion of glucagon-like peptide-1 in patients with type 2 diabetes mellitus: Systematic review and meta-analyses of clinical studies. **Diabetologia**, v. 56, n. 5, p. 965–972, 2013.

CARTONI, C. et al. Taste preference for fatty acids is mediated by GPR40 and GPR120. **The Journal of Neuroscience**, v. 30, n. 25, p. 8376–8382, 2010.

CHRISTIANSEN, E. et al. Discovery of potent and selective agonists for the free fatty acid receptor 1 (FFA(1)/GPR40), a potential target for the treatment of type II diabetes. **Journal of Medicinal Chemistry**, v. 51, n. 22, p. 7061–4, 2008.

CHRISTIANSEN, E. et al. Discovery of TUG-770: A Highly Potent Free Fatty Acid Receptor 1 (FFA1/GPR40) Agonist for Treatment of Type 2 Diabetes. **ACS Med Chem Lett**, v. 4, n. 5, p. 441–445, 2013.

CINTRA, D. E. et al. Unsaturated fatty acids revert diet-induced hypothalamic inflammation in obesity. **PloS one**, v. 7, n. 1, p. e30571, 2012.

CORNISH, J. et al. Modulation of osteoclastogenesis by fatty acids. **Endocrinology**, v. 149, n. 11, p. 5688–5695, 2008.

D. OH, S. T. et al. GPR120 is an Omega-3 Fatty Acid Receptor Mediating Potent Anti-Inflammatory and Insulin Sensitizing Effects. **Cell**, v. 142, n. 5, p. 687–698, 2011.

DAVIS, T. M. E. et al. Prevalence, incidence, and prognosis of hepatobiliary disease in community-based patients with type 2 diabetes: the Fremantle Diabetes Study. **The Journal of clinical endocrinology and metabolism**, v. 97, n. 5, p. 1581–8, 2012.

DEFOSSA, E.; WAGNER, M. Recent developments in the discovery of FFA1 receptor agonists as novel oral treatment for type 2 diabetes mellitus. **Bioorganic & Medicinal Chemistry Letters**, v. 24, p. 2991–3000, 2014.

DEWIRE, S. M. et al.  $\beta$ -Arrestins and Cell Signaling. **Annual Review of Physiology**, v. 69, n. 1, p. 483–510, 2007.

DONG, C. et al. Interacting genetic loci on chromosomes 20 and 10 influence extreme human obesity. **American journal of human genetics**, v. 72, n. 1, p. 115–24, 2003.

EDFALK, S.; STENEBERG, P.; EDLUND, H. Gpr40 is expressed in enteroendocrine cells and mediates free fatty acid stimulation of incretin secretion. **Diabetes**, v. 57, n. 9, p. 2280–2287, 2008.

FAKHRUDIN, N. et al. Identification of plumericin as a potent new inhibitor of the NF-

$\kappa$ B pathway with anti-inflammatory activity in vitro and in vivo. **British Journal of Pharmacology**, v. 171, n. 7, p. 1676–1686, 2014.

FAN, H. Y.; HEERKLOTZ, H. Digitonin does not flip across cholesterol-poor membranes. **Journal of Colloid and Interface Science**, v. 504, p. 283–293, 2017.

FENG, D. D. et al. Reduction in voltage-gated K<sup>+</sup> currents in primary cultured rat pancreatic beta-cells by linoleic acids. **Endocrinology**, v. 147, n. 2, p. 674–682, 2006.

FENG, X. T. et al. GPR40: A therapeutic target for mediating insulin secretion (Review). **International Journal of Molecular Medicine**, v. 30, n. 6, p. 1261–1266, 2012.

FERREIRA, J. V. et al. Cannabinoid Type 1 Receptor (CB1) Ligands with Therapeutic Potential for Withdrawal Syndrome in Chemical Dependents of Cannabis sativa. **ChemMedChem**, v. 12, n. 16, p. 1408–1416, 2017.

FILMORE, D. It's a GPCR world. **Modern Drug Discovery**, v. 7, n. 11, p. 24–27, 2004.

FLOCK, T. et al. Universal allosteric mechanism for G $\alpha$  activation by GPCRs. **Nature**, 2015.

FLODGREN, E. et al. GPR40 is expressed in glucagon producing cells and affects glucagon secretion. **Biochemical and Biophysical Research Communications**, v. 354, n. 1, p. 240–245, 2007.

FORTI, A. C. E. Estratégias terapêuticas baseadas nas vias do GLP-1. **Johns Hopkins Advanced Studies in Medicine**, v. 6, p. 618–626, 2006.

FREDRIKSSON, R. et al. Seven evolutionarily conserved human rhodopsin G protein-coupled receptors lacking close relatives. **FEBS Letters**, v. 554, n. 3, p. 381–388, 2003.

FUKUSHIMA, K. et al. Different roles of GPR120 and GPR40 in the acquisition of malignant properties in pancreatic cancer cells. **Biochemical and Biophysical Research Communications**, v. 465, n. 3, p. 512–515, 2015.

FUKUSHIMA, K. et al. Different effects of GPR120 and GPR40 on cellular functions stimulated by 12-O-tetradecanoylphorbol-13-acetate in melanoma cells. **Biochemical and Biophysical Research Communications**, v. 475, n. 1, p. 25–30, jun. 2016.

GALINDO, M. M. et al. G protein-coupled receptors in human fat taste perception. **Chemical Senses**, v. 37, n. 2, p. 123–139, 2012.

GAO, B. et al. Dose-response estrogen promotes osteogenic differentiation via GPR40 (FFAR1) in murine BMMSCs. **Biochimie**, v. 110, p. 36–44, 2015.

GARRIDO, D. M. et al. Synthesis and activity of small molecule GPR40 agonists. **Bioorganic & Medicinal Chemistry Letters**, v. 16, p. 1840–1845, 2006.

GEELLEN, M. J. H. The use of digitonin-permeabilized mammalian cells for measuring enzyme activities in the course of studies on lipid metabolism. **Analytical**

**Biochemistry**, v. 347, n. 1, p. 1–9, 2005.

GONG, Z. et al. G protein-coupled receptor 120 signaling regulates ghrelin secretion in vivo and in vitro. **AJP: Endocrinology and Metabolism**, v. 306, n. 1, p. E28–E35, 2014.

GOODMAN & GILMAN. **As bases farmacológicas da terapêutica**. 10. ed. Rio de Janeiro: McGraw-Hill, 2005.

GOTOH, C. et al. The regulation of adipogenesis through GPR120. **Biochemical and Biophysical Research Communications**, v. 354, n. 2, p. 591–597, 2007.

GOWDA, N. et al. Treatment with CNX-011-67, a novel GPR40 agonist, delays onset and progression of diabetes and improves beta cell preservation and function in male ZDF rats. **BMC Pharmacology and Toxicology**, v. 14, n. 1, p. 1, 2013.

GUO, D. Y. et al. Yhhu4488, a novel GPR40 agonist, promotes GLP-1 secretion and exerts anti-diabetic effect in rodent models. **Biochemical and Biophysical Research Communications**, v. 466, n. 4, p. 740–747, 2015.

GUREVICH, E. V.; GUREVICH, V. V. Arrestins: Ubiquitous regulators of cellular signaling pathways. **Genome Biology**, v. 7, n. 9, 2006.

HAMDOUCHI, C. et al. The Discovery, Preclinical, and Early Clinical Development of Potent and Selective GPR40 Agonists for the Treatment of Type 2 Diabetes Mellitus (LY2881835, LY2922083, and LY2922470). **Journal of Medicinal Chemistry**, v. 59, n. 24, p. 10891–10916, 2016.

HAMDOUCHI, C.; LINESWALA, J. P.; MAITI, P. **Spiropiperidine compounds and pharmaceutical use thereof for treating diabetes**. US Google Patents, , 21 abr. 2011. Disponível em: <<https://encrypted.google.com/patents/WO2011046851A1?cl=ar>>

HARA, T. et al. Novel selective ligands for free fatty acid receptors GPR120 and GPR40. **Naunyn-Schmiedeberg's Archives of Pharmacology**, v. 380, n. 3, p. 247–255, 2009.

HARDY, S. et al. Oleate promotes the proliferation of breast cancer cells via the G protein-coupled receptor GPR40. **The Journal of Biological Chemistry**, v. 280, n. 14, p. 13285–13291, 2005.

HIRASAWA, A. et al. Free fatty acids regulate gut incretin glucagon-like peptide-1 secretion through GPR120. **Nature Medicine**, v. 11, n. 1, p. 90–94, 2005.

HOPKINS, A. L.; GROOM, C. R. The druggable genome. **Nature Reviews. Drug Discovery**, v. 1, n. 9, p. 727–30, 2002.

HOPKINS, M. M. et al. Eicosopentaneic Acid and Other Free Fatty Acid Receptor Agonists Inhibit Lysophosphatidic Acid- and Epidermal Growth Factor-Induced Proliferation of Human Breast Cancer Cells. **Journal of Clinical Medicine**, v. 5, n. 2, p. 16, 26 fev. 2016.

HOUTHUIJZEN, J. M. et al. Fatty acid 16:4(n-3) stimulates a GPR120-induced signaling cascade in splenic macrophages to promote chemotherapy resistance. **FASEB Journal**, v. 31, n. 5, p. 2195–2209, 2017.

- HU, H. et al. A novel class of antagonists for the FFAs receptor GPR40. **Biochemical and Biophysical Research Communications**, v. 390, n. 3, p. 557–63, 2009.
- HUDSON, B. D. et al. The pharmacology of TUG-891, a potent and selective agonist of the free fatty acid receptor 4 (FFA4/GPR120), demonstrates both potential opportunity and possible challenges to therapeutic agonism. **Molecular Pharmacology**, v. 84, n. 5, p. 710–25, 2013.
- HUDSON, B. D. et al. The molecular basis of ligand interaction at free fatty acid receptor 4 (FFA4/GPR120). **Journal of Biological Chemistry**, v. 289, n. 29, p. 20345–20358, 2014.
- ICHIMURA, A. et al. Dysfunction of lipid sensor GPR120 leads to obesity in both mouse and human. **Nature**, v. 483, n. 7389, p. 350–354, 2012.
- INSEL, P. A. et al. GPCR expression in tissues and cells: Are the optimal receptors being used as drug targets? **British Journal of Pharmacology**, v. 165, n. 6, p. 1613–1616, 2012.
- ISHIHARA, G. et al. Expression of G protein coupled receptors in a cell-free translational system using detergents and thioredoxin-fusion vectors. **Protein Expression and Purification**, v. 41, n. 1, p. 27–37, 2005.
- ISHII, S. et al. Opposite effects of GPR120 and GPR40 on cell motile activity induced by ethionine in liver epithelial cells. **Biochemical and Biophysical Research Communications**, v. 456, n. 1, p. 135–138, jan. 2015a.
- ISHII, S. et al. Role of GPR120 in cell motile activity induced by 12-O-tetradecanoylphorbol-13-acetate in liver epithelial WB-F344 cells. **Molecular and Cellular Biochemistry**, v. 400, n. 1–2, p. 145–151, 8 fev. 2015b.
- ISHII, S. et al. Negative effects of G-protein-coupled free fatty acid receptor GPR40 on cell migration and invasion in fibrosarcoma HT1080 cells. **Molecular Carcinogenesis**, v. 55, n. 11, p. 1553–1559, nov. 2016.
- ITO, J. et al. Anatomical and histological profiling of orphan G-protein-coupled receptor expression in gastrointestinal tract of C57BL/6J mice. **Cell and Tissue Research**, v. 338, n. 2, p. 257–69, 2009.
- ITOH, Y. et al. Free fatty acids regulate insulin secretion from pancreatic beta cells through GPR40. **Nature**, v. 422, n. 6928, p. 173–176, 2003.
- JOHANSSON, S. et al. Cytotoxicity of digitoxin and related cardiac glycosides in human tumor cells. **Anti-Cancer Drugs**, v. 12, n. 5, p. 475–483, 2001.
- JONES, B. et al. Aequorin functional assay for characterization of G-protein-coupled receptors: Implementation with cryopreserved transiently transfected cells. **Analytical Biochemistry**, v. 400, n. 2, p. 184–189, 2010.
- JOOST, P.; METHNER, A. Phylogenetic analysis of 277 human G-protein-coupled receptors as a tool for the prediction of orphan receptor ligands. **Genome biology**, v. 3, n. 11, p. RESEARCH0063, 2002.
- KALIS, M. et al. Variants in the FFAR1 Gene Are Associated with Beta Cell Function. **PLoS ONE**, v. 2, n. 11, p. e1090, 2007.

- KATSUMA, S. et al. Free Fatty Acids Inhibit Serum Deprivation-induced Apoptosis through GPR120 in a Murine Enteroendocrine Cell Line STC-1. **Journal of Biological Chemistry**, v. 280, n. 20, p. 19507–19515, 20 maio 2005.
- KATZUNG, B.G. **Farmacologia Básica e Clínica**. 10. ed. Rio de Janeiro: Artmed/McGraw-Hill, 2010.
- KEBEDE, M. A. et al. Lipid receptors and islet function: therapeutic implications? **Diabetes, Obesity & Metabolism**, v. 11 Suppl 4, p. 10–20, 2009.
- KITA, T. et al. Diverse effects of G-protein-coupled free fatty acid receptors on the regulation of cellular functions in lung cancer cells. **Experimental Cell Research**, v. 342, n. 2, p. 193–199, 2016.
- KOTARSKY, K. et al. A human cell surface receptor activated by free fatty acids and thiazolidinedione drugs. **Biochemical and Biophysical Research Communications**, v. 301, n. 2, p. 406–410, 2003.
- KRISTINSSON, H. et al. FFAR1 is involved in both the acute and chronic effects of palmitate on insulin secretion. **Endocrinology**, 2013.
- LAMRI, A. et al. Interaction between GPR120 p.R270H loss-of-function variant and dietary fat intake on incident type 2 diabetes risk in the D.E.S.I.R. study. **Nutrition, Metabolism and Cardiovascular Diseases**, v. 26, n. 10, p. 931–936, 2016.
- LAN, H. et al. Lack of FFAR1 / GPR40 Does Not Protect Mice From High-Fat Diet – Induced Metabolic Disease. **Diabetes**, v. 57, n. November, p. 2999–3006, 2008.
- LATOUR, M. G. et al. GPR40 is necessary but not sufficient for fatty acid stimulation of insulin secretion in vivo. **Diabetes**, v. 56, n. 4, p. 1087–94, 2007.
- LEE, J. et al. 3,3'-Diindolylmethane Suppresses Adipogenesis Using AMPK  $\alpha$  - Dependent Mechanism in 3T3-L1 Adipocytes and *Caenorhabditis elegans*. **Journal of Medicinal Food**, v. 20, n. 7, p. 646–652, 2017.
- LEFKOWITZ, R. J.; RAJAGOPAL, K.; WHALEN, E. J. New Roles for  $\beta$ -Arrestins in Cell Signaling: Not Just for Seven-Transmembrane Receptors. **Molecular Cell**, v. 24, n. 5, p. 643–652, 2006.
- LEISER, M.; FLEISCHER, N. cAMP-Dependent Phosphorylation of the Cardiac-Type  $\alpha_1$  Subunit of the Voltage-Dependent  $\text{Ca}^{2+}$  Channel in a Murine Pancreatic B-Cell Line. **Diabetes**, v. 45, n. October, p. 25–29, 1996.
- LI, H. et al. Discovery of Potent and Orally Bioavailable GPR40 Full Agonists Bearing Thiophen-2-ylpropanoic Acid Scaffold. **Journal of Medicinal Chemistry**, v. 60, n. 7, p. 2697–2717, 2017.
- LI, Z. et al. Free fatty acid receptor agonists for the treatment of type 2 diabetes: drugs in preclinical to phase II clinical development. **Expert Opinion on Investigational Drugs**, v. 25, n. 8, p. 871–890, 2016a.
- LI, Z. et al. Discovery of novel pyrrole-based scaffold as potent and orally bioavailable free fatty acid receptor 1 agonists for the treatment of type 2 diabetes. **Bioorganic & Medicinal Chemistry**, v. 24, n. 9, p. 1981–1987, 2016b.

- LIN, D. C.-H. et al. Identification and pharmacological characterization of multiple allosteric binding sites on the free fatty acid 1 receptor. **Molecular Pharmacology**, v. 82, n. 5, p. 843–59, 2012.
- LIN, D. C. H. et al. AMG 837: A novel GPR40/FFA1 agonist that enhances insulin secretion and lowers glucose levels in rodents. **PLoS ONE**, v. 6, n. 11, 2011.
- LIU, D. et al. G-protein coupled receptor 120 is involved in glucose metabolism in fat cells. **Cellular and Molecular Biology (Noisy-le-Grand, France)**, v. Suppl.58, p. 1757–1762, 2012.
- LIU, Y. et al. The fish oil ingredient, docosahexaenoic acid, activates cytosolic phospholipase A2 via GPR120 receptor to produce prostaglandin E2 and plays an anti-inflammatory role in macrophages. **Immunology**, v. 143, n. 1, p. 81–95, 2014.
- LIU, Z. et al. Omega-3 Fatty Acids and Other FFA4 Agonists Inhibit Growth Factor Signaling in Human Prostate Cancer Cells. **J Pharmacol Exp Ther**, v. 352, p. 380–394, 2015.
- LU, H. et al. Discovery of novel orally bioavailable GPR40 agonists. **Bioorganic & Medicinal Chemistry Letters**, v. 23, n. 10, p. 2920–2924, maio 2013.
- LU, S. Y. et al. Insight into analysis of interactions of GW9508 to wild-type and H86F and H137F GPR40: A combined QM/MM study and pharmacophore modeling. **Journal of Molecular Graphics and Modelling**, v. 29, n. 6, p. 818–825, 2011.
- LU, X. et al. Postprandial inhibition of gastric ghrelin secretion by long-chain fatty acid through GPR120 in isolated gastric ghrelin cells and mice. **American Journal of Physiology. Gastrointestinal and Liver Physiology**, v. 303, n. 3, p. G367-76, 2012.
- LUO, J. et al. A Potent Class of GPR40 Full Agonists Engages the Enteroinular Axis to Promote Glucose Control in Rodents. **PLoS ONE**, v. 7, n. 10, 2012.
- MAEHLE, A. H. A binding question: the evolution of the receptor concept. **Endeavour**, v. 33, n. 4, p. 135–140, 2009.
- MANCINI, A. D. et al. B-Arrestin Recruitment and Biased Agonism At Free Fatty Acid Receptor 1. **Journal of Biological Chemistry**, v. 290, n. 34, p. 21131–21140, 2015.
- MANCINI, A. D.; POITOUT, V. The fatty acid receptor FFA1/GPR40 a decade later: How much do we know? **Trends in Endocrinology and Metabolism**, v. 24, n. 8, p. 398–407, 2013.
- MATSUMURA, S. et al. GPR expression in the rat taste bud relating to fatty acid sensing. **Biomedical Research (Tokyo, Japan)**, v. 28, n. 1, p. 49–55, 2007.
- MATSUMURA, S. et al. Colocalization of GPR120 with phospholipase-Cbeta2 and alpha-gustducin in the taste bud cells in mice. **Neuroscience Letters**, v. 450, n. 2, p. 186–90, 2009.
- MCDONALD, P. H. et al. Beta-arrestin 2: a receptor-regulated MAPK scaffold for the activation of JNK3. **Science**, v. 290, n. 5496, p. 1574–7, 24 nov. 2000.
- MILTON, F. A. et al. PPAR $\gamma$  partial agonist GQ-16 strongly represses a subset of



genes in 3T3-L1 adipocytes. **Biochemical and Biophysical Research Communications**, v. 464, n. 3, p. 718–723, 2015.

MIYAUCHI, S. et al. Distribution and regulation of protein expression of the free fatty acid receptor GPR120. **Naunyn-Schmiedeberg's Archives of Pharmacology**, v. 379, n. 4, p. 427–434, 2009.

MOORE, K. et al. Cloning, expression, and pharmacological characterization of the GPR120 free fatty acid receptor from cynomolgus monkey: Comparison with human GPR120 splice variants. **Comparative Biochemistry and Physiology**, v. 154, n. 4, p. 419–26, 2009.

MOREADITH, R. W.; FISKUM, G. Isolation of mitochondria from ascites tumor cells permeabilized with digitonin. **Analytical Biochemistry**, v. 137, n. 2, p. 360–367, 1984.

MUNKARAH, A. et al. Targeting of free fatty acid receptor 1 in EOC: A novel strategy to restrict the adipocyte-EOC dependence. **Gynecologic Oncology**, v. 141, n. 1, p. 72–79, 2016.

NAKAMOTO, K. et al. Involvement of the long-chain fatty acid receptor GPR40 as a novel pain regulatory system. **Brain Res**, v. 1432, p. 74–83, 2012.

NAKAMOTO, K. et al. Dysfunctional GPR40/FFAR1 signaling exacerbates pain behavior in mice. **PLOS ONE**, v. 12, n. 7, p. e0180610, 19 jul. 2017.

NAVARRO-TITO, N.; ROBLEDO, T.; SALAZAR, E. P. Arachidonic acid promotes FAK activation and migration in MDA-MB-231 breast cancer cells. **Experimental Cell Research**, v. 314, n. 18, p. 3340–3355, 2008.

NEGORO, N. et al. Discovery of TAK-875: A potent, selective, and orally bioavailable GPR40 agonist. **ACS Medicinal Chemistry Letters**, v. 1, n. 6, p. 290–294, 2010.

NISHIKAWA, M. et al. Interaction of digitonin and its analogs with membrane cholesterol. **Journal of Biochemistry**, v. 96, n. 4, p. 1231–1239, 1984.

OH, D. Y. et al. A Gpr120-selective agonist improves insulin resistance and chronic inflammation in obese mice. **Nature Medicine**, v. 20, n. 8, p. 942–947, 6 jul. 2014.

OH, D. Y.; OLEFSKY, J. M. Omega 3 fatty acids and GPR120. **Cell Metabolism**, v. 15, n. 5, p. 564–565, 2012.

OH, D. Y.; WALENTA, E. Omega-3 Fatty Acids and FFAR4. **Frontiers in Endocrinology**, v. 5, n. 115, p. 115, 16 jul. 2014.

PARKER, H. E. et al. Nutrient-dependent secretion of glucose-dependent insulinotropic polypeptide from primary murine K cells. **Diabetologia**, v. 52, n. 2, p. 289–98, 2009.

PELÉ, J. et al. Multidimensional scaling reveals the main evolutionary pathways of class A G-protein-coupled receptors. **PLoS ONE**, v. 6, n. 4, p. 1–10, 2011.

PIERCE, K. L.; PREMONT, R. T.; LEFKOWITZ, R. J. Seven-transmembrane receptors. **Nature Reviews. Molecular Cell Biology**, v. 3, n. 9, p. 639–650, 2002.

PILLAIYAR, T. et al. Diindolylmethane Derivatives: Potent Agonists of the

Immunostimulatory Orphan G Protein-Coupled Receptor GPR84. **Journal of Medicinal Chemistry**, v. 60, n. 9, p. 3636–3655, 2017.

PILLAIYAR, T. et al. 6-(Ar)Alkylamino-Substituted Uracil Derivatives: Lipid Mimetics with Potent Activity at the Orphan G Protein-Coupled Receptor 84 (GPR84). **ACS Omega**, v. 3, n. 3, p. 3365–3383, 2018.

PRIHANDOKO, R. et al. Distinct Phosphorylation Clusters Determine the Signaling Outcome of Free Fatty Acid Receptor 4/G Protein-Coupled Receptor 120. **Molecular Pharmacology**, v. 89, n. 5, p. 505–20, 2016.

QIAN, J. et al. Agonist-induced activation of human FFA1 receptor signals to extracellular signal-regulated kinase 1 and 2 through Gq- and Gi-coupled signaling cascades. **Cellular and Molecular Biology Letters**, v. 22, n. 1, p. 1–12, 2017.

QUESADA-LÓPEZ, T. et al. The lipid sensor GPR120 promotes brown fat activation and FGF21 release from adipocytes. **Nature Communications**, v. 7, 2016.

RANKOVIC, Z.; BRUST, T. F.; BOHN, L. M. Biased agonism: An emerging paradigm in GPCR drug discovery. **Bioorganic & Medicinal Chemistry Letters**, v. 26, n. 2, p. 241–250, jan. 2016.

REGARD, J. B.; SATO, I. T.; COUGHLIN, S. R. Anatomical Profiling of G Protein-Coupled Receptor Expression. **Cell**, v. 135, n. 3, p. 561–571, out. 2008.

ROSEN, E. D. et al. C/EBP $\alpha$  induces adipogenesis through PPAR $\gamma$ : a unified pathway. **Genes & Development**, n. 16, p. 22–26, 2002.

ROSENBAUM, D. M.; RASMUSSEN, S. G. F.; KOBILKA, B. K. The structure and function of G-protein-coupled receptors. **Nature**, v. 459, n. 7245, p. 356–363, 2009.

SABRAUTZKI, S. et al. Point mutation of Ffar1 abrogates fatty acid-dependent insulin secretion, but protects against HFD-induced glucose intolerance. **Molecular Metabolism**, v. 6, n. July, 2017.

SAWZDARGO, M. et al. A cluster of four novel human G protein-coupled receptor genes occurring in close proximity to CD22 gene on chromosome 19q13.1. **Biochemical and Biophysical Research Communications**, v. 239, n. 2, p. 543–547, 1997.

SCHIÖTH, H. B.; FREDRIKSSON, R. The GRAFS classification system of G-protein coupled receptors in comparative perspective. **General and Comparative Endocrinology**, v. 142, n. 1–2 SPEC. ISS., p. 94–101, 2005.

SCHNELL, S.; SCHAEFER, M.; SCHÖFL, C. Free fatty acids increase cytosolic free calcium and stimulate insulin secretion from beta-cells through activation of GPR40. **Molecular and Cellular Endocrinology**, v. 263, n. 1–2, p. 173–80, 15 jan. 2007.

SHIMPUKADE, B. et al. Discovery of potent and selective GPR120 agonists. **Abstracts of Papers of the American Chemical Society**, v. 243, 2012.

SMRCKA, A. et al. Regulation of polyphosphoinositide-specific phospholipase C activity by purified Gq. **Science**, v. 251, n. 4995, p. 804–807, 15 fev. 1991.

SOLFRIZZO, M. et al. Production of a toxin stemphol by *Stemphylium* species.

**Natural Toxins**, v. 2, n. 1, p. 14–18, 1994.

SONG, T. et al. GPR120 promotes adipogenesis through intracellular calcium and extracellular signal-regulated kinase 1/2 signal pathway. **Molecular and Cellular Endocrinology**, v. 434, p. 1–13, 2016.

SOTO-GUZMAN, A. et al. Oleic acid induces ERK1/2 activation and AP-1 DNA binding activity through a mechanism involving Src kinase and EGFR transactivation in breast cancer cells. **Molecular and Cellular Endocrinology**, v. 294, n. 1–2, p. 81–91, 2008.

SPARKS, S. M. et al. Identification of diarylsulfonamides as agonists of the free fatty acid receptor 4 (FFA4/GPR120). **Bioorganic and Medicinal Chemistry Letters**, v. 24, n. 14, p. 3100–3103, 2014.

STENEBERG, P. et al. The FFA receptor GPR40 links hyperinsulinemia, hepatic steatosis, and impaired glucose homeostasis in mouse. **Cell Metabolism**, v. 1, n. 4, p. 245–258, 2005.

STODOLA, F. H.; WEISLEDER, D.; VESONDER, R. F. A new dialkylresorcinol from *Stemphylium majusculum*. **Phytochemistry**, v. 12, n. 7, p. 1797–1798, 1973.

SUM, C. S. et al. Identification of Residues Important for Agonist Recognition and Activation in GPR40. **Journal of Biological Chemistry**, v. 282, n. 40, p. 29248–29255, 15 ago. 2007.

SUN, P. et al. DC260126: A Small-Molecule Antagonist of GPR40 that Protects against Pancreatic  $\beta$ -Cells Dysfunction in db/db Mice. **PLoS ONE**, v. 8, n. 6, 2013.

SUZUKI, T. et al. Identification of G protein-coupled receptor 120-selective agonists derived from PPAR $\gamma$  agonists. **Journal of Medicinal Chemistry**, v. 51, n. Table 1, p. 7640–7644, 2008.

TAKAESU, G. et al. TAK1 is critical for I $\kappa$ B kinase-mediated activation of the NF- $\kappa$ B pathway. **Journal of Molecular Biology**, v. 326, n. 1, p. 105–115, 2003.

TAKAHASHI, K. et al. Different effects of G-protein-coupled receptor 120 (GPR120) and GPR40 on cell motile activity of highly migratory osteosarcoma cells. **Biochemical and Biophysical Research Communications**, v. 484, n. 3, p. 675–680, 2017.

TAKANO, R. et al. Discovery of DS-1558: A potent and orally bioavailable GPR40 agonist. **ACS Medicinal Chemistry Letters**, v. 6, n. 3, p. 266–270, 2015.

TAKEDA, S. et al. Identification of surrogate ligands for orphan G protein-coupled receptors. **Life Sciences**, v. 74, n. 2–3, p. 367–377, 2003.

TAKEUCHI, M. et al. FFA1-selective agonistic activity based on docking simulation using FFA1 and GPR120 homology models. **British Journal of Pharmacology**, v. 168, n. 7, p. 1570–1583, 2013.

TAN, C. P. et al. Selective small-molecule agonists of G protein-coupled receptor 40 promote glucose-dependent insulin secretion and reduce blood glucose in mice. **Diabetes**, v. 57, n. 8, p. 2211–9, 2008.

- TANAKA, T. et al. Cloning and characterization of the rat free fatty acid receptor GPR120: in vivo effect of the natural ligand on GLP-1 secretion and proliferation of pancreatic  $\beta$  cells. **Naunyn-Schmiedeberg's Archives of Pharmacology**, v. 377, n. 4–6, p. 515–522, 2008.
- TIKHONOVA, I. G. et al. Bidirectional, Iterative Approach to the Structural Delineation of the Functional “Chemoprint” in GPR40 for Agonist Recognition. **Journal of Medicinal Chemistry**, v. 50, n. 13, p. 2981–2989, jun. 2007.
- TIKHONOVA, I. G. et al. Discovery of novel agonists and antagonists of the free fatty acid receptor 1 (FFAR1) using virtual screening. **Journal of Medicinal Chemistry**, v. 51, n. 3, p. 625–633, 2008.
- TRZASKOWSKI, B. et al. Action of Molecular Switches in GPCRs - Theoretical and Experimental Studies. **Current Medicinal Chemistry**, v. 19, n. 8, p. 1090–1109, 2012.
- TSUDA, N. et al. A novel free fatty acid receptor 1 (GPR40/FFAR1) agonist, MR1704, enhances glucose-dependent insulin secretion and improves glucose homeostasis in rats. **Pharmacology Research and Perspectives**, v. 5, n. 4, p. 1–12, 2017.
- TUTEJA, N. Signaling through G protein coupled receptors. **Plant Signaling & Behavior**, v. 4, n. 10, p. 942–947, 2009.
- VANDREY, R.; HANEY, M. Pharmacotherapy for cannabis dependence: How close are we? **CNS Drugs**, v. 23, n. 7, p. 543–553, 2009.
- VASSILATIS, D. K. et al. The G protein-coupled receptor repertoires of human and mouse. **Proceedings of the National Academy of Sciences of the United States of America**, v. 100, n. 8, p. 4903–4908, 2003.
- VESTMAR, M. A. et al. Functional and genetic epidemiological characterisation of the FFAR4 (GPR120) p.R270H variant in the Danish population. **Journal of Medical Genetics**, v. 53, n. 9, p. 616–623, 2016.
- WALSH, S. P. et al. 3-Substituted 3-(4-aryloxyaryl)-propanoic acids as GPR40 agonists. **Bioorganic and Medicinal Chemistry Letters**, v. 21, n. 11, p. 3390–3394, 2011.
- WANG, X. et al. Synthesis and biological evaluation of phenoxyacetic acid derivatives as novel free fatty acid receptor 1 agonists. **Bioorganic & Medicinal Chemistry**, v. 23, n. 1, p. 132–140, 2015.
- WANG, Y. et al. Discovery and optimization of potent GPR40 full agonists containing tricyclic spirocycles. **ACS Medicinal Chemistry Letters**, 2013.
- WATSON, S.-J.; BROWN, A. J. H.; HOLLIDAY, N. D. Differential signaling by splice variants of the human free fatty acid receptor GPR120. **Molecular Pharmacology**, v. 81, n. 5, p. 631–42, 2012.
- WETTSCHURECK, N.; OFFERMANN, S. Mammalian G Proteins and Their Cell Type Specific Functions. **Physiological Review**, p. 1159–1204, 2005.
- WU, Q. et al. Identification of G-protein-coupled receptor 120 as a tumor-promoting receptor that induces angiogenesis and migration in human colorectal carcinoma.

**Oncogene**, v. 32, n. 49, p. 5541–5550, 2013.

YAN, Y. et al. Omega-3 Fatty Acids Prevent Inflammation and Metabolic Disorder through Inhibition of NLRP3 Inflammasome Activation. **Immunity**, v. 38, n. 6, p. 1154–1163, 2013.

YANG, L. et al. Synthesis and biological evaluation of GPR40/FFAR1 agonists containing 3,5-dimethylisoxazole. **European Journal of Medicinal Chemistry**, v. 116, p. 46–58, 2016.

ZHANG, D.; LEUNG, P. S. Potential roles of GPR120 and its agonists in the management of diabetes. **Drug Design, Development and Therapy**, 2014.

ZHOU, X.-M. et al. Two new stemphol sulfates from the mangrove endophytic fungus *Stemphylium* sp. 33231. **The Journal of Antibiotics**, v. 68, n. October 2014, p. 1–3, 2015.